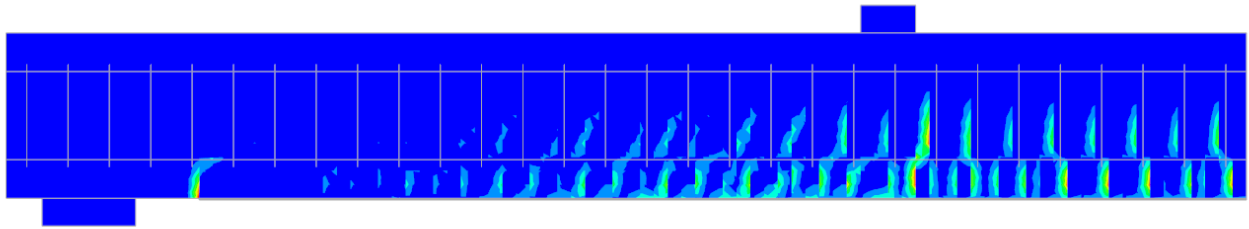




CHALMERS
UNIVERSITY OF TECHNOLOGY



Flexural Strengthening of Concrete Structures with Prestressed FRP Composite

A Parametric study with Finite Element Modelling

Master's thesis in Structural Engineering and Building Technology

PER AHLGREN
JOACIM EDWIJN

Department of Civil and Environmental Engineering
Division of Structural Engineering
Steel and Timber Structures
CHALMERS UNIVERSITY OF TECHNOLOGY
Gothenburg, Sweden 2017
Master's thesis BOMX02-17-20

MASTER'S THESIS BOMX02-17-20

Flexural Strengthening of Concrete Structures with Prestressed FRP Composite

A Parametric study with Finite Element Modelling

Master's thesis in Structural Engineering and Building Technology

PER AHLGREN
JOACIM EDWIJN

Department of Civil and Environmental Engineering
Division of Structural Engineering
Steel and Timber Structures
CHALMERS UNIVERSITY OF TECHNOLOGY
Gothenburg, Sweden 2017

Flexural Strengthening of Concrete Structures with Prestressed FRP Composite
A Parametric study with Finite Element Modelling
PER AHLGREN
JOACIM EDWIJN

© PER AHLGREN , JOACIM EDWIJN, 2017

Master's thesis BOMX02-17-20
ISSN 1652-8557
Department of Civil and Environmental Engineering
Division of Structural Engineering
Steel and Timber Structures
Chalmers University of Technology
SE-412 96 Gothenburg
Sweden
Telephone: +46 (0)31-772 1000

Colophon:

The thesis was created using $\text{\LaTeX} 2_{\epsilon}$ and `biblatex` and edited on `www.sharelatex.com`. The typesetting software was the `TEX Live` distribution. The text is set in Times New Roman. Graphs were created using MS Excel. Figures were created using SNIPPING TOOL.

Cover:

Concrete beam, DIANA FEA, CFRP

Chalmers
Gothenburg, Sweden 2017

Flexural Strengthening of Concrete Structures with Prestressed FRP Composite
A Parametric study with Finite Element Modelling
Master's thesis in Structural Engineering and Building Technology

PER AHLGREN

JOACIM EDWIJN

Department of Civil and Environmental Engineering
Division of Structural Engineering
Steel and Timber Structures
Chalmers University of Technology

ABSTRACT

This master thesis presents the results from a parametric study, with Finite Element Modelling, using a new prestressing method where a Carbon Fiber Reinforced Polymer (CFRP) laminate is Externally Bonded (EB) to a reinforced concrete beam. The results from the parametric study are compared with the results from already executed experiments.

By prestressing the CFRP laminate the capacity of the composite material can be utilized more and by externally bond it to a reinforced concrete structure the Serviceability Limit State (SLS) will improve due to cracks closing up and the Ultimate Limit State (ULS) will improve due to higher ultimate strength.

The objective of this thesis is to create a model using the Finite Element Method (FEM) and optimizing the prestressing force, using the new method, in order to improve the structure in both SLS and ULS. The main focus of the project is to check for and optimize against crack width, ductility, and ultimate strength.

There are methods for strengthening concrete structures using prestressed Fiber Reinforced Polymer (FRP), but most of them require metal anchorage at the end of the laminate. Anchorage is needed due to the high shear forces created by the prestressing force and to transfer stresses into the structure to avoid debonding of the FRP laminate.

A new method has been developed at Chalmers University of Technology where the prestressing force is applied in segments, reducing the shear force at the end of the laminate, making the need for anchorage redundant.

Initial experimental tests have been done on three 4.5 m long reinforced concrete beams subjected to four point bending at Chalmers, using the new prestressing method. One reference beam, one beam with EB passive CFRP, and one beam with EB prestressed CFRP.

The results from the Finite Element Analysis (FEA) show that, by prestressing the CFRP laminate to the concrete members, crack width can be reduced if the prestressing level is within a certain range. Prestressing with too high force will cause the concrete to crack on the top side and reducing the ductility of the beam. According to the results from the FEA and the optimization strategy, an optimal prestressing force will be between 27.90-29.17% utilization of the CFRPs ultimate tensile strength. The optimal prestressing force according to this thesis is when the top side cracking is kept at a minimum, failure of the concrete occurs as late as possible, and that there is sufficient utilization of the CFRP laminate.

Keywords: Flexural strengthening, Carbon Fiber Reinforced Polymer, CFRP, Concrete, Cracking, FEM, Finite element modelling, Externally bonded, DIANA, Prestress

Böjförstärkning av Betongkonstruktioner med hjälp av Förspända Fiberarmerade Polymerkompositer
En Parametrisk studie med Finita Element Modellerings
Examensarbete inom Structural Engineering

PER AHLGREN

JOACIM EDWIJN

Institutionen för Bygg- och miljöteknik
Avdelningen för Konstruktionsteknik
Stål- och träbyggnad
Chalmers tekniska högskola

SAMMANFATTNING

Detta examensarbete presenterar resultaten från en parametrisk studie, med Finita Element Metoden, där en ny metod används för att förspänna laminat av kolfiberarmerade polymerer till en armerad betongbalk. Resultaten från den parametriska studien har sedan jämförts med resultaten från redan utförda experiment.

Genom att förspänna laminat av kolfiberarmerade polymerer och fästa dessa på armerade betongkonstruktioner kan man öka kapaciteten i bruksgränstillståndet på grund av sprickor som stänger sig och i brottgränstillståndet på grund av en ökad brottlast.

Målet för detta examensarbete är att skapa en modell med hjälp av Finita Element Metoden och optimera förspänningskraften, genom att använda den nya metoden, för att förbättra konstruktionen i brott- och bruksgränstillståndet. Huvudfokus ligger på att kontrollera sprickbredd, seghet och brottlast.

Det finns idag metoder för att förstärka betongkonstruktioner med hjälp av förspända fiberarmerade polymerer, men majoriteten av dessa kräver någon form av metallförankring i änden av laminatet. Förankringen är nödvändig på grund av den höga skjuvspänningen som bildas tack vare förspänningen, och för att överföra spänningarna till konstruktionen och undvika att laminatet släpper från betongen.

En ny metod har utvecklats på Chalmers Tekniska Högskola där förspänningskraften är applicerad i segment vilket reducerar skjuvspänningen i laminatets ändar och därför gör användandet av metallförankring redundant.

Experimentella tester har, på Chalmers, utförts på tre 4.5 m långa armerade betongbalkar utsatta för fyrpunktsböjning. En referensbalk, en balk med ett passivt kolfiberarmerat polymerlaminat, och en balk med ett förspänt kolfiberarmerat polymerlaminat.

Resultatet från Finita Element Analyserna visar att man, genom att förspänna laminatet på betongelementet, kan reducera sprickbredd om man håller sig inom ett visst förspänningsintervall. Vid för höga förspänningskrafter visar det sig att balken spricker på ovansidan och att det leder till försämrad seghet hos balken. Enligt resultaten från Finita Element Analyserna ligger den optimala förspänningskraften mellan 27.90-29.17% utnyttjandegrad av det kolfiberarmerade polymerlaminatet.

Nyckelord: Böjförstärkning, Reparation, Kolfiberarmerad Polymer, Betong, Sprickor, DIANA, Förspänning

CONTENTS

Abstract	i
Sammanfattning	ii
Contents	iii
Preface	vii
Acronyms	ix
Nomenclature	x
1 Introduction	1
1.1 Background	1
1.2 Scope of study	1
1.3 Aim and objectives	1
1.4 Method	3
1.5 Limitations	3
2 Theory	4
2.1 Fiber reinforced polymer	4
2.1.1 Glass FRP	4
2.1.2 Carbon FRP	4
2.1.3 Carbon FRP for external bonding	5
2.2 Reinforced concrete beams	6
2.2.1 Cracks in concrete structures	6
2.2.2 Crack criterion's in Concrete	6
2.3 Ductility of strengthened RC beams	8
2.4 Strengthening of RC beam with FRP	9
2.4.1 Non-prestressed FRP	9
2.4.2 Externally bonded prestressed FRP	10
2.4.3 Benefits with EB prestressed FRP	13
2.4.4 Challenges with prestressed externally bonded CFRP	13
2.4.5 Near-surface mounted FRP	15
2.4.6 Optimization of the prestressed externally bonded CFRP	15
2.5 Failure modes of FRP	16
2.6 Tenroc method	17
3 Full-scale tests of strengthened beams	20
3.1 Results of full-scale tests	20
3.2 Results from lab tests	21

4	Finite element modelling	22
4.1	FE model	22
4.1.1	Boundary conditions	23
4.1.2	Element types and mesh	23
4.1.3	Convergence study	26
4.1.4	Interface between materials	26
4.2	Material indata	27
4.2.1	Concrete	27
4.2.2	Reinforcement	27
4.2.3	CFRP	28
4.2.4	Epoxy adhesive	28
4.3	Compressive Behavior	29
4.4	Nonlinear tension softening	30
4.4.1	Influence of lateral cracking	31
4.4.2	Crack bandwidth	32
5	Results	33
5.1	Verification of the FE model	33
5.1.1	Reference beam vs FE	34
5.1.2	Beam with passive CFRP vs FE	34
5.1.3	Beam with prestressed CFRP vs FE	35
5.1.4	FE vs hand calculation	35
5.1.5	Visualisation of cracking load, yielding load and ultimate load for real tests, FE simulations and hand calculations	36
5.2	Increasing prestressing force in the CFRP	38
5.2.1	Failure modes	40
5.3	Axial force profile in the CFRP laminate	42
5.4	Shear stress results	43
5.5	Crack pattern and crack width	44
5.6	Ductility of the beam strengthened with prestressed CFRP laminate	49
5.7	Strain in CFRP laminate	50
5.8	Optimization of prestressing force	51
5.8.1	Work flow for optimizing prestressing force	52
6	Discussion	56
6.1	Source of error	57
7	Conclusion	58
8	Further studies	59
	References	61
	Appendix A Hand Calculations	63

Appendix B	CFRP Manufacture	78
Appendix C	Reinforcement lab test	82
Appendix D	Concrete lab test	85
Appendix E	CFRP lab test	87

PREFACE

We would like to thank our supervisors Larry and Valbona for all their help and advice, especially during times where everything didn't go as anticipated. We would also like to thank our examiner Reza Haghani Dogaheh for constructive input.

A special thank goes to "Fikagruppen" for their contributing energy and positive attitude. This thesis would not have been the same without you.

Joacim Edwijn and Per Ahlgren, Göteborg 2017

Acronyms

ACI American Concrete Institute.

CFRP Carbon Fiber Reinforced Polymer.

CHBDC Canadian Highway Bridge Design Code.

DIANA DIsplacement ANAlyser.

DIE DIANA Interactive Environment.

EB Externally Bonded.

FEA Finite Element Analysis.

FEM Finite Element Method.

FRP Fiber Reinforced Polymer.

LVDT Linear Variable Differential Transducers.

NSM Near-Surface Mounted.

PAN Polyacrylonitrile.

RC Reinforced Concrete.

Rebars Reinforcement Bars.

SLS Serviceability Limit State.

ULS Ultimate Limit State.

Nomenclature

Greek letters

α_{lat}	Average lateral damage variable (-)
α_p	Peak strain value in Thorenfeldt curve (-)
α_p	Strain value in Thorenfeldt curve (-)
β	Material and geometrical parameter (-)
$\beta_{\sigma_{cr}}$	Reduction factor (-)
$\beta_{\varepsilon_{cr}}$	Reduction factor (-)
η	Shape function (-)
μ	Ductility index (-)
ν	Poisson's ratio (-)
σ_{cm}	Stress from pure bending (MPa)
σ_{cn}	Stress from the axial force (MPa)
τ	Shear stress (MPa)
ε_0	Initial strain at the extreme tensile fibre before strengthening (-)
ε_{CFRP}	CFRP strain (-)
ε_{cu}	Concrete strain at ultimate (-)
$\varepsilon_{fu,c}$	FRP strain (-)
$\varepsilon_{su,c}$	Internal steel strain (-)
ε_{sud}	Design Reinforcement strain (-)
ε_{suk}	Characteristic Reinforcement strain (-)
ε_s	Reinforcement strain (-)
ε_p	Strain value in Thorenfeldt curve (-)
$\varphi_{0.001}^c$	Curvature at $M_{0.001}^c$ (-)
φ_{ult}	Curvature at M_{ult} (-)
ξ	Ductility index (-)
ξ	Shape function (-)

Roman lower case letters

$\Delta u_{n,ult}$	Crack width at zero crack stress (-)
Δu_n	Crack width for nonlinear tension softening (-)
a_i	Shape function factor (-)
b_t	mean width of the part of the cross-section in tension (m)
c	Distance from extreme compression fibers to the neutral axis (m)
d	Effective depth of the tension reinforcement (m)
f_p	Peak stress (MPa)
f_u	Ultimate strength (MPa)

f_y	Yield stress (MPa)
f_{cc}	Concrete compressive strength in Thorenfeldt curve (MPa)
f_{cf}	Compressive stress in Thorenfeldt curve (MPa)
f_{cm}	Mean compressive strength (MPa)
$f_{ct,fl}$	Bending resistance (MPa)
f_{ctm}	Mean axial tensile strength of concrete (MPa)
f_n	Nonlinear tension softening factor (-)
f_t	Tensile strength (MPa)
f_{yk}	Characteristic yield strength of longitudinal reinforcement (MPa)
h	Crack bandwidth (m)
h	Height (m)
k	Reduction factor (-)
k	Thorenfeldt parameter (-)
n	Thorenfeldt parameter (-)
t	Tensile strain (-)
x	Compression zone (m)
d	effective depth of the cross-section (m)

Roman capital letters

ΔP	Prestressing force difference (kN)
A	Element area (m ²)
$A_{s,min}$	Minimum area of bending reinforcement (m ²)
C	Ductility factor (-)
E	Young's modulus (MPa)
F	Axial force (kN)
F_{pres}	Total prestressing force (kN)
G_f	Fracture Energy (N/m)
J	Performance factor (-)
$M_{0.001}^c$	Moment when the maximum concrete compressive strain reaches 0.001 (kN m)
M_{ult}	Moment capacity of the current section (kN m)
P_{max}	Total prestressing force (kN)
$U_{ultimate}$	Ultimate mid-span deflection (m)
$U_{yielding}$	Mid-span deflection at yielding (m)

1 Introduction

1.1 Background

Concrete structures have been used for a long time and there are now many structures that are in need of repair (Täljsten, Carolin, and Nordin, 2003). Concrete performs well under compression but will easily crack when subjected to tension. Cracking of concrete affects its performance and have a negative impact on the aesthetics as well. Concrete structures are designed for a long lifespan and, due to the rapidly improving technology of today, the structures might be subjected to higher loads than what was intended in the design phase. Instead of rebuilding structures, techniques for strengthening have been developed.

Fiber Reinforced Polymer (FRP) has been used as reinforcement for flexural strengthening of existing Reinforced Concrete (RC) structures, both as Externally Bonded (EB) and Near-Surface Mounted (NSM) to the soffit tension side. The FRP is usually bonded with structural epoxy adhesive and both EB and NSM acts passively and increases the load-bearing capacity of the RC member. In Serviceability Limit State (SLS) the FRP, independent of which way it is used, does not contribute that much, considering stiffness and cracking load, crack width and crack pattern. There is also a high risk of debonding at low utilization ratio of the FRP material.

To be able to utilize the true tensile strength of the FRP composites and make it act in a more active way, the FRP could be prestressed before installed onto the RC member. When the FRP is prestressed there is one main critical issue concerning peak shear stress at the end of the FRP. This force cannot be transferred to the RC member without a mechanical anchor due to the limitation of strength in the concrete. Mechanical anchors are commonly used today, but they involve challenges with corrosion and inspection.

To make the process of installing and maintaining the strengthening with FRP more simple, a new method has been developed Haghani and Al-Emrani, 2016. In this method, the need for mechanical anchorage is made redundant. This is done by prestressing the FRP in small steps to avoid the peak shear stress at the end of the FRP. In order to test this new method and comparing it with present methods, full-scale tests were conducted at Chalmers University of Technology prior to this Master Thesis.

1.2 Scope of study

The scope of the master thesis project is to investigate different methods of externally bonded fiber reinforced polymers and the efficiency by comparing prestressed Carbon Fiber Reinforced Polymer (CFRP) to passive CFRP in serviceability limit state of a reinforced concrete member.

1.3 Aim and objectives

The objectives of the master thesis are to conduct a parametric study by Finite Element Method (FEM) and a case study about commonly used techniques for strengthening reinforced concrete beams. The thesis is followed up with a parametric study of reinforced concrete beams, reinforced with externally bonded FRP subjected to different prestressing levels.

- A comparison between present methods on prestressed FRP and the new method.
- Present challenges to deal with in order to fully take advantage of the prestressed FRP and what solutions are available at the market as of now.
- Investigate how the prestressed FRP influence the serviceability limit state of the RC member and how much the crack size can be decreased.

To carry out the parametric study, three main objectives are studied:

1. Modeling of three RC beams under four point bending, see figure 1.1

- Beam 1 is the control beam and not strengthened.
- Beam 2 is externally bonded with CFRP laminate.
- Beam 3 is externally bonded with CFRP laminate prestressed with the new method

2. Analyze the structural behavior and cross-sectional strain/stress of the beams in terms of:

- Flexural stiffness of each beam — load and deflection curve
- The cracking load
- Identify the proper failure mode of each beam and estimate the ultimate load bearing capacity
- The utilization ratio of the CFRP laminate when prestressed — load and strain curve along the span

3. Analyze crack-width in SLS and optimize the prestressing force and design an optimization work flow.

- How does the ductility change with different prestressing force.

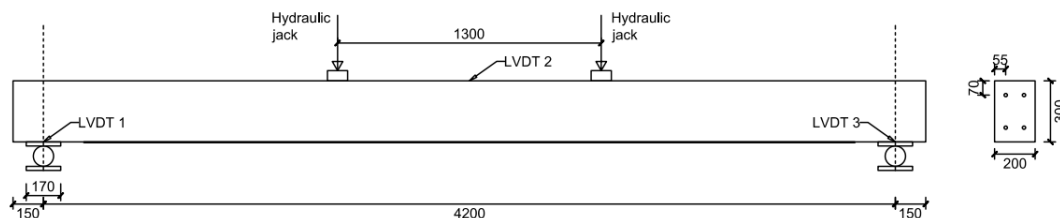


Figure 1.1: Dimensions and layout of RC beam

1.4 Method

To gain knowledge about strengthening of reinforced concrete beams with FRP, a review of the most common methods was the focus to meet the case study aims and gain knowledge about externally bonded, near-surface-mounted, mechanical anchor systems, adhesives and prestressing of FRP.

The parametric study was carried out with help of Finite Element Method (FEM) with the program DIplacement ANALyser (DIANA) to verify against the full-scale tests.

1.5 Limitations

One limitation that leads to insecurity in the verification phase, was that the control beams were already cracked before the introduction of CFRP. This meant that the cracking load in the FE simulations would be a lot higher than in the control beams, both for the reference beam, beam with passive CFRP and beam with prestressed CFRP. Also, the fact that only three tests were conducted is not representative enough. To be able to find the margin of error, more experimental tests should have been performed. Other limitations in this master thesis were:

- Relaxation in the prestressed CFRP, due to tie constraints, is not taken into account.
- The aggregate engagement is not treated.
- Reinforcement is assumed to have a perfect bond with the concrete in all FE simulations.
- Debonding of CFRP in the FE model is neglected.
- Selfweight in the FE model is neglected.

2 Theory

2.1 Fiber reinforced polymer

Fiber reinforced polymer is a composite material consisting of different phases. There can be one or several discontinuous phases embedded in a continuous phase.

The discontinuous phase is the reinforcement consisting of fibers, which are strong and/or stiff and will give the composite its strength. The fibers are embedded in a matrix (continuous phase), which transfers load and protect them. They are bonded together with an either strong or weak interface. Both the reinforcement and the matrix are typically lightweight.

FRP can consist of both organic and inorganic fibers and the most common FRP in structural engineering is glass (GFRP), carbon (CFRP) and aramid (AFRP) together with a bonding thermoset resin epoxy, vinylester or unsaturated polyester. The fiber part is the largest volume part with about 60-70% of the composite. This is due to the fibers being the main stress bearing component while the thermoset resin (matrix or binder) is transferring the stresses between the fibers and protecting them. FRP's strength lies in the load-bearing capacity due to all small fibers working together and they are extremely defect free orientation and microstructure.

Since the matrix (binder) is the stress transferring part of the composite, it will allow a smooth load transfer between broken or damaged fibers and adjacent intact fibers, and also between intact fibers. The matrix system also leads to decreasing local stress concentration and an increase of the unidirectional composite strength. It also protects the fibers mechanical damage and effects from the environment (Zoghi, 2013).

2.1.1 Glass FRP

Glass fibers are the most commonly used fiber to reinforce polymers with and has a wide range of different material properties. The fibers are a composition of silicon oxide and additional oxides that are very surface active and hydrophilic. To improve the fibers behavior, individual fibers are processed with sizing to ensure enough protection against degradation and sufficient embedment within the matrix.

There are different types of glass fibers and they can be divided into groups depending on their chemical compound. The most common glass fiber is the E-glass, which is a low-cost fiber with adequate strength and electrical resistivity. The S-glass fiber is stronger than the E-glass, with higher stiffness and thermal stability. C-glass is used for its resistance against acids and AR-glass is good for its resistance against alkalies, especially from cement.

Even though glass fibers have good mechanical properties, like high tensile strength, good electrical resistivity, and good thermal resistance, generally, they suffer from a lack of protection against water, acids and alkalies. The fibers do not perform well against creep and show a stress rupture behavior under constant stress (Zoghi, 2013).

2.1.2 Carbon FRP

Carbon fibers are made from Polyacrylonitrile (PAN), pitch, or rayon. Low E-modulus fibers are produced with isotropic pitch and rayon. High E-modulus/strength fibers (mostly used in FRP) are produced with PAN or liquid crystalline pitch.

For composites like FRP, carbon fibers are the strongest and stiffest. Carbon fiber also has excellent properties against creep and fatigue, and show great chemical-, UV-light- and moisture resistance, which is why they are durable (Zoghi, 2013). The E-modulus and strength of carbon fibers are not affected by high temperature changes. This combined with all other properties makes them insensitive to the exposed environment around a construction. The carbon fiber is behaving linearly elastic until rupture (Täljsten, Blanksvärd, and Sas, 2016). When producing CFRP, the matrix usually consists of an epoxy. CFRP is much more expensive compared to GFRP (Zoghi, 2013).

For constant long term loading, both GFRP and AFRP show a major decrease in tensile strength compared to CFRP, which shows a very little loss in tensile strength (Nordin, 2005).

2.1.3 Carbon FRP for external bonding

External steel reinforcement, both as prestressed and non-prestressed, has been used for a long time to strengthen concrete structures, but due to the high density of steel and its inability to withstand corrosion, engineers had to find a new material that could fulfill the demands of being light weight, corrosion resistant, strong and stiff, which CFRP is capable of (Nordin, 2003). CFRP is a better option compared to AFRP and GFRP because of its good behavior in long-term loading.

Table 2.1: Material properties of different fibers and steel (Dyresjö and Eskilsson, 2016).

Material	Density [kg/m ³]	Tensile strength [MPa]	Modulus of elasticity [GPa]	Ultimate strain [%]
E/AR-glass	2500-2600	1800-3500	70-75	2.0-3.5
S-glass	2500-2600	3400-4800	85-100	3.5-5.0
Carbon(HS)	1700-1800	3500-5000	200-260	1.2-1.8
Carbon(HM)	1800-2000	2500-4000	350-700	0.4-0.8
Aramid(HM)	1400-1450	2700-4500	115-130	2.5-3.5
PBO	1540-1560	5800	180-270	2.5-3.5
Steel reinforcement	7500	500-600	200	3.5-7.5
Prestressing steel	7500	1680	195	3.5

Table 2.2: Material properties of AFRP, CFRP and GFRP (Zoghi, 2013).

Material	Coefficient of thermal expansion $\frac{10^{-6}}{^{\circ}\text{C}}$		Tensile Strength [MPa]	Modulus of elasticity [GPa]	Ultimate strain [%]
	Longitudinal	Transverse			
AFRP	≈ -2	≈ 30	600-2500	30-125	1.8-4.0
CFRP	≈ 0	≈ 25	600-3000	80-500	0.5-1.8
GFRP	≈ 5	≈ 25	400-1600	30-60	1.2-3.7

2.2 Reinforced concrete beams

2.2.1 Cracks in concrete structures

Cracks in concrete structures appear due to its limited tensile strength when subjected to stress. When examining cracks in concrete structures and evaluating whether or not these cracks are to be considered damage, it is important to know the design method of the structure (Engström, 2014). Cracking of the concrete is to be expected and is calculated for in the design, by limiting the crack width. The calculations are based on simplified models and do not consider much detailing that might occur in the final stage of the design. Therefore it might be hard to distinguish "normal" cracks, that are calculated for, from cracks that might cause unexpected damage to the structure.

When designing a reinforced concrete structure, the important factors to consider are the amount of Reinforcement Bars (Rebars) and to arrange them in a way so that the structure and the applied loads will stay in equilibrium after cracking of the concrete. Cracking is expected but when designing structures that are lightly reinforced, cracking might imply danger as there is a risk of brittle failure. This will happen when the concrete cracks and the tensile force that caused the crack will have to be transferred by the reinforcement instead of the concrete. This sudden reaction will cause some dynamic effect that, in worst case scenario, might lead to sudden rupture of the rebars. There are minimum requirements that need to be fulfilled in order to avoid brittle rupture of lightly reinforced concrete structures in regard to bending as can be seen in equation 2.1 (Engström, 2014).

$$A_{s,min} \geq 0.26 \frac{f_{ctm}}{f_{yk}} b_t d \geq 0.0013 b_t d \quad (2.1)$$

$A_{s,min}$	minimum area of bending reinforcement
f_{ctm}	mean axial tensile strength of concrete
f_{yk}	characteristic yield strength of longitudinal reinforcement
b_t	mean width of the part of the cross-section in tension
d	effective depth of the cross-section

In the case where a concrete structure is prestressed, compressive forces have been added to the structure and crack propagation are delayed. The structure will be subjected to compressive stresses already during manufacture and when the service load is applied these loads will cancel out each other. Full prestressing means that the structure is designed in a way so that the compressive forces from the prestressing are larger than the tensile forces from the service load, and thus the beam will be in compression and cannot crack (Engström, 2014).

2.2.2 Crack criterion's in Concrete

When checking if the concrete structure is cracked or uncracked, four different scenarios exists that needs to be evaluated according to Engström, Al-Emrani, Johansson, and Johansson (2013):

1. Estimate which type of calculation model, uncracked concrete or cracked concrete, to use at a certain load in serviceability limit state.

2. Estimate the risk of cracks in a certain situation in SLS.
 - When cracks are unfavorable, e.g in serviceability.
 - When cracks are favorable, e.g regarding applied stress.
3. Estimate if cracks will develop in a certain situation in SLS, e.g when to expect crack propagation in the concrete.
4. Estimate the risk of cracking in an uncracked state when using full load carrying capacity.

Which value of the tensile strength to use when evaluating these criteria depends on the acting situation, since the tensile strength is uncertain and has a wide range. Mean value f_{ctm} is most commonly used to investigate crack propagation, which means, statistically, that the probability for cracks is 50% (Engström et al., 2013).

In the case when investigating crack propagation in pure bending with an axial compressive force the criteria for the uncracked state is:

$$\sigma_{cn} + \sigma_{cm} \leq f_{ct,fl} \quad (2.2)$$

and where:

$$f_{ct,fl} = k \cdot f_{ctm} \quad (2.3)$$

σ_{cm} is the stress from pure bending and σ_{cn} is the stress from the axial force. K is a height reduction factor according to equation 2.4 (Engström et al., 2013).

$$k = 1.6 - \frac{h}{1000} \geq 1 \quad (2.4)$$

where h is the height of the beam.

Failure criteria for concrete and reinforcement

Since both concrete and reinforcement are showing plastic behavior after reaching maximum stress, there will not be a clear failure point and the failure will, therefore, be determine with the material's ability to deform. The following failure criteria are stated in Eurocode 2 according to Engström et al. (2013):

For concrete:

$$|\epsilon_{cu}| \leq 3.5 \cdot 10^{-3} \quad (2.5)$$

For reinforcement:

$$\epsilon_s \leq \epsilon_{sud} \quad (2.6)$$

where $\epsilon_{sud} = 0.9\epsilon_{suk}$ (national parameter) and ϵ_{suk} is the characteristic reinforcement strain. ϵ_{sud} is the limiting strain in the reinforcement.

2.3 Ductility of strengthened RC beams

Ductility is the ability of a structural member to withstand plastic deformation without decreasing the load carrying capacity (Rezazadeh, Barros, and Costa, 2014). Ductility is, however, a controversial subject, mainly because there is no generic definition of how to express ductility. There are different methods that quantify the ductile behavior of beams, like curvature ductility, displacement ductility, energy ductility, and deformability factors (Kim, Shi, and Green, 2008).

RC beams externally strengthened or retrofitted with FRP ought to be designed in manners to achieve appropriate ductility as suggested by codes or design guides, by making sure that the internal reinforcement yields before failure in the FRP. General parameters that are affecting the ductile behavior of a structure according to Kim et al. (2008) are:

- Reinforcement ratio.
- The geometry of a structure.
- Strengthening schemes.
- Environmental exposure
- Concrete strength
- Confinement
- Rate of loading

The ductility index measured with displacement ductility is the ratio between ultimate mid-span deflection and the deflection corresponding to yielding in the reinforcement.

$$\mu = \frac{U_{ultimate}}{U_{yielding}} \quad (2.7)$$

$$\frac{U_{ultimate}}{U_{yielding}} > C \quad (2.8)$$

Rezazadeh et al. (2014) impose that the ductility index μ , see equation 2.7-2.8, must be greater than C , where C is between 1.25 – 1.5.

When an RC beam is strengthened with prestressed FRP, the load carrying capacity will increase and the deflection will decrease, compared with non-prestressed FRP, both for SLS and Ultimate Limit State (ULS). Rezazadeh et al. (2014) suggest that the ductility index will decrease with increasing prestressing force, which will make the RC beam behave in a more brittle manner, and might compromise its ductility performance. To ensure that the beam will perform in a ductile manner, they suggest adopting an upper limit of the prestressing force (Rezazadeh et al., 2014).

Cement Association of Canada propose another way to measure ductility, by introducing a ductile failure mode for RC members by controlling the ratio between $\frac{c}{d}$. c is the distance between the fibers subjected to the most compression and the neutral axis. d is the effective depth of the tension reinforcement.

The American Concrete Institute (ACI) advise a ductility condition by limiting the net minimum tensile strain in the reinforcement to $t = 0.005$, except for structures with high demands on ductility (Kim et al., 2008).

The Canadian Highway Bridge Design Code (CHBDC) suggest a deformability factor (performance factor), J , that was developed especially for FRP-reinforced structures, based on the moment-curvature relations, see equation 2.9.

$$J = \frac{M_{ult} \varphi_{ult}}{M_{0.001}^c \varphi_{0.001}^c} \quad (2.9)$$

M_{ult} is equal to the moment capacity of the current section, φ_{ult} is the curvature at M_{ult} , $M_{0.001}^c$ is the moment when the maximum concrete compressive strain reaches 0.001 and $\varphi_{0.001}^c$ is the curvature at $M_{0.001}^c$. CHBDC recommends that the performance factor J is 4.0 for rectangular sections and 6.0 for T-sections (Kim et al., 2008).

In this thesis, ductility will be measured accordingly to Fib Bulletin 14 (2001). For concrete class C35/45 or lower the ductility index ξ is calculated $\xi = x/d$, where x is the height of the compression zone at ultimate capacity and d the effective depth of the beam. ξ must be lower than equation 2.10.

$$\xi \leq 0.45 \quad (2.10)$$

Fib Bulletin 14 (2001) also reformulates equation 2.10 with help of ultimate concrete strain $\varepsilon_{cu} = 0.0035$ and $h/d \approx 1.1$ so the following requirement can be stated, in terms of minimum FRP strain at ultimate. ε_0 is the initial strain at the extreme tensile fiber.

$$\varepsilon_{fu,c} \geq 0.0050 - \varepsilon_0 \quad (2.11)$$

Equation 2.11 applies for concrete class C35/45 or lower and where $\varepsilon_{fu,c}$ is the strain in the FRP at the ultimate critical section. In terms of a minimum strain in the internal steel reinforcement at ultimate, equation 2.10 will correspond to:

$$\varepsilon_{su,c} \geq 0.0043 \quad (2.12)$$

where $\varepsilon_{su,c}$ is the strain in the internal steel at ultimate critical section.

2.4 Strengthening of RC beam with FRP

2.4.1 Non-prestressed FRP

FRP plates/sheets have been used as an addition to steel plates when it comes to strengthening of RC beams in the tension bed and they have shown good and effective behavior. They increase the shear- and/or flexural strength as well as reduce crack width and deflection. According to El-Hacha, Wight, and Green (2001), they impose that a 1-2 mm thick FRP plates could provide the same strength equal to a 6 mm thick steel plate.

Strengthening an RC beam with a non-prestressed FRP sheet/plate leads to increased flexural capacity and stiffness, see figure 2.1. The overall performance of the RC beam under service load is slightly improved and the ultimate strength is remarkably increased. The cracking pattern is more evenly spread

over the RC beam and the overall sum of all crack widths is reduced. Non-prestressed FRP has one main disadvantage and that is the anchorage of the FRP onto the RC beam. The FRP laminate may debond if it is mounted in a high shear stress zone or if it is not utilized enough. There are special stirrups and anchorage systems that can prevent this kind of behavior and introduction of a prestressing force in the FRP is a good solution to be able to increase the utilization rate of the FRP.

Since the FRP is showing a brittle behavior, this must be taken into account when designing the FRP reinforcement. The FRP must fail after the internal steel reinforcement yields and before crushing of the concrete (El-Hacha et al., 2001).

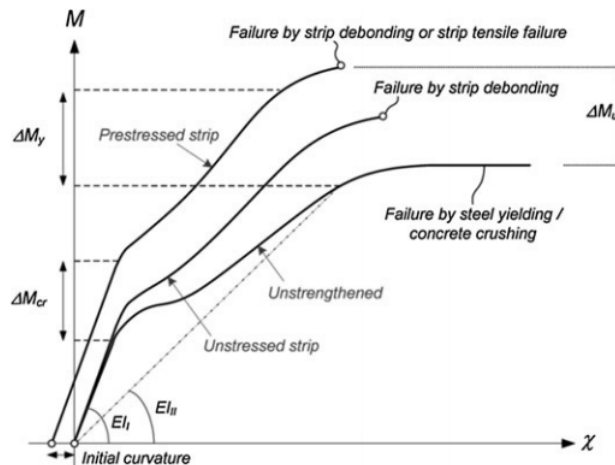


Figure 2.1: Moment and deflection curve of different RC beams (Michels et al., 2016).

2.4.2 Externally bonded prestressed FRP

Non-prestressed FRP only utilizes a small part of the ultimate strength compared with prestressed FRP. Externally bonded prestressed FRP has all the advantages of a non-prestressed system, as well as the advantages of a prestressed system, great durability, and enhancements in serviceability and ultimate capacity, see figure 2.2. With these improvements the load carrying capacity can increase before any further deformations will occur and crack control will be induced, which leads to closing of cracks and delaying the development of new ones. A benefit with crack control is that it will provide better moisture resistance for both the concrete and the adhesive layer. The FRP even prevents the RC beam from premature failure modes.

There are different methods on how to introduce the prestressing force in the FRP laminates and they mostly end up in three different categories. Cambered beam systems, systems that tension the FRP laminate against an independent external reaction frame and systems that tension the FRP laminate against the strengthened beam itself.

Prestressed FRP tends to have high shear stress at the ends of the FRP laminate and the shear stress tends to peel or flake off the concrete cover between the FRP laminate and steel reinforcement, even with low prestressing forces. To avoid this problem some kind of anchorage system needs to be taken into account when designing the FRP reinforcement (El-Hacha et al., 2001).

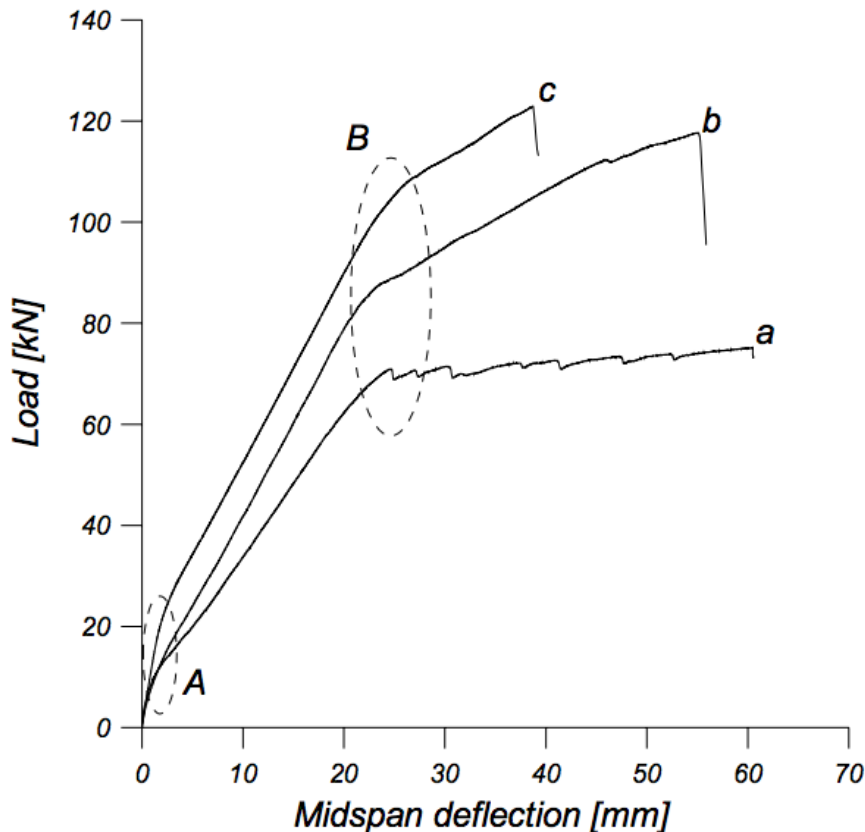


Figure 2.2: A) Cracking and B) yielding. a) Unstrengthened member, b) strengthened with non-prestressed CFRP and c) strengthened with prestressed CFRP (Nordin, 2003).

Cambered beam system

The cambered beam system, see figure 2.3, is indirectly prestressing the FRP laminate with the help of hydraulic jacks, mounted in the mid-span of the RC beam, pushing the beam upwards into a deflected state. The FRP is then mounted onto the beam with the help of epoxy and when it has cured the jacks are removed and a prestressing force is introduced in the FRP laminate. The prestressing force gained with this method is low and it is hard to utilize the full capacity of the FRP. There is also a risk of overstressing the RC beam (El-Hacha et al., 2001).

Tensioning against an independent beam system

Tensioning against an independent beam system, see figure 2.3, is a different method to induce prestressing force into the FRP laminate. The ends of the laminate are connected to steel plates and stretched by a jacking device that is mounted on an external steel frame, acting as a stressing bed, independent of the RC beam. Once the FRP laminate is tensioned, the upper part will be bonded together with the RC beam with epoxy. After curing of the epoxy, the system is released and the prestressing force is transferred into the RC beam gradually.

Laboratory experiments have been carried out with this method and results show that a prestressing force at 50% of the FRP laminate's ultimate strength, increase the flexural strength of the RC member

with 32%. Fatigue testing shows no evidence of damaging the concrete or the FRP laminate. Research also shows that if you increase the prestressing force up to 75% of the ultimate strength, the strength of the RC beam will decrease, due to little strain capacity left in the FRP laminate, which leads to premature rupture.

This method suffers from debonding at the FRP's ends due to high shear stresses, but there is a concept to avoid this problem, except using external anchorage. The epoxy is heated to cure faster, starting in the middle and gradually working towards the ends of the FRP laminates, lowering the prestressing force in the end region. The shear stress in the concrete will also decrease, leading to no need for anchorage (El-Hacha et al., 2001).

Tensioning against the strengthened beam

When tensioning against the strengthened beam, the FRP laminate is fitted with anchors at the laminate ends. The beam is fitted with separate anchors and the FRP is tensioned by pulling the FRP anchors towards the anchors mounted on the beam, see figure 2.3,.

Like in the method with tensioning against an independent beam system, this method suffers from debonding at the FRP ends due to high shear stresses, but with help of staggering the termination points of the laminate, a desirable prestress profile is created and the shear stress in the interface is lowered (El-Hacha et al., 2001).

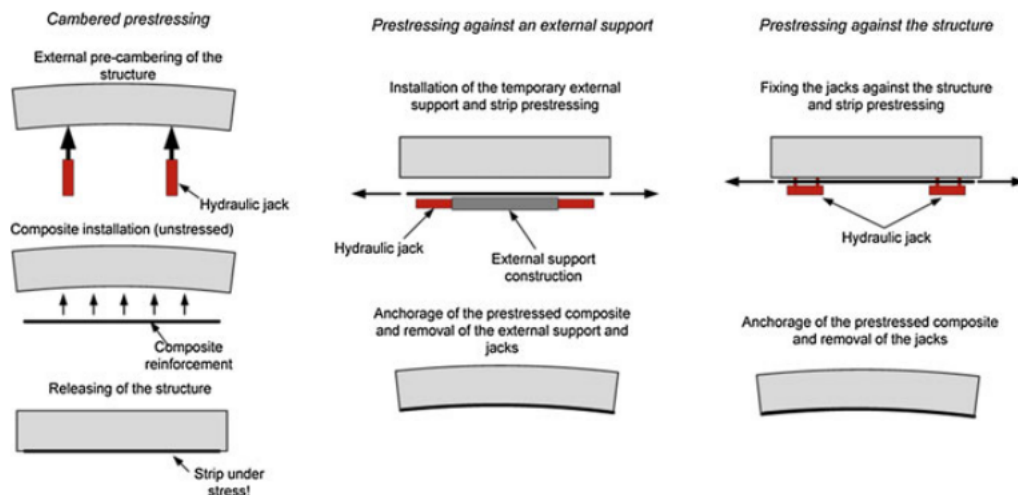


Figure 2.3: Different ways of prestressing FRP laminates (Michels et al., 2016).

2.4.3 Benefits with EB prestressed FRP

The main benefits with external bonded prestressed FRP are:

- Serviceability might be improved and deflections will be reduced.
- Reduces crack widths and delaying development of new cracks.
- Unburden strains from the internal steel reinforcement.
- Introduce compressive stresses which help to resist fatigue failure.
- The internal steel reinforcement will yield at a higher proportion of the ultimate load.
- Efficiency will increase, both for the concrete and FRP.
- Antagonize stresses from dead and live loads.
- The risk of premature failure will decrease.
- Ultimate capacity increases.
- Increase prestressing force in the member if it has been lost, e.g prestressed concrete.
- Increased shear capacity.

2.4.4 Challenges with prestressed externally bonded CFRP

Externally bonded CFRP comes with challenges that must be taken into account when designing the reinforcement system for the RC member. The design of the beam will decide what failure mode will be the governing one, and this can be chosen by making adjustments in the design. Hong and Park (2013) states that the prestressing level of the CFRP will tell what type of failure mode to expect. Prestressing levels below 60% will lead to debonding of the CFRP plate, starting from mid-span, before rupturing of the CFRP. They also propose that with prestressing levels above 40% the ductility of the member will not be fulfilled and thereby the failure will be brittle. In figure 2.4, different failure modes depending on the prestressing level can be seen, both for prestressed and non-prestressed CFRP plate.

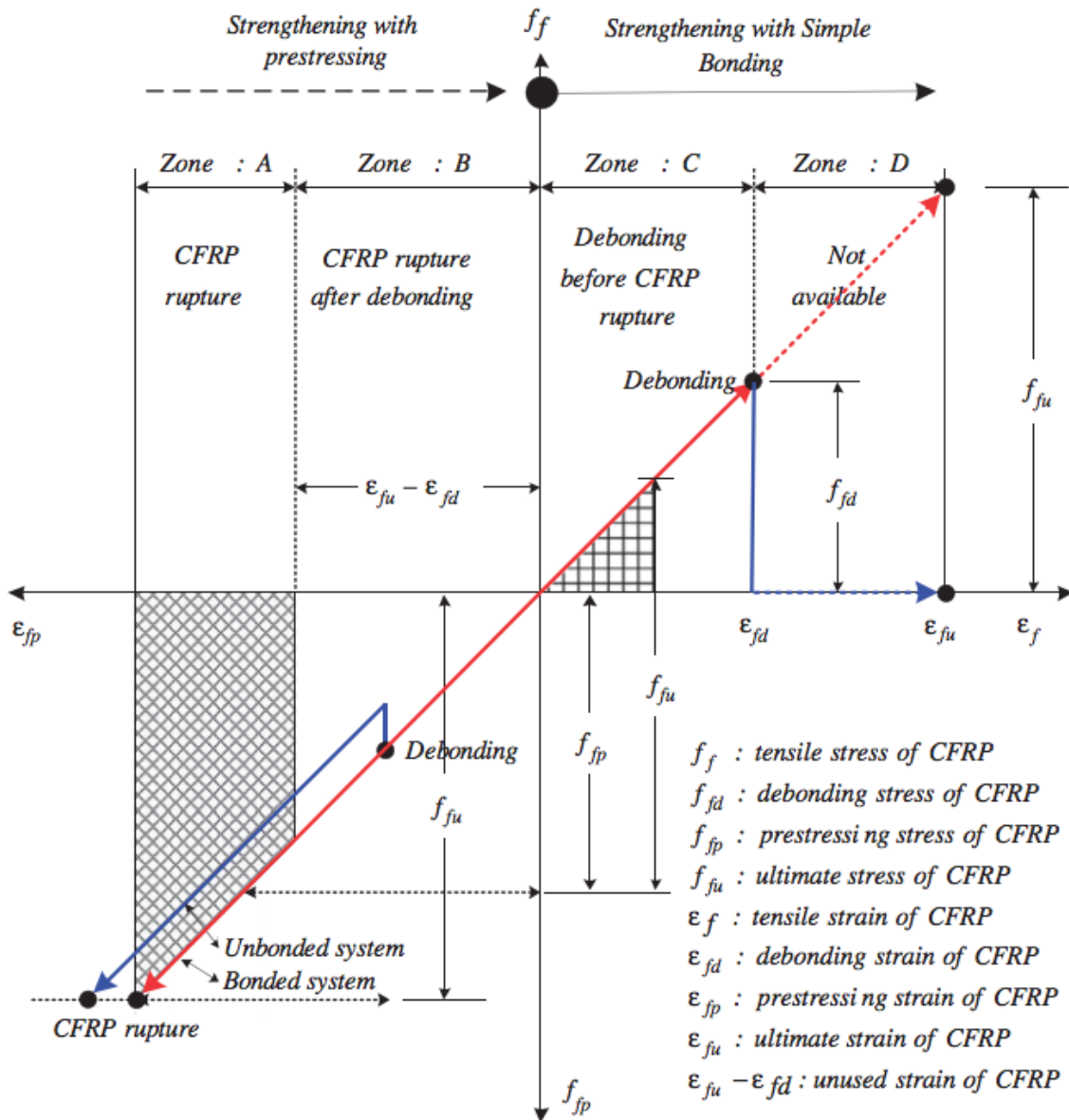


Figure 2.4: Relationship between level of prestress and debonding failure mechanism for CFRP plate (Hong and Park, 2013).

To utilize the full potential of the prestressed CFRP, the plate must be properly anchored with either a mechanical anchorage system or a gradient system (Hong and Park, 2013). When designing a mechanical system, challenges like stress concentration in the CFRP, adhesive and concrete need to be taken into account to prevent premature failure. Other aspects that need to be considered are the risk for corrosion and the maintenance of the anchors (Dyresjö and Eskilsson, 2016). Gradient systems have other challenges compared to mechanical, especially regarding premature debonding of the adhesive/concrete and the level of prestressing force.

2.4.5 Near-surface mounted FRP

Near-surface mounted FRP reinforcement is a strengthening method that possesses some advantages over externally bonded FRP. Where externally bonded FRP is installed on the surface of existing RC structures, the near-surface mounted FRP is installed into grooves which are cut out of the existing RC structure. Since the FRP is embedded in the structure, it is protected against outer influences such as impact and is, therefore, a good alternative when strengthening RC structures over supports, where the top side is in tension.

To transport the stresses between the RC structure and the FRP reinforcement, the grooves are filled with epoxy or some type of other appropriate groove-filler e.g. cement paste. The most important properties of these are the tensile and shear strength.

Another benefit that simplifies the installation of near-surface mounted FRP reinforcement over supports, where the grooves are on the top side (negative moment), is the possibility to use a low viscosity epoxy and pour it in the groove. This cannot be used on the soffit (positive moment) and therefore an epoxy with high viscosity must be chosen. The shape and type of the FRP element will affect a lot of parameters and should be chosen accordingly. By choosing a thin FRP strip the contact area with the adhesive will be larger, lowering the risk of debonding. A thin FRP strip needs a thicker adhesive cover. A square bar will maximize the sectional area and a round bar will be easier to find at a manufacturer and easier to use if the FRP is prestressed. Which type of shape to choose will be defined by existing constraints, concrete cover depth, availability and cost (Lorenzis and Teng, 2007).

2.4.6 Optimization of the prestressed externally bonded CFRP

The theoretically most optimal case will be when the concrete beam crushes on the top side at the same time as the CFRP laminate ruptures. In this case, the utilization of the RC beam and the CFRP laminate is utilized to its fullest. However, the beam must fulfill other requirements such as sufficient yielding of the reinforcement steel, ductility demands and crack widths.

2.5 Failure modes of FRP

When reinforcing concrete with an externally bonded CFRP laminate there are five possible failure modes (Täljsten et al., 2016), which can be seen in Figure 2.5

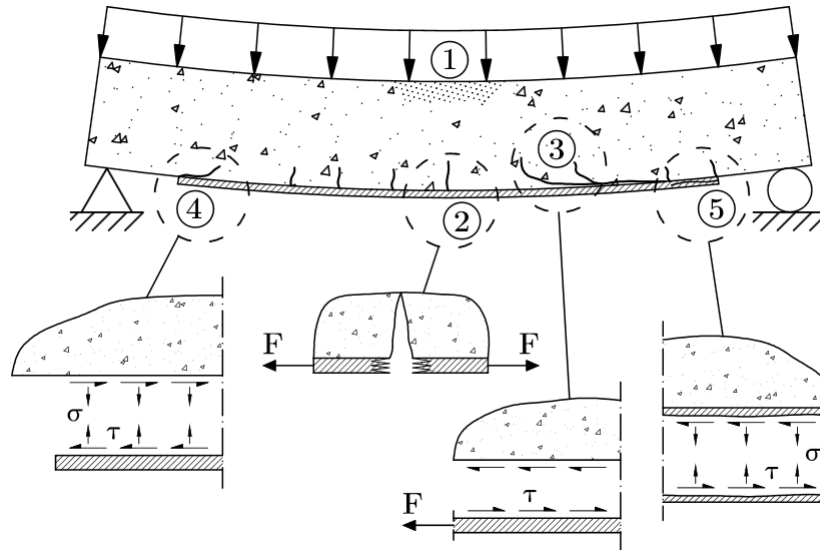


Figure 2.5: Failure modes in concrete with externally bonded CFRP. 1) Crushing of concrete. 2) Rupture of CFRP laminate. 3) Adhesion debonding. 4) End plate debonding. 5) FRP delamination. (Täljsten, Blanksvärd, and Sas, 2016).

There are several ways in which debonding between the concrete and the CFRP laminate can occur. Either by adhesive debonding, end plate debonding or CFRP delamination.

The crushing of concrete will happen when the beam is over-reinforced and the ultimate load of concrete is reached before the reinforcement starts to yield. By designing the beam in a way that allows for the reinforcement to yield before crushing of the concrete the behavior of the beam will be more ductile and less brittle.

Rupture of the CFRP laminate happens when the ultimate tensile force is reached. In the case where the CFRP ruptures the failure will be brittle as CFRP show little to none plastic behaviour. When rupture occurs the material is utilized to its fullest, although the brittle failure of the CFRP is not desirable since there will be no warning in the structure.

Debonding failure consists of different modes. If the adhesive is correctly applied the weakest link will always be the concrete, therefore the most common failure is concrete cover separation as can be seen in figure 2.6.

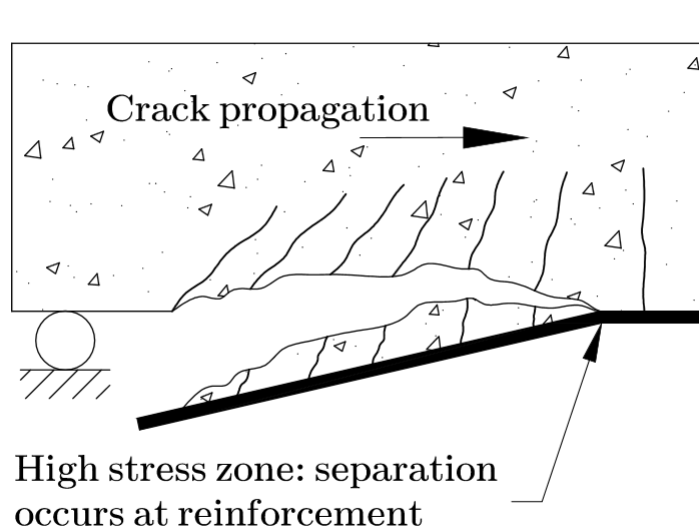


Figure 2.6: Concrete cover separation. (Täljsten, Blanksvärd, and Sas, 2016).

2.6 Tenroc method

The Tenroc method is a new prestressing technique developed by Haghani and Al-Emrani (2016) at Chalmers University of Technology. The authors show that if you calculate the shear stress magnitude along the FRP laminate, there is a direct relationship with the rate at which the axial force is increasing inside the laminate. This means that the shear stress is directly proportional to the first derivative of the axial force in the laminate, as seen in equation 2.13.

$$\tau(x) = \beta \frac{d(F)}{dx} \quad (2.13)$$

Where τ is the shear stress, F is the axial force in the FRP laminate and β is a function of the material and its geometrical properties. To control the magnitude of the shear stress, equation 2.13 can be multiplied with the prestressing force along the anchorage length.

Compared to the method using heat curing of the epoxy to gradually decrease the axial force in the laminate, this method proposes that you introduce the prestressing force in a stepwise manner. The authors propose that this transfer mechanism would reduce the shear force to a level that can be tolerated and leads to no need for any mechanical anchorage system.

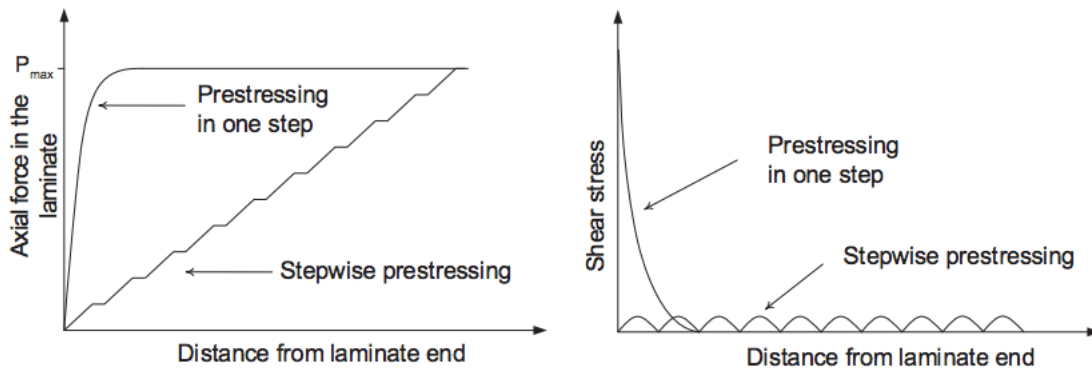


Figure 2.7: Theoretical introduction of the axial force and corresponding shear force in the laminate (Haghani and Al-Emrani, 2016).

The Tenroc method works by dividing the length of strengthening into different prestressing steps. In each step, the axial force will be held constant, but the magnitude difference between the different steps as low as possible. This will lead to breaks, between each step, in the shear force curve and the shear force will be distributed over a certain length of the laminate. Haghani and Al-Emrani (2016) states that both numerical and experimental studies prove that it is possible to decrease the stress in the interface to levels below 1 and 0.2 MPa, for a prestressing force with the magnitude of 100 kN, by dividing it into 10 steps. In order to divide the anchorage length into 10 steps, a device was developed which consist of a number of discrete points, attached to the FRP laminate. They are connected to each other with a series of different springs with different stiffness, see figure 2.8.

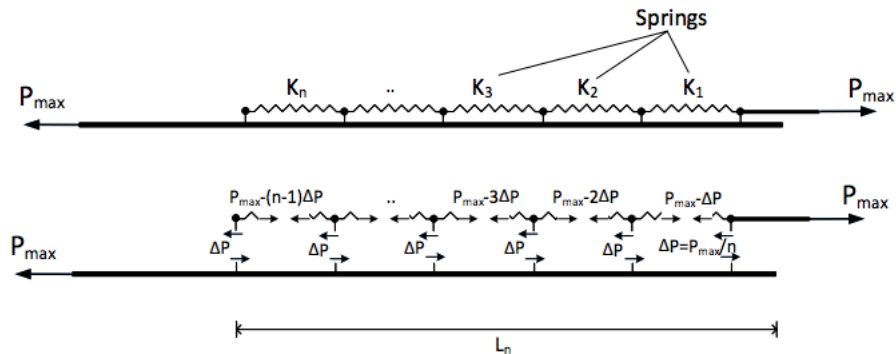


Figure 2.8: Principle of distributing the prestressing force over the FRP laminate using a spring system (Haghani and Al-Emrani, 2016).

The spring system is designed in a way that, between each discrete point, a fixed part of the difference in prestressing force, ΔP , of the total prestressing force, P_{max} , delivers a certain stress in the laminate. The device consists of 10 tabs connected to each other, using metallic rods as springs. The metallic rod's stiffness is designed to deliver 10% of the total prestressing force to each tab. The strengthening laminate is CFRP and it is connected to the device with help of a GFRP plate, which is bolted to the device. See figure 2.9 for the full setup.

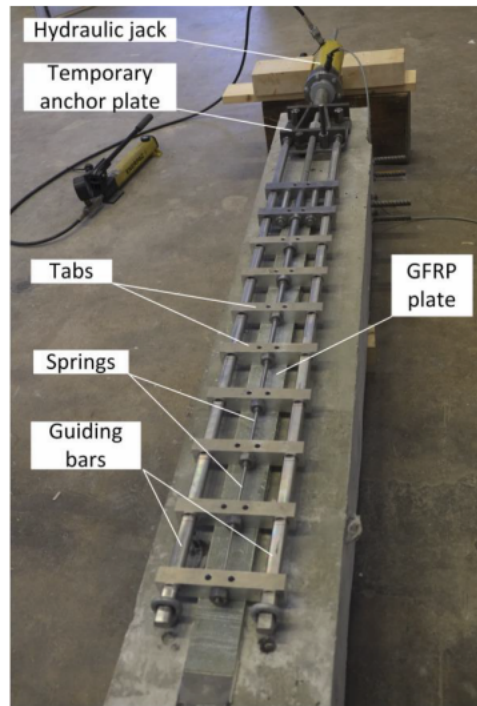


Figure 2.9: The prestressing device and set up during prestressing (Haghani and Al-Emrani, 2016).

This new method to introduce prestressing force show benefits compared to traditional methods. These benefits are the elimination of anchorage system, ease of application and less time consumption, better durability and no risk of galvanic corrosion, better inspectability, and lower cost. The experimental work described by the authors succeeded to use a prestressing force of 110 kN (43% of ultimate strength of the CFRP) and they demonstrated that the technique works without the use of mechanical anchors. The study also states that only a minor loss, 1%, of the total prestressing force was found after full curing of the adhesive (Haghani and Al-Emrani, 2016).

Table 2.3: Pros and cons, Tenroc method vs Traditional methods

	Tenroc method	Traditional methods
Shear force at laminate end	Low	High without anchorage
Need of anchorage	No	Yes, due to high shear force
Need of inspections	No	Yes, if there is an anchorage system
Ease of application	Yes	Depends on chosen system
Time consumption	Low	Moderate
Cost	Low	Moderate
Durability	Good	Moderate
Debonding risk	Low	Low, with an anchorage system
Risk of corrosion	No	Yes, if there is an anchorage system

3 Full-scale tests of strengthened beams

During the autumn of 2016 experimental tests were conducted at Chalmers University of Technology with the aim of verifying the feasibility of the Tenroc method. Three identical RC beams were tested under four point bending, see figure 3.1. One control beam, one beam with passive externally bonded CFRP and one beam with prestressed externally bonded CFRP. The dimension of the beams that were tested was 4500 mm x 200 mm x 300 mm (L,W,H) and they had two steel reinforcement bars with a diameter $\phi 16$ in both the tension and compression side. $\phi 10$ stirrups were located along the beam with a spacing of 75 mm. Accordingly, to the beam manufacture, the concrete class was C30/37 and the characteristic yield strength of the reinforcement was 500 MPa (Yang, Haghani, and Al-Emrani, 2017).

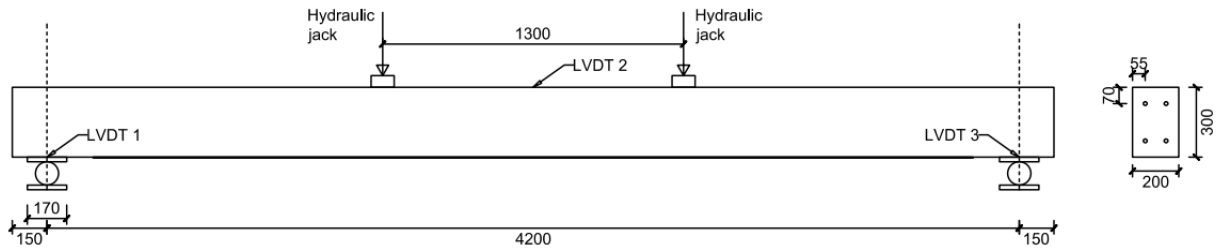


Figure 3.1: Test setup and layout (Yang, Haghani, and Al-Emrani, 2017).

The CFRP laminate that was used for both the beam with prestressed and passive CFRP was 3800 mm x 80 mm x 1.4 mm and had an average elastic modulus of 210 GPa and an average tensile strength of 3300 MPa, accordingly to the manufacture. More information about the material properties for the CFRP can be seen in Appendix B. The prestressing force in the experiment was equivalent to 22% of the CFRP ultimate tensile strength, corresponding to a force of 80 kN.

The beams were loaded with a displacement-control of 1 mm/minute. To capture all necessary data, strain gauges and Linear Variable Differential Transducers (LVDT) were installed (Yang et al., 2017).

3.1 Results of full-scale tests

Strains were measured during the prestressing phase and the descending axial force in the laminate ends was captured. The result provides a gradual decrease of strains in the laminate ends, which corresponds to a gradual decrease of the axial force as expected. The test result shows an increase in ultimate load bearing capacity which can be seen in figure 3.2.

The failure mode for the CFRP reinforced beams was debonding for the beam with passive CFRP and rupture of the laminate for the beam with prestressed CFRP. The debonding happened at a strain corresponding to $\epsilon_{CFRP} = 4.97$ micro strain and rupture took place at a maximum strain of $\epsilon_{CFRP} = 10.29$ micro strain.

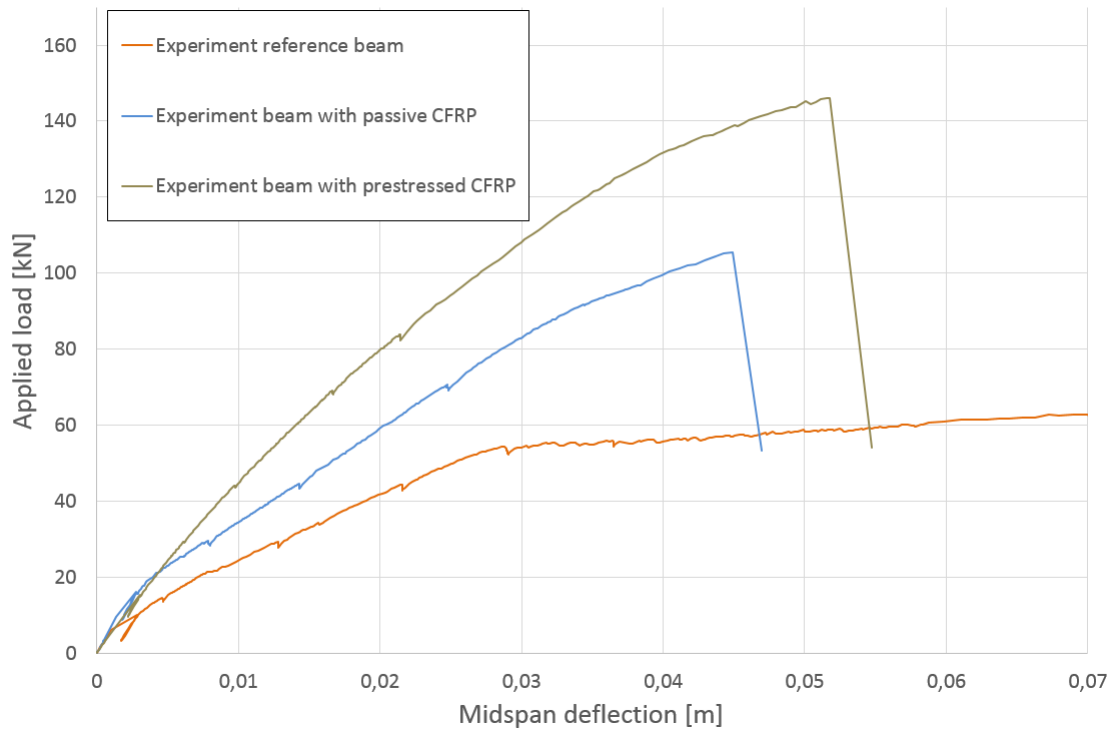


Figure 3.2: Load-deflection curve (Yang, Haghani, and Al-Emrani, 2017).

3.2 Results from lab tests

Reinforcement, CFRP, and concrete samples have been tested in the laboratory at Chalmers University of Technology to collect appropriate data to use in the FE model. All concrete samples showed that the compressive strength was higher than C30/37 that was specified from the supplier. C30/37 is the concrete class used in all FE simulations. CFRP samples showed that the ultimate strain was between 10-15 micro strain, but the most reliable result showed 14 micro strain. See Appendices C-E for the full analysis of the tests.

Table 3.1: Lab test results

Specimen	E-modulus [GPa]	Yield Stress [MPa]	Ultimate strain [micro strain]	Concrete class
Reinforcement	210	560	-	-
CFRP	230	3520	14	-
Concrete Cube 1	-	-	-	C35/45
Concrete Cube 2	-	-	-	C45/55

4 Finite element modelling

In this master thesis the finite element method program DIANA were used to conduct Finite Element Analysis (FEA) of RC members strengthened with externally bonded CFRP in passive and active manner.

4.1 FE model

The models created in DIANA were 2D-models with regular plane stress elements. The models were created using DIANA Interactive Environment (DIE) and consisted of: a concrete beam, a CFRP strip, epoxy, a loading print, a support plate, two rebars and stirrups at certain intervals. The model can be seen in Figure 4.1.

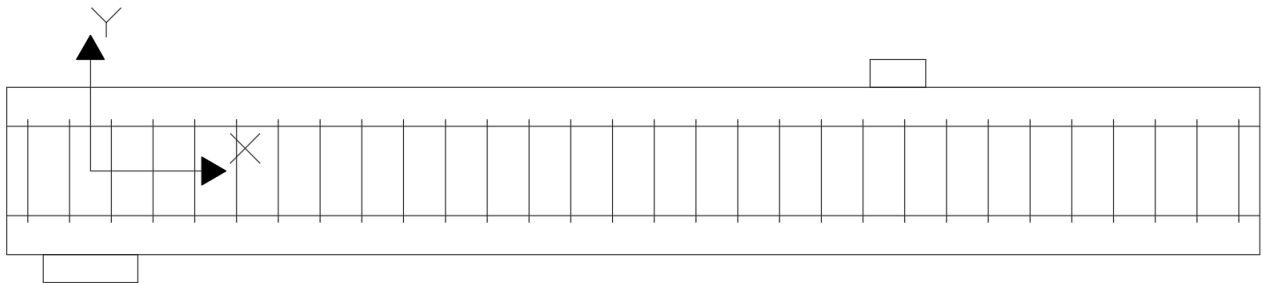


Figure 4.1: FE-Model of a strengthened beam in DIANA/FEA consisting of: Concrete beam, Support plate, Load print, CFRP, Epoxy, Rebars, and Stirrups.

Nominal dimensions taken from the test specimens that were used in the models can be seen in table 4.1 and 4.2.

Table 4.1: Parts parameters of the reference beam

Part	Length [mm]	Depth [mm]	Height [mm]	Diameter [mm]	Spacing [mm]
Concrete beam	2250	100	300	-	-
Rebar	2250	-	-	15.3	-
Stirrup	-	-	-	10	75

Due to symmetry only half of the beam was modeled, instead of using the full length of 4.5 m and full width of 0.2 m the model has a length of 2.25 m and a width of 0.1 m. The amount of reinforcement steel used in the model were also changed in order to match this. Since the model is in 2D, the exact profile of

Table 4.2: Parts parameters of the beams strengthened with passive and prestressed CFRP laminates

Part	Length [mm]	Depth [mm]	Height [mm]	Diameter [mm]	Spacing [mm]
Concrete beam	4500	200	300	-	-
Rebar	4500	-	-	15.3	-
Stirrup	-	-	-	10	75
Epoxy	3800	80	1.4	-	-
CFRP	3800	80	1.4	-	-

the beam cannot be taken into consideration. In the model, the beam is modeled with half the width and use the cross-section area of one rebar and one stirrup. If the full width were to be used the cross-section area would have to be doubled since there are two reinforcement bars at the same height in the beam.

4.1.1 Boundary conditions

To mimic the conditions in the experimental tests boundary conditions were implemented. The tests were conducted as four point bending where the concrete beam is supported on both side and the load is applied at two points at equal length from the supports. As can be seen in Figure 4.2 the boundary conditions which were used in the model were restricted against translation in the Y-direction at the bottom center node of the support plate. In order to model the effect taken from symmetry the center of the beam, in this case, the right side of the model, were restricted from translation in the X-direction and restricted from rotation around the Y- and Z-axis.

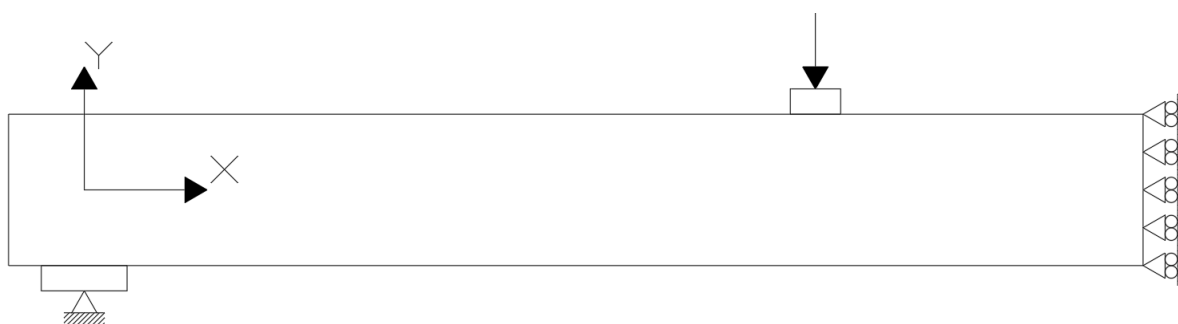


Figure 4.2: Boundary conditions used in the model.

4.1.2 Element types and mesh

The main element type used in the model was CQ16M, see figure 4.3, which is an eight-node quadrilateral isoparametric plane stress element that uses Gauss integration and quadratic interpolation according to DIANA FEA (2015). Displacements are described according to equation 4.1.

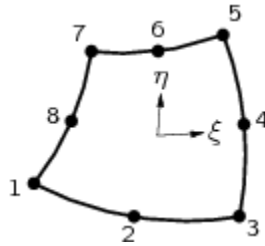


Figure 4.3: The element type "CQ16M" used in DIANA (DIANA FEA, 2015).

$$u_i(\xi, \eta) = a_0 + a_1\xi + a_2\eta + a_3\xi\eta + a_4\xi^2 + a_5\eta^2 + a_6\xi^2\eta + a_7\xi\eta^2 \quad (4.1)$$

The secondary element type used in the model were CT12M, see figure 4.4, which is a six-node triangular isoparametric plane stress element that uses Area integration and quadratic interpolation according to DIANA FEA (2015). The displacements can be described according to equation 4.2. Main difference between these two element types is number of nodes and how DIANA solves the displacement equation.

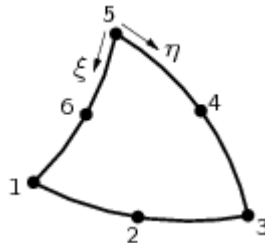


Figure 4.4: The element type "CT12M" used in DIANA (DIANA FEA, 2015).

$$u_i(\xi, \eta) = a_0 + a_1\xi + a_2\eta + a_3\xi\eta + a_4\xi^2 + a_5\eta^2 \quad (4.2)$$

Both the CQ16M and CT12M is used for the concrete in the FE models, see figure 4.5-4.6. This is due to irregularities in the geometry. The support is 0.170 m long and element size is 0.025 m and this will make DIANA, in best possible way, try to mesh the model. DIANA creates four CT12M elements in the model to compensate for this irregularity to result in the best possible mesh along the CFRP laminate and concrete.

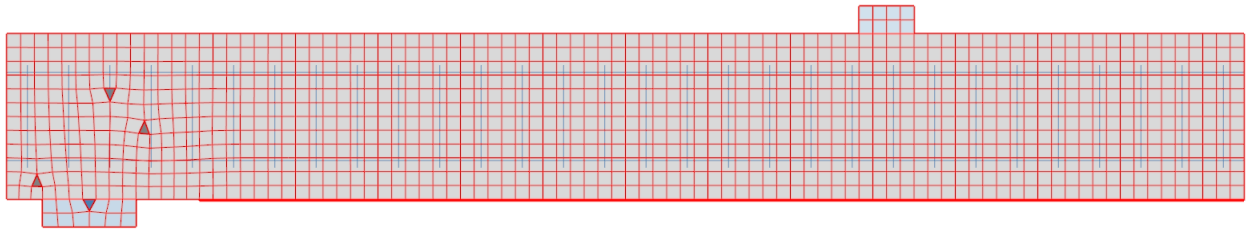


Figure 4.5: Mesh of the model in DIANA where the element type "CQ16M" is highlighted.

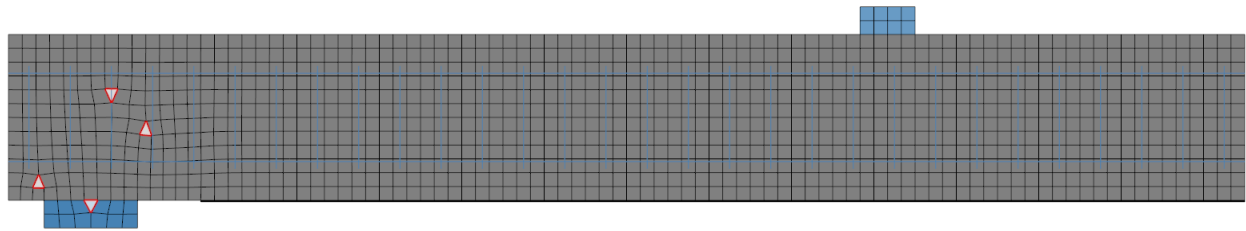


Figure 4.6: Mesh of the model in DIANA where the element type "CT12M" is highlighted in red.

4.1.3 Convergence study

To be able to run the solver with reasonable accuracy, a convergence study of the mesh were conducted for the beam with passive CFRP laminate. Load and displacement were measured with different mesh sizes, which can be found in table 4.3. The result of the convergence study can be seen in figure 4.7. The mesh size of 0.025 m was chosen as it generated good results from the solver as well as keeping the run time at a reasonable length.

Mesh size [m]
0.025
0.030
0.040
0.050
0.100

Table 4.3: Different mesh sizes for the convergence study

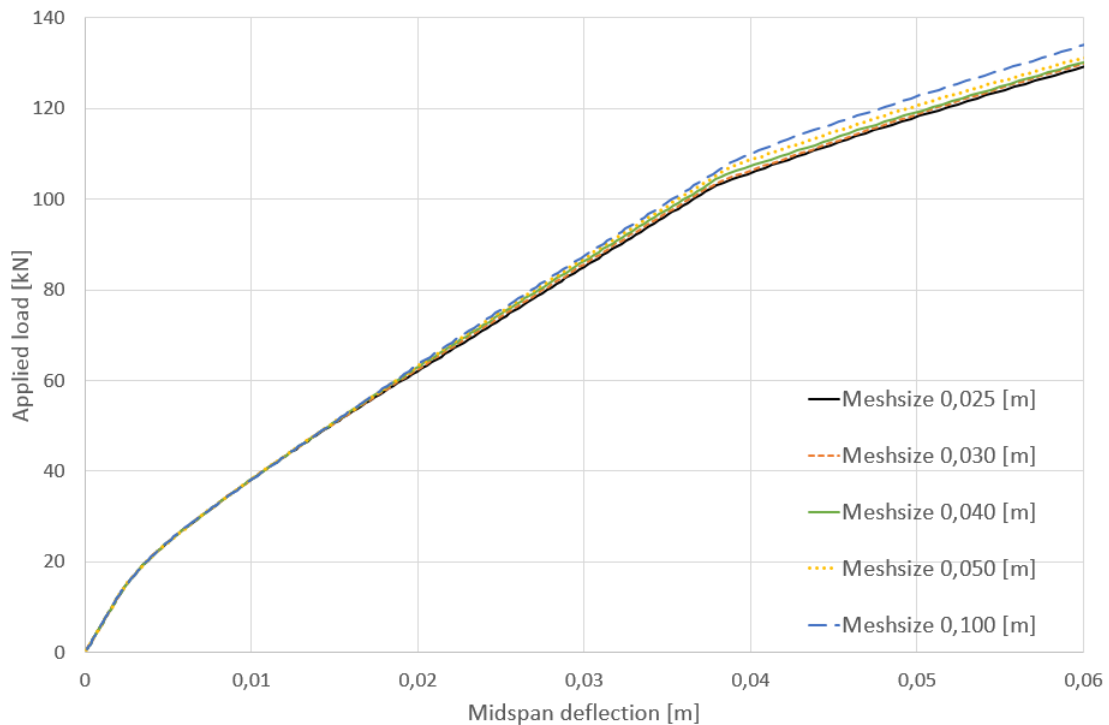


Figure 4.7: Result of the convergence study

4.1.4 Interface between materials

A tie constraint was used to model the interaction between the different materials. The assumption that all material had a perfect bond to one another were made.

4.2 Material indata

4.2.1 Concrete

To derive appropriate input data for concrete C30/37 these equations from ACI (1999) has been used:

Mean cube compressive strength

$$f_{cm} = 38 \text{ MPa} \quad (4.3)$$

Tensile strength

$$f_t = 0.33 \cdot \sqrt{f_{cm}} \quad (4.4)$$

E-modulus

$$E = 4700 \cdot \sqrt{f_{cm}} \quad (4.5)$$

Fracture energy

$$G_f = 73 \cdot \sqrt{f_t} \quad (4.6)$$

Poisson's ratio

$$\nu = 0.2 \quad (4.7)$$

4.2.2 Reinforcement

Reinforcement indata used in the FE model, according to section 3.2. Strain hardening is included and is illustrated in figure 4.8. Values can be found in Appendix C.

E-modulus

$$E = 210 \text{ GPa} \quad (4.8)$$

Yield strength

$$f_y = 560 \text{ MPa} \quad (4.9)$$

Poisson's ratio

$$\nu = 0.3 \quad (4.10)$$

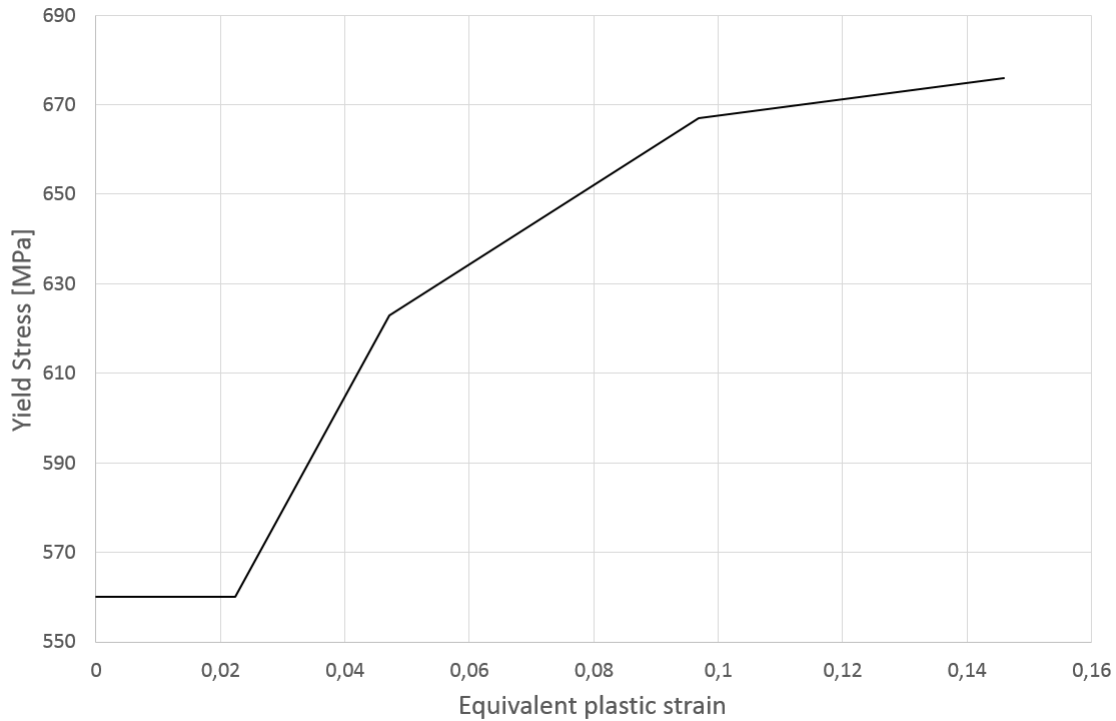


Figure 4.8: Strain hardening

4.2.3 CFRP

CFRP indata used in the FE model, according to section 3.2. The CFRP is modeled as perfectly linear elastic until failure.

E-modulus

$$E = 230GPa \quad (4.11)$$

Ultimate strength

$$f_u = 3520MPa \quad (4.12)$$

Poisson's ratio

$$\nu = 0.3 \quad (4.13)$$

4.2.4 Epoxy adhesive

The epoxy adhesive is assumed to be a perfectly linear elastic material. E-modulus accordingly to Fib Bulletin 14 (2001) is 0.5-20 GPa and is chosen to be 10 GPa.

E-modulus

$$E = 10GPa \quad (4.14)$$

Poisson's ratio

$$\nu = 0.3 \quad (4.15)$$

4.3 Compressive Behavior

Concrete which is exposed to compressive stresses will show a pressure-dependent behavior, i.e. the concrete strength and ductility will increase with increasing stress. Lateral confinement is an aspect that needs to be taken into account. It is assumed that the compressive behavior is influenced by lateral cracking. To model these effects, the parameters of the compressive stress-strain curve, f_{cf} and ϵ_p , are determined with help of a failure function, which gives the compressive stress which causes failure as a function of the confining stresses in the lateral direction.

If the concrete is cracked in the lateral direction, the peak strain is reduced with a factor $\beta_{\epsilon_{cr}}$ and the peak stress with a factor $\beta_{\sigma_{cr}}$. In summary, the peak stress and the peak strain can be expressed as: (DIANA FEA, 2015)

$$f_p = \beta_{\sigma_{cr}} \cdot f_{cf} \quad (4.16)$$

$$\alpha_p = \beta_{\epsilon_{cr}} \cdot \epsilon_p \quad (4.17)$$

In this master thesis, these base equations are modeled with the curve, see figure 4.9, according to Thorenfeldt (DIANA FEA, 2015):

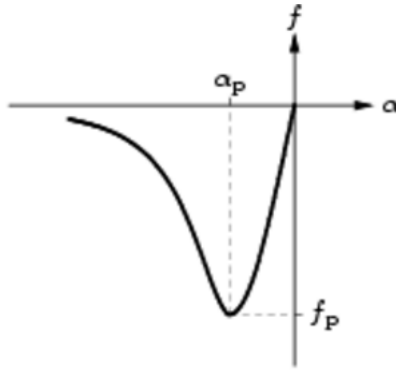


Figure 4.9: Thorenfeldt compression curve (DIANA FEA, 2015).

$$f = -f_p \frac{\alpha}{\alpha_p} \left(\frac{n}{n - \left(1 - \left(\frac{\alpha}{\alpha_p} \right)^{nk} \right)} \right) \quad (4.18)$$

where:

$$n = 0.80 + \frac{f_{cc}}{17}; k = \begin{cases} 1 & \text{if } \alpha_p < \alpha < 0 \\ 0.67 + \frac{f_{cc}}{62} & \text{if } \alpha \leq \alpha_p \end{cases} \quad (4.19)$$

and

$$\beta_{\sigma_{cr}} = \beta_{\epsilon_{cr}} = 1 \quad (4.20)$$

$$\alpha = \varepsilon_p = \text{Concrete strain} \quad (4.21)$$

$$f_{cc} = f_{cf} = \text{Concrete compressive strength} \quad (4.22)$$

The Thorenfeldt curve is related to the size of the concrete specimen and to take this relationship into account the softening part of the curve needs to be multiplied with a value of $\frac{300}{\text{Concrete element size}}$ from the FE model. The reason for this is an assumption that compressive failure in the concrete can take place in one element row, instead of between several element rows in the FE model (Petre and Zapalowicz, 2012).

4.4 Nonlinear tension softening

In the DIANA manual Hordijk, Cornelissen and Reinhardt propose an expression for the softening behavior of concrete, which results in a crack stress equal to zero at crack width $\Delta u_{n,ult}$. This is illustrated in figure 4.10.

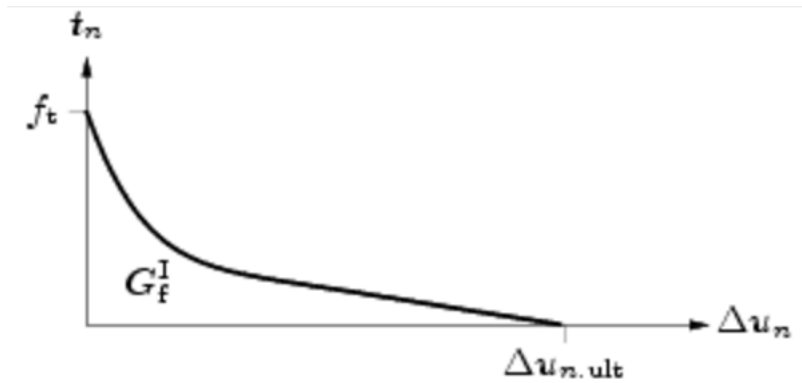


Figure 4.10: Nonlinear tension softening (DIANA FEA, 2015).

The equation is defined by:

$$\frac{f_n(\Delta u_n)}{f_t} = \begin{cases} (1 + (c_1 \frac{\Delta u_n}{\Delta u_{n,ult}})^3) \exp(-c_2 \frac{\Delta u_n}{\Delta u_{n,ult}}) \dots & \text{if } 0 < \Delta u_n < \Delta u_{n,ult} \\ -\frac{\Delta u_n}{\Delta u_{n,ult}} (1 + c_1^3) \exp(-c_2) & \text{if } \Delta u_{n,ult} < \Delta u_n < \infty \\ 0 & \text{if } \Delta u_n < \Delta u_{n,ult} < \infty \end{cases} \quad (4.23)$$

And with the parameters $c_1 = 3$ and $c_2 = 6.93$ and with the ultimate crack strain defined by:

$$\Delta u_{n,ult} = 5.56 \frac{G_F^I}{f_t} \quad (4.24)$$

and

$$\Delta u_n = \text{Crack width} \quad (4.25)$$

$$G_F^I = \text{Fracture energy} \quad (4.26)$$

$$f_t = \text{Concrete tensile strength} \quad (4.27)$$

$$f_n(\Delta u_n) = \text{Corresponding tensile strength at certain crack width} \quad (4.28)$$

4.4.1 Influence of lateral cracking

In DIANA it is possible to take the influence of lateral cracking, cracks in x-direction in the FE model, into account. Cracked concrete with large tensile strains perpendicular to the principal compressive direction reduces the concrete compressive strength. In this thesis, it is described by the model from Vecchio and Collins (DIANA FEA, 2015), which is illustrated in figure 4.11.

$$\beta_{\sigma_{cr}} = \frac{1}{1 + K_c} \leq 1 \quad (4.29)$$

where

$$K_c = 0.27 \left(-\frac{\alpha_{lat}}{\varepsilon_0} - 0.37 \right) \quad (4.30)$$

and

$$\beta_{\varepsilon_{cr}} = 1 \quad (4.31)$$

$$\alpha_{lat} = \text{Average lateral damage} \quad (4.32)$$

$$\varepsilon_0 = \text{Concrete strain at uncracked section} \quad (4.33)$$

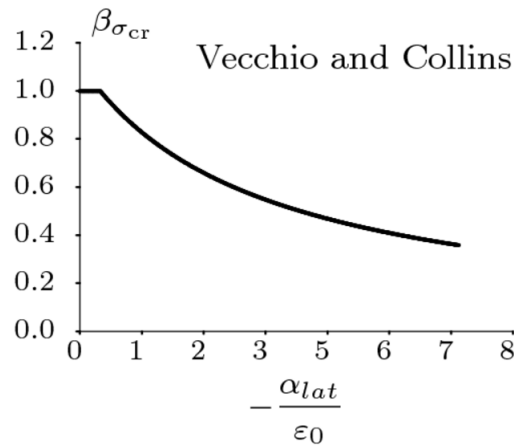


Figure 4.11: Vecchio and Collins reduction factor due to lateral cracking (DIANA FEA, 2015).

4.4.2 Crack bandwidth

Crack bandwidth is assumed to be equal to 0.004 m, due to convergence problems in the FE model.

As default in DIANA, crack bandwidth is calculated as $h = \sqrt{2 \cdot A}$, where h is crack bandwidth and A is total area of an element, for a linear two-dimensional element (DIANA FEA, 2015).

5 Results

5.1 Verification of the FE model

When the FE models and all verification simulations were completed some discrepancies between simulations and FE results were found. The FE models in all three cases, the reference beam and the strengthened beam with active and passive CFRP, had higher cracking load compared to the reality and this can be explained by the fact that the concrete already was cracked from the beginning. The reference beam and the beam with passive CFRP due to transportation and shrinkage and the beam with prestressed CFRP, because it was loaded til some level between cracking load and yielding load before the CFRP was applied. In figure 5.1 the result from the FE-simulations is plotted versus the experimental tests.

The FE model is behaving in a perfect manner, e.g. the FE model does not have any imperfections. The concrete, in reality, is not perfect in itself and this lead to some values that needed to be derived may not match. Cracking load is highly affected by the tensile strength which is really hard to classify and in some way needs to be empirically evaluated.

To perform the parametric study, the E-modulus of the concrete had to be modified from the proposed E-modulus calculated accordingly to equation 4.5, to E-modulus = $15GPa$. This is done to be able to remove the effects of the concrete in the model. CFRP and reinforcement input data is used from obtained lab tests instead of proposed input data from the manufacturer.

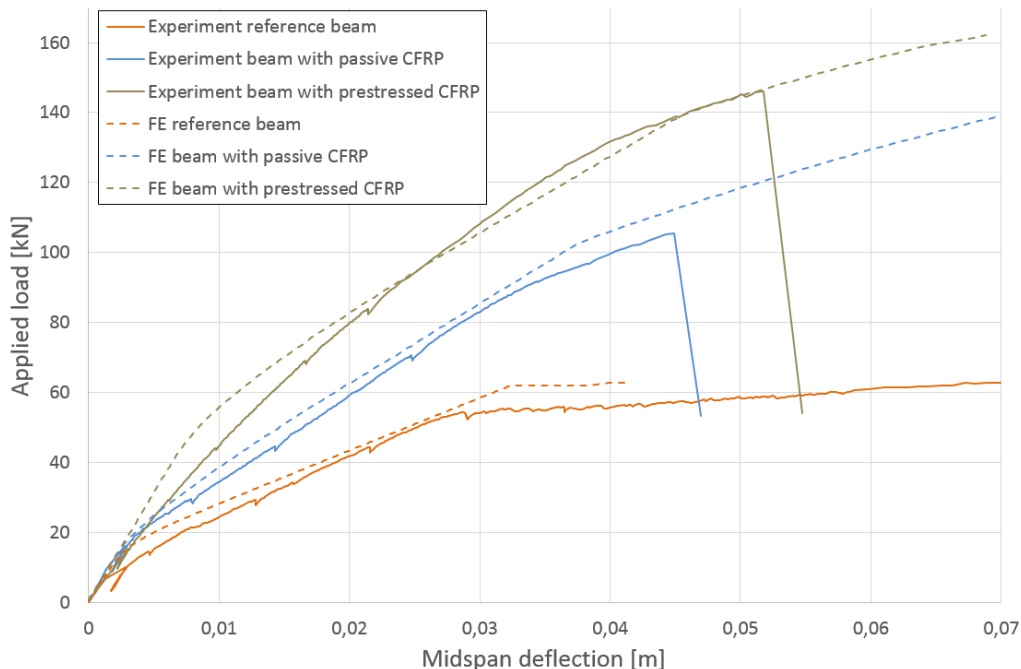


Figure 5.1: Load and deflection curve, FE vs real beams

Figure 5.1 is showing the midspan deflection of the loaded beam versus applied force on the load cell, for all three FE beams and lab beams.

Table 5.1: Cracking load, yield load and ultimate load for FE- and real beams

Beam	Cracking load [kN]	Yield load [kN]	Ultimate load [kN]
Reference beam	5.9	54.8	56
Reference beam FE	10.9	61.9	62.9
Tested beam with passive CFRP	16.78	92.56	105.4
FE beam with passive CFRP	18.8	102.4	111.2
Tested beam with prestressed CFRP	15.68	108.8	146
FE beam with prestressed CFRP	41.92	138.96	161.3

Table 5.2: FE vs real beams

Beam	Cracking load [%]	Yield load [%]	Ultimate load [%]
Reference beam	84	13	12
Beam with passive CFRP	12	10.6	5.5
Beam with prestressed CFRP	167.3	27.7	9.8

When extracting data from the FE models, cracking load, crack widths were studied to distinguish which load step it took place. For yielding load, stress was checked, when it reached ≥ 560 MPa and to distinguish ultimate load failure modes were studied. Since the FE model could not capture debonding, the beam with passive CFRP laminate did not end with the same failure mode as the experimental beam with passive CFRP laminate, which can be seen in figure 5.1 and it ended with concrete failure. This applies to the FE model with prestressed CFRP laminate as well, due to a premature rupture of the experimental beam with prestressed CFRP.

5.1.1 Reference beam vs FE

When comparing the FE results with experimental results from the reference beam, yielding and ultimate load is matching well as seen both in table 5.2 and the figure 5.1, which indicates, with a standard deviation, that the FE model is providing reasonably good predictions. The cracking load is deviating and this is explained by already existing cracks before tested.

5.1.2 Beam with passive CFRP vs FE

The FE model for the beam with passive CFRP is also, as seen in table 5.2 and figure 5.1, matching well comparing to the experimental results. The FE beam is showing a stiffer behavior after it starts to yield, but still, lie within reasonable deviation. The experimental beam failed when the CFRP debonded from the concrete and the FE beam is assumed to debond at a similar strain as the experimental beam, ~ 5 micro strain. This happened after the FE beam yielded.

5.1.3 Beam with prestressed CFRP vs FE

The biggest deviation can be seen in the prestressed FE model. Cracking in the FE model is taking place at almost three times higher load compared to the tested beam. This can be explained by the fact that it was already cracked before it got strengthened with CFRP. This means that the tested prestressed beam will lose stiffness, in the beginning, comparing to the FE model, which can be seen in figure 5.1. An explanation to why the tested beam is stiffer before yielding of the steel is that the prestressing process is handled differently in reality versus modeling. In reality, the CFRP were bonded in one end of the beam and pulled in the other end to create the prestressing force. During the prestressing phase, the hydraulic jacks cause some pressure on the end of the beam. This applied pressure will create additional compression in the beam leading to a higher stiffness. In the FE model, the CFRP adhere to the concrete without any applied force, explaining the difference in stiffness before yielding of the steel.

When comparing the strain from the FE model at the yielding point of reinforcement, 2.688 micro strain, with the experimental beam, it corresponds to an equivalent load of 112.88 kN for the experimental beam. This indicates some deviation from FE modeling and hand calculations. When looking at yielding the main difference comes from the testing of the prestressed beam. Strain gauges do not always work as anticipated and it was assumed that the steel yield when the strain gauge showed 2.5 micro strain. When checking the applied load in this step, the lab results showed that the yielding load was 108 kN, which is deviating from lab test and hand calculations for the yielding point. It is more reasonable to assume that this is not the right value since the steel showed in lab tests, that it had a yield limit around 560 MPa, which would confirm that the yield point is too low.

Since the FE model does not prestress the CFRP in the same way as when prestressing in the reality, it is reasonable to assume that the prestressing force of 80 kN will not represent the prestressing force in the FE model. When looking at strains from the experimental beam, an equivalent strain of 4 micro strain matched 80 kN, but it did not take into account that the concrete in this phase already was compressed and when released it would have increased the prestressing force. To match this in the FE model, 4 micro strain were kept as an index and an equivalent prestressing force was calculate from E-modulus of 230 GPa and this force corresponds to 103 kN.

Ultimate load in the FE model comparing to the tested beam is higher due to stress concentration in the CFRP laminate (which lead to premature rupture) from the prestressing phase, which the FE model can not capture.

5.1.4 FE vs hand calculation

To further verify the FE model, hand calculations were made accordingly to beam theory and Fib Bulletin 14 (2001), to make sure that hand calculations match the FE result within reasonable deviation and verify the assumption of decreasing the E-modulus and use lab test data for the reinforcement and CFRP. For full hand calculations, see Appendix A.

It seems that the FE model is matching rather well with reasonable deviation from hand calculations. The biggest difference can be found in the FE beam with passive CFRP and the reference beam compared to the FE beam with prestressed CFRP, that matches well.

Table 5.3: Cracking load, yield load and ultimate load from hand calculations

Beam	Cracking load [kN]	Yield load [kN]	Ultimate load [kN]
Reference beam	9.59	55.68	65.7
Beam with passive CFRP	19.03	92.25	101.1
Beam with prestressed CFRP	40.36	132.1	150.4

Table 5.4: FE vs hand calculations

Beam	Cracking load [%]	Yield load [%]	Ultimate load [%]
Reference beam	13.3	11.1	4.26
Beam with passive CFRP	12	11	9.98
Beam with prestressed CFRP	3.9	5.1	7.2

5.1.5 Visualisation of cracking load, yielding load and ultimate load for real tests, FE simulations and hand calculations

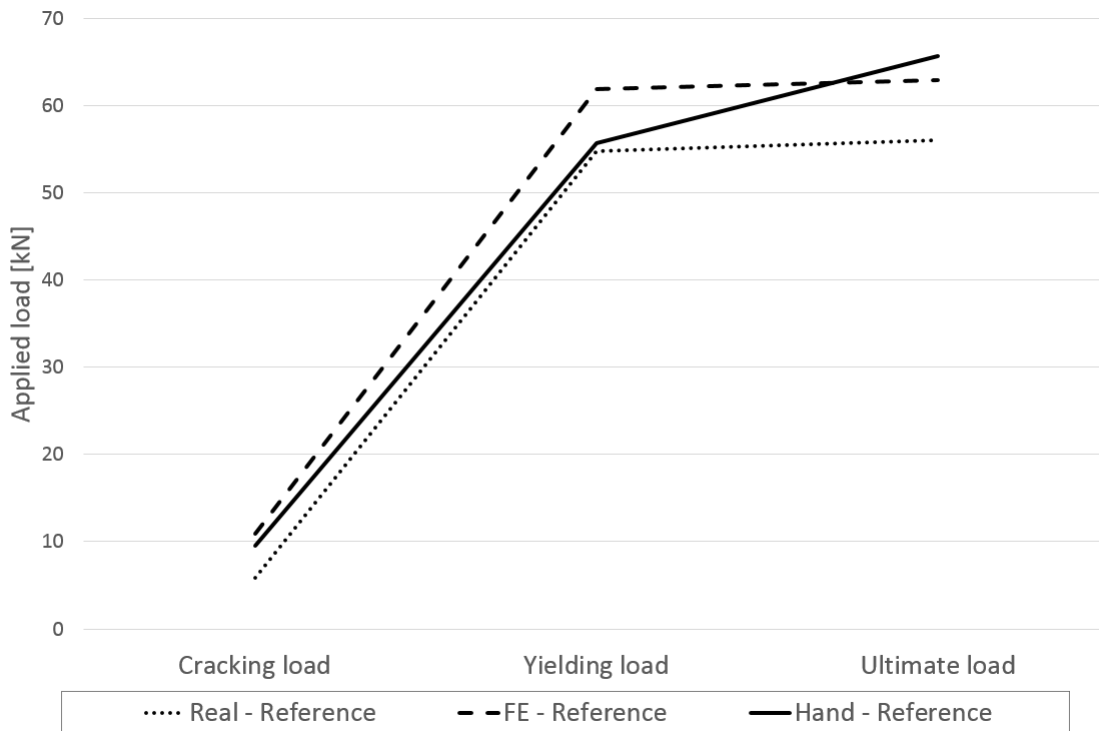


Figure 5.2: Reference beam

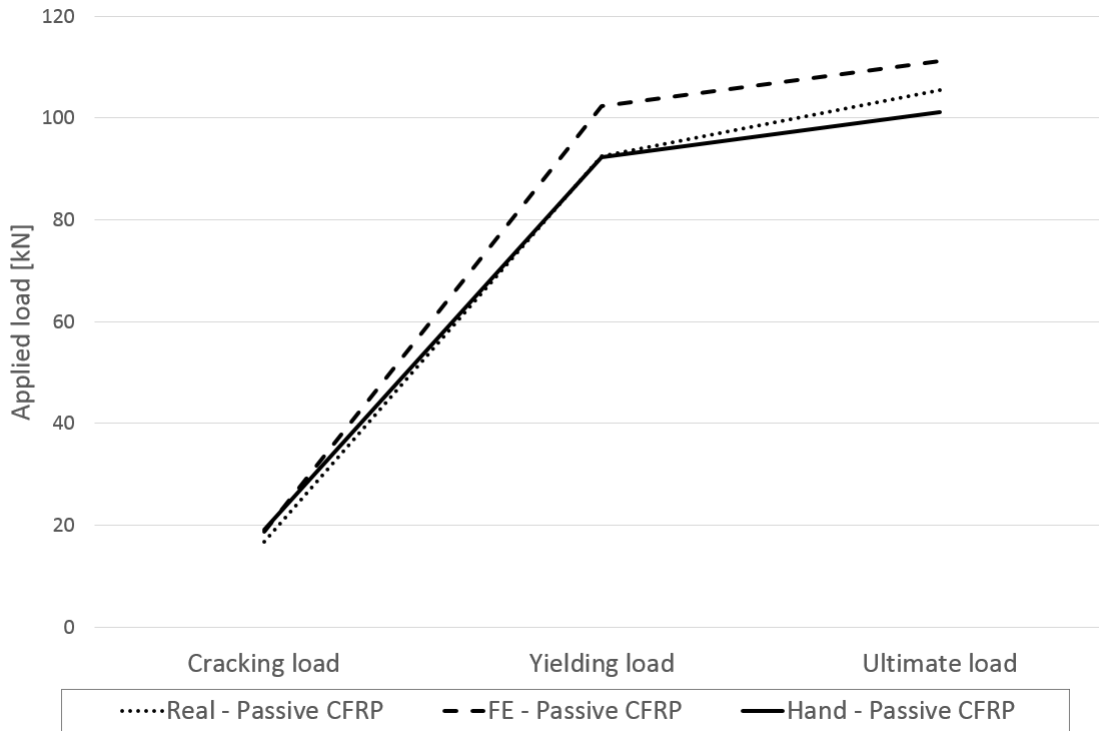


Figure 5.3: Beam with passive CFRP

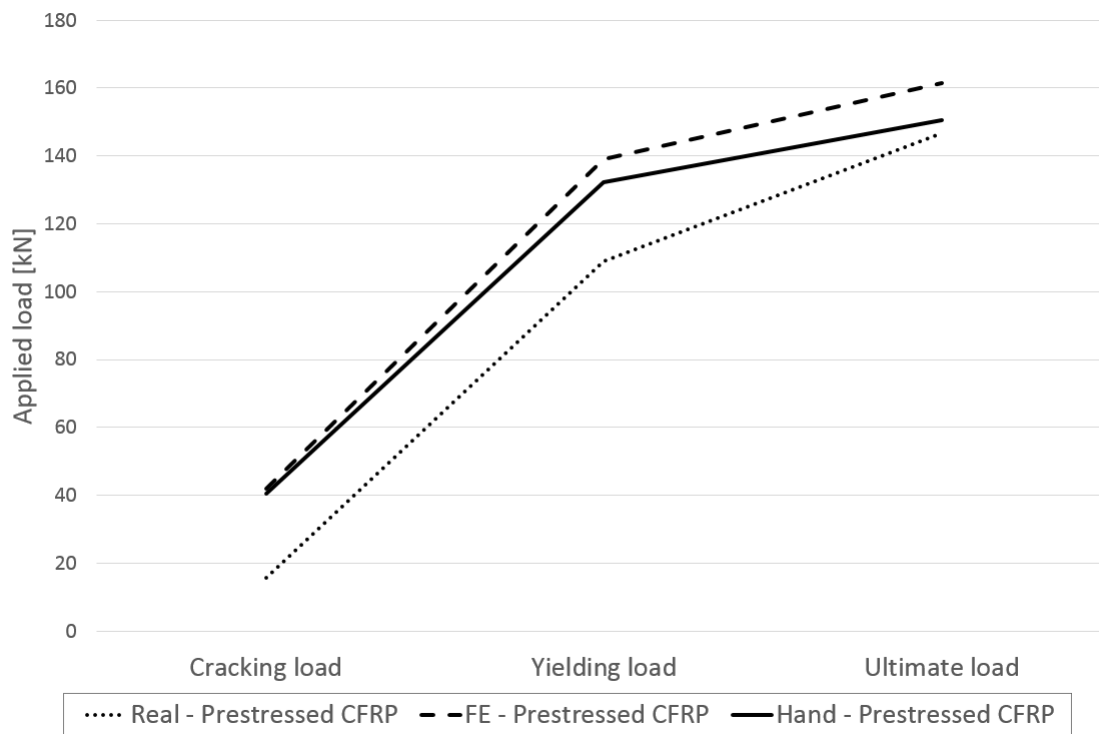


Figure 5.4: Beam with prestressed CFRP

5.2 Increasing prestressing force in the CFRP

Next step to finding the optimal prestressing force was to increase the force from zero until reached desired failure mode in the beam with prestressed CFRP, which is CFRP rupture at the same time as the concrete crushes. As the lab tests showed different failure strain comparing to the strain the CFRP manufacturer propose, it is reasonable to assume that the CFRP will rupture at $\epsilon_{cfRP} = 14$ micro strain. In all increasing steps, the beams will be checked for ductility and crack widths.

Table 5.5: Prestressing force

Prestressing force [kN]	Utilization [Prestressing force vs Ultimate strength %]	Theoretical CFRP strain [10^{-3}]
30	7.6	1.16
60	15.22	2.33
103	26.14	4.00
120	30.4	4.65
135	34.2	5.24
150	38	5.82
180	45.6	6.98
210	53.3	8.15
240	60.9	9.31

Theoretical CFRP strain is calculated from test result from the CFRP coupons.

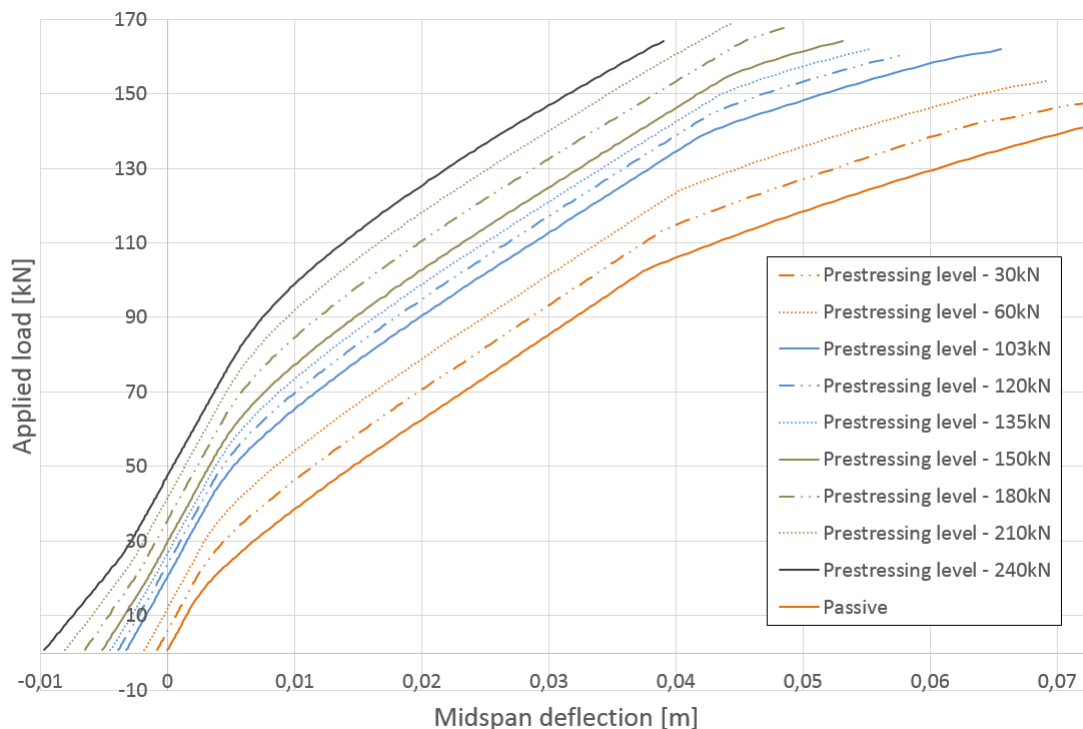


Figure 5.5: Load-deflection curve, increase prestressing force

When the prestressing force increases, the beam will gain higher cracking load, yield load and ultimate load as seen in figure 5.5. A major issue that is observed is when the prestressing force is increased to $F_{pres} \geq 120kN$ is that the top of the beam will sustain cracking and the beam will lose stiffness in the beginning before reaching cracking load (from external load), see figure 5.5. This is happening due to the beam is getting cambered from the prestressed CFRP laminate which is illustrated as the negative deflection in figure 5.5. All beams that sustain a prestressing force will be subjected to cambering, thus as soon as it sustains a force larger than the tensile strength, it will start to crack.

In figure 5.6 all load and deflection curves for different prestressing levels is plotted from the same starting point to be able to visualize the stiffness loss due to cracking of top side and the cambering effect. The cracks will eventually start to disappear when the beam is loaded and they will disappear as soon as the beam gets back to its original start position when the beam is completely straight again. When the cracks start to close the beam will regain stiffness, which can be seen in figure 5.6.

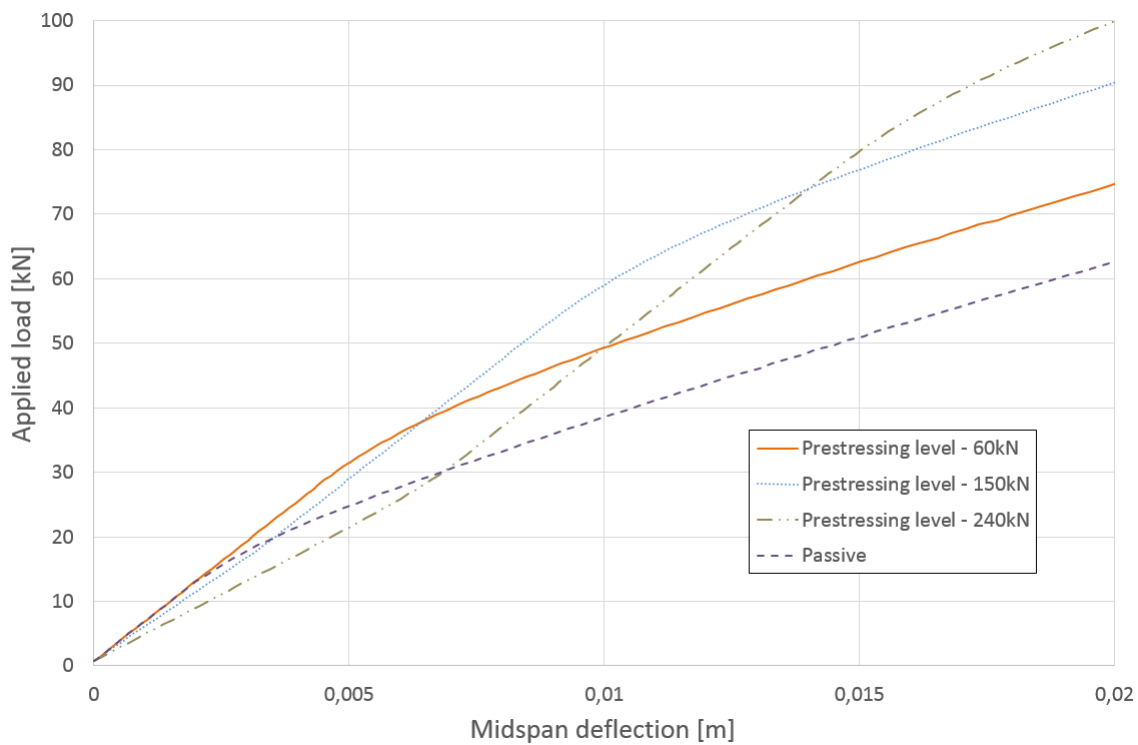


Figure 5.6: Load-deflection curve, point when the beam is regaining stiffness

5.2.1 Failure modes

Since lab tests showed a rupture strain of $\epsilon_{cfrrp} = 14$ micro strain of and full-scale test showed $\epsilon_{cfrrp} = 10$ micro strain, it is reasonable to assume that the CFRP will rupture at $\epsilon_{cfrrp} = 14$ micro strain.

Fib Bulletin 14 (2001) states that:

$$\epsilon_f + \epsilon_0 \leq \epsilon_{fud} \quad (5.1)$$

where:

$$\epsilon_f = \text{FRP strain} \quad (5.2)$$

$$\epsilon_0 = \text{Initial concrete strain at the extreme tensile fiber before strengthening} \quad (5.3)$$

$$\epsilon_{fud} = \text{Ultimate FRP strain} \quad (5.4)$$

The experimental beam with prestressed CFRP was sustained to some loading before strengthening and it induced some initial strain ϵ_0 . Since the FE model is not sustained to any loading before it is strengthened with prestressed CFRP, the initial strain will be $\epsilon_0 = 0$. In all FE simulations, the concrete will fail before the CFRP, which means that the initial strain ϵ_0 is an important factor for reaching theoretical rupture strain of the CFRP.

Concrete crushing is checked with the principal strain in elements that are reasonable to believe will sustain crushing. Adhesive debonding is negligible since the FE model can not capture that failure mode.

Desired failure mode for the FE model is when the reinforcement is yielding, CFRP is rupturing and the concrete crushes, which can be seen in table 5.6 for all different prestressing levels. Lateral confinement in the model will decrease the compressive strength when the FE model sustain more cracks, which will lead to crushing earlier for beams that have sustained larger prestressing forces from the CFRP and the effect due to cambering of the beam. When the prestressing force increases, the beam will also sustain local crushing in the middle of the beam. Ultimate load is taken from the last step in the FE-simulation, when the concrete fails.

Table 5.6: Failure modes in the FE simulations

Prestressing force [kN]	CFRP strain [10^{-3}]	Yielding in rebars	Ultimate load [kN]	Failure mode
30	10.04	Yes	147.6	Concrete crushing
60	10.46	Yes	153.36	Concrete crushing
103	11.37	Yes	161.3	Concrete crushing
120	11.19	Yes	160.6	Concrete crushing
135	11.34	Yes	162	Concrete crushing
150	11.57	Yes	164.2	Concrete crushing
180	11.95	Yes	167.8	Concrete crushing
210	12.53	No	169.2	Concrete crushing
240	12.92	No	164.2	Concrete crushing

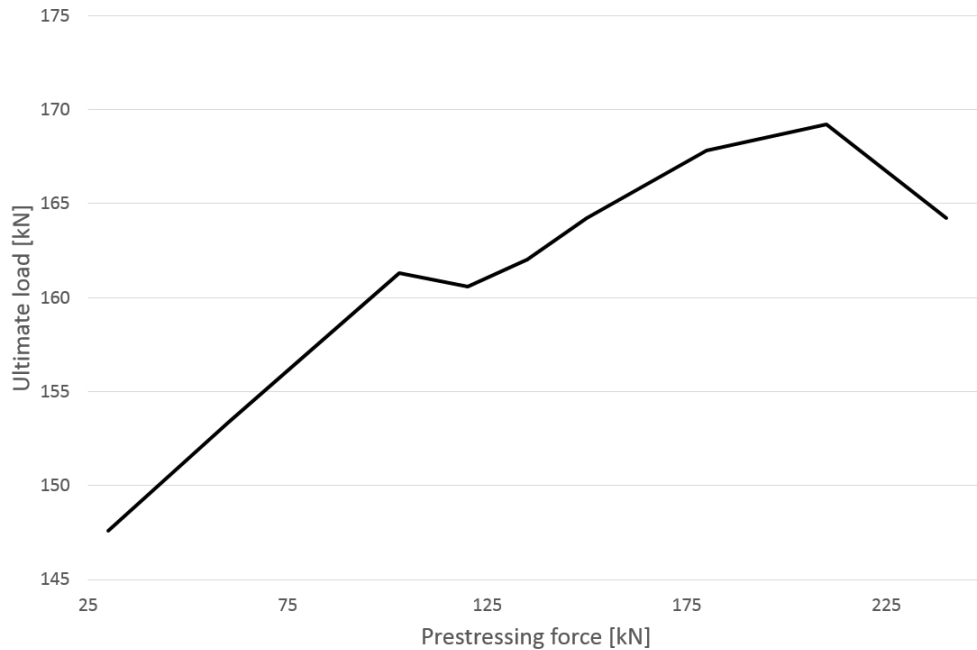


Figure 5.7: Ultimate load vs prestressing force

In figure 5.7 ultimate load is plotted versus prestressing force for all prestressing levels. Here it is easy to see the part when the prestressing force is affecting the concrete and the prestressing force can not increase anymore due to lateral cracking/confinement. There are some small deviations between different FE simulations due to convergence issues.

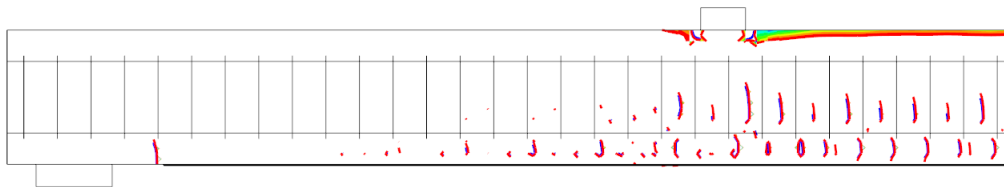


Figure 5.8: Concrete crushing as a result from the FE model in DIANA

5.3 Axial force profile in the CFRP laminate

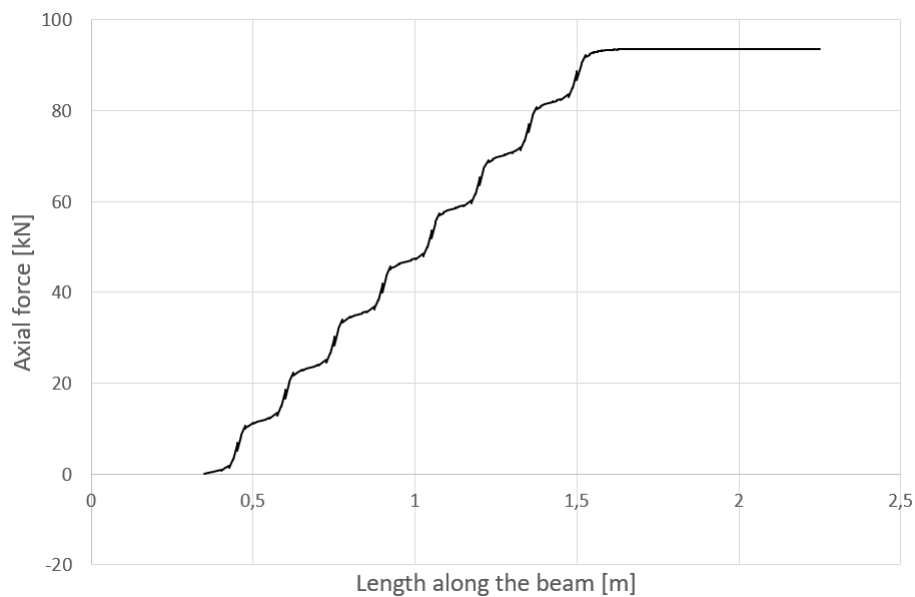


Figure 5.9: Axial force at prestressing level 103 kN

As anticipated and described in chapter 2.6, the axial force in the CFRP laminate in the FE mode is behaving, see figure 2.7, as stated in chapter 2.6. It decreases along the CFRP segments which result in an axial force almost at zero at the laminate end.

5.4 Shear stress results

Shear stress between the CFRP and concrete for prestressing level 103 kN can be seen in figure 5.10. It is plotted along the FE model, starting from the left end of the beam in the model. This is directly connected with the Tenroc method and for verifying that the FE model is behaving as it should.

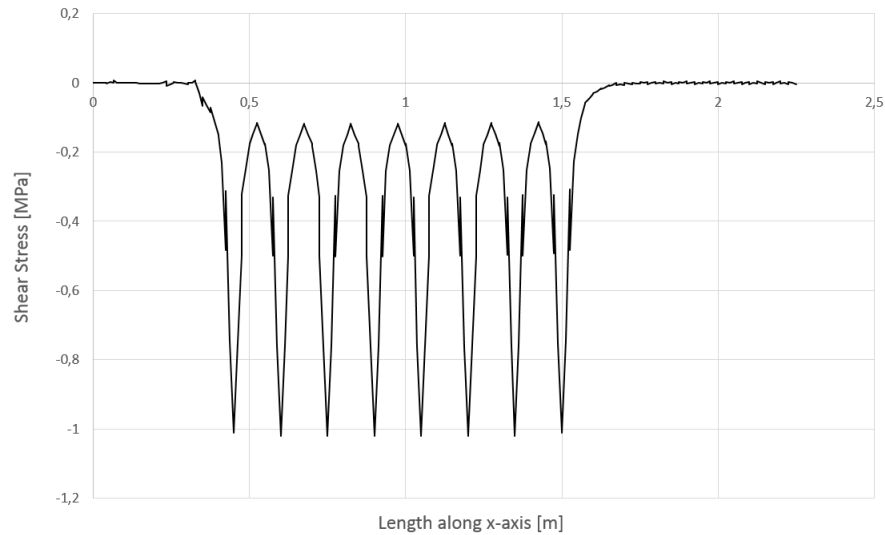


Figure 5.10: Shear stress between CFRP and concrete

Shear stress in the epoxy adhesive for prestressing level 103 kN can be seen in figure 5.11. It is plotted along the FE model, starting from the left end of the beam in the model.

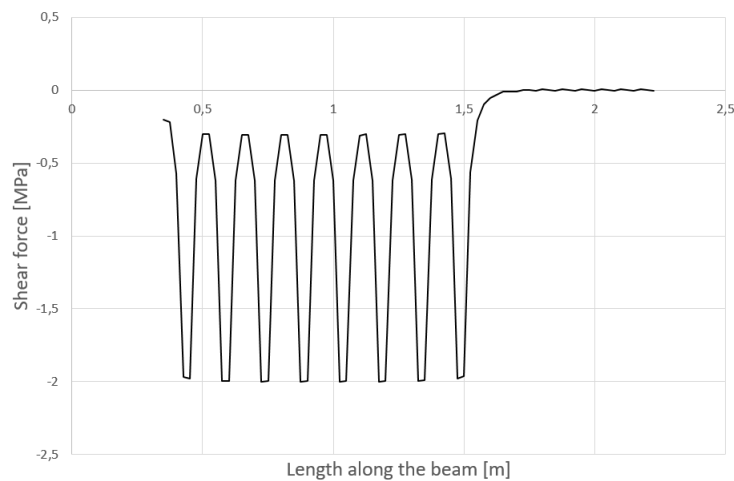


Figure 5.11: Shear stress in the epoxy

5.5 Crack pattern and crack width

To find a valid point for all simulations and compare crack widths, a deflection point was chosen that correlate to all simulations. When the prestressing force increased, it was observed that the crack width decreased and became more evenly distributed (smeared) over the cross section. To visualize this, crack widths are shown with help of trend lines, seen in figure 5.14. Figure 5.14 is based on figure 5.13 and due to difficulties in visualizing, it had to be formatted into trend lines to see the effect of decreasing crack widths. It was also observed that a major crack appeared at the laminate end, seen in figure 5.12, that is developed from the prestressing phase in the FE analysis. When the CFRP is attached to the beam after the prestressing phase, the prestressing force is not gradually released as it is done in the reality and the effect of this could resemble a sudden stress concentration, which makes the concrete crack at the CFRP laminate end. Since this phenomenon is not happening in the reality this crack can be neglected. In figure 5.15, 5.16 and 5.17 the crack pattern is shown for three different prestressing levels. This is to visualize the decreased crack widths and the effect of evenly distributed cracks.

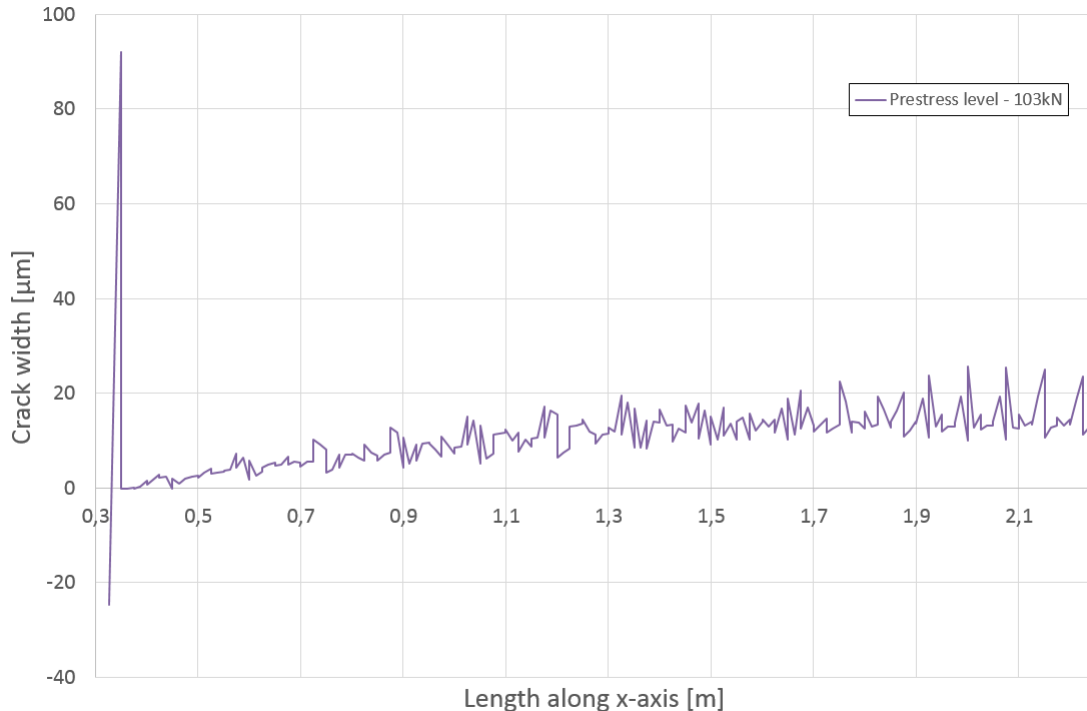


Figure 5.12: Major crack at CFRP laminate end

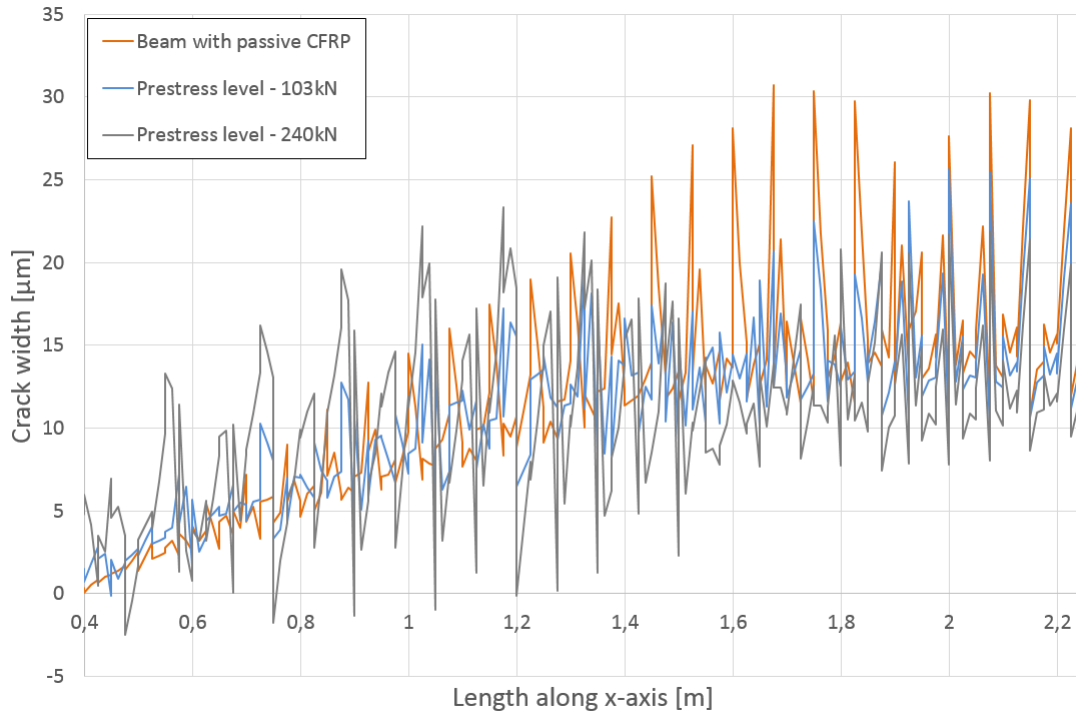


Figure 5.13: Crack widths at different prestressing levels

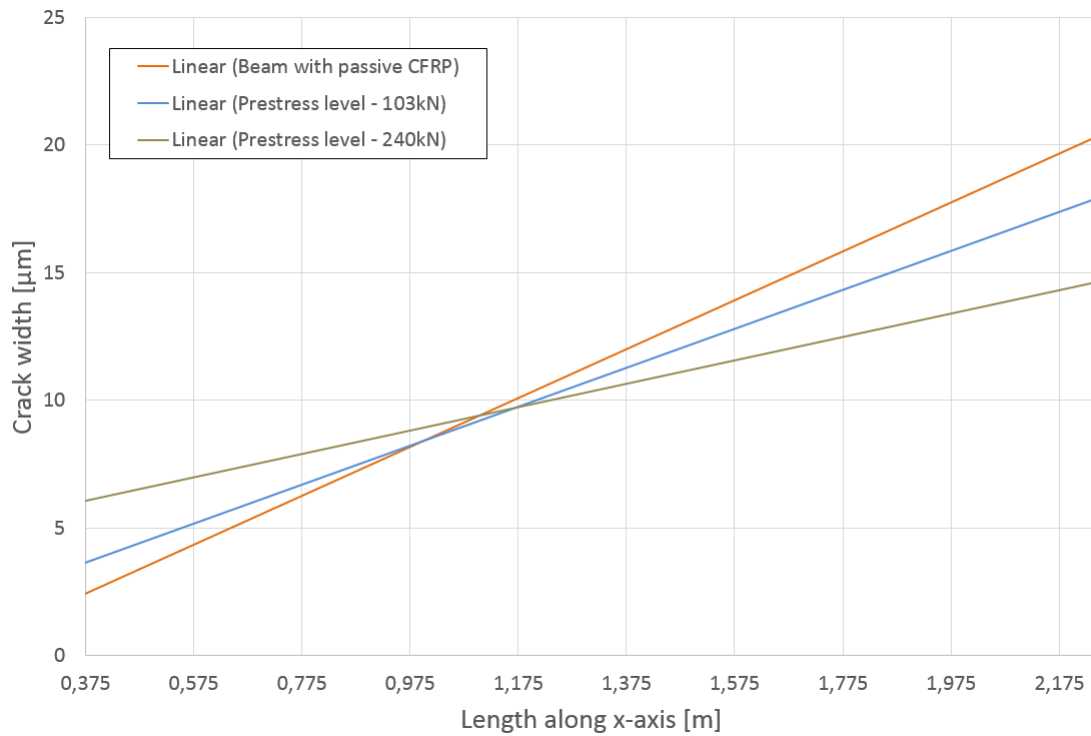


Figure 5.14: Crack trends at different prestressing levels

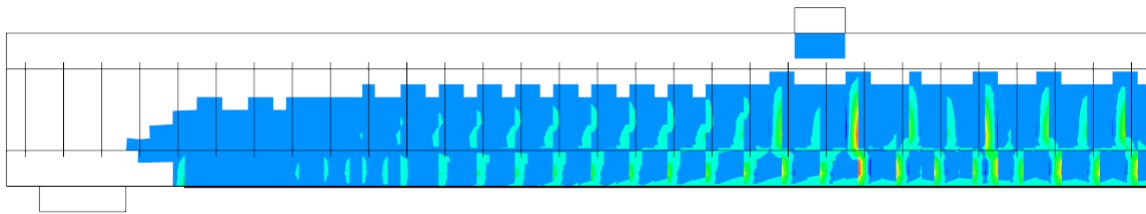


Figure 5.15: Crack pattern at applied load 120 kN with passive CFRP

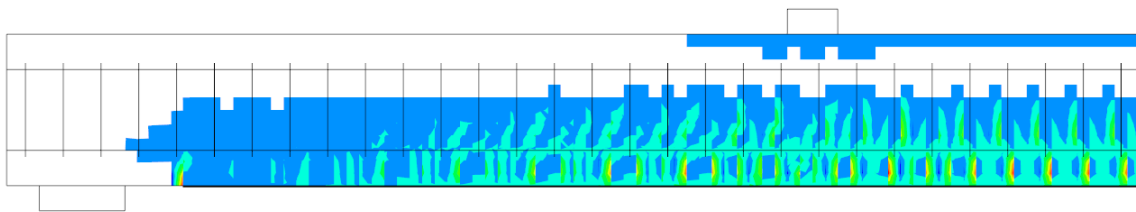


Figure 5.16: Crack pattern at applied load 120 kN with prestressing level 103 kN

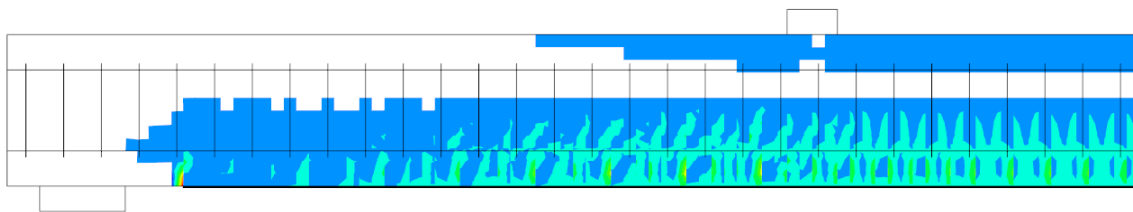


Figure 5.17: Crack pattern at applied load 120 kN with prestressing level 150 kN

When the beam started to camber due to high prestressing levels, the top side started to crack. These cracks grew as the prestressing force increased, illustrated in figure 5.18.

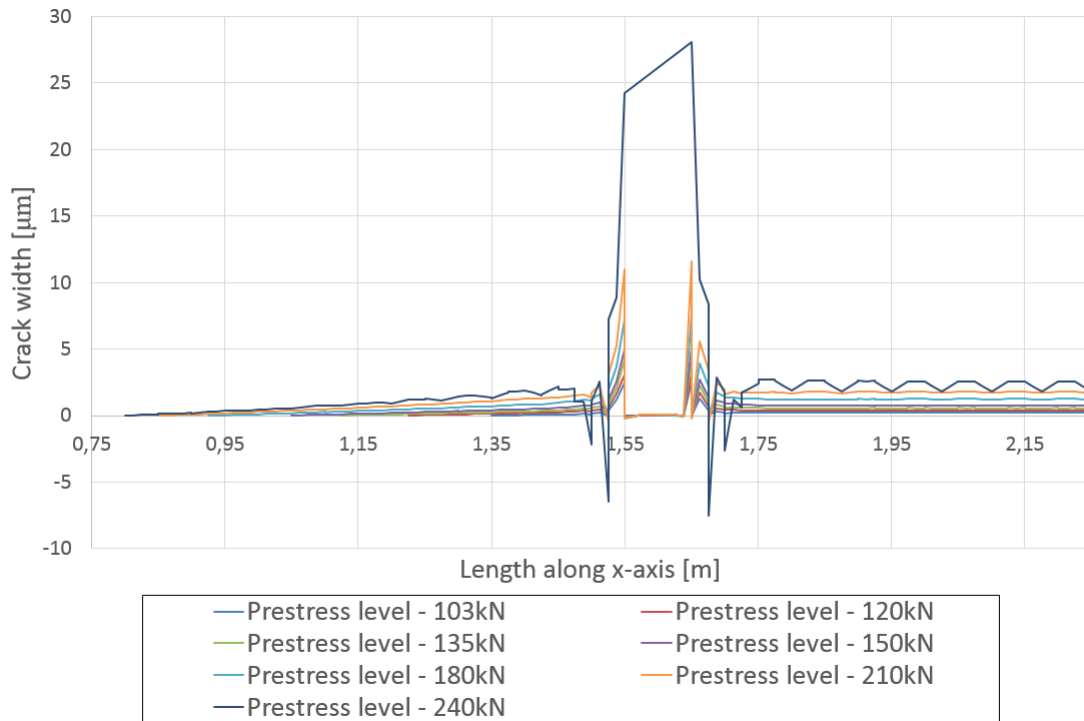


Figure 5.18: Crack growth on top side

Cracking locally where the load print is attached to the FE model (seen as the major cracks in figure 5.18) is negligible since the load print, in reality, is not perfectly tied to the beam, but in the FE model it had to be perfectly tied and that is why these cracks appeared in the simulations just right by the load print.

Figure 5.19 shows crack widths precisely after the load print to mid section of the beam and how they increase with increasing prestressing force.

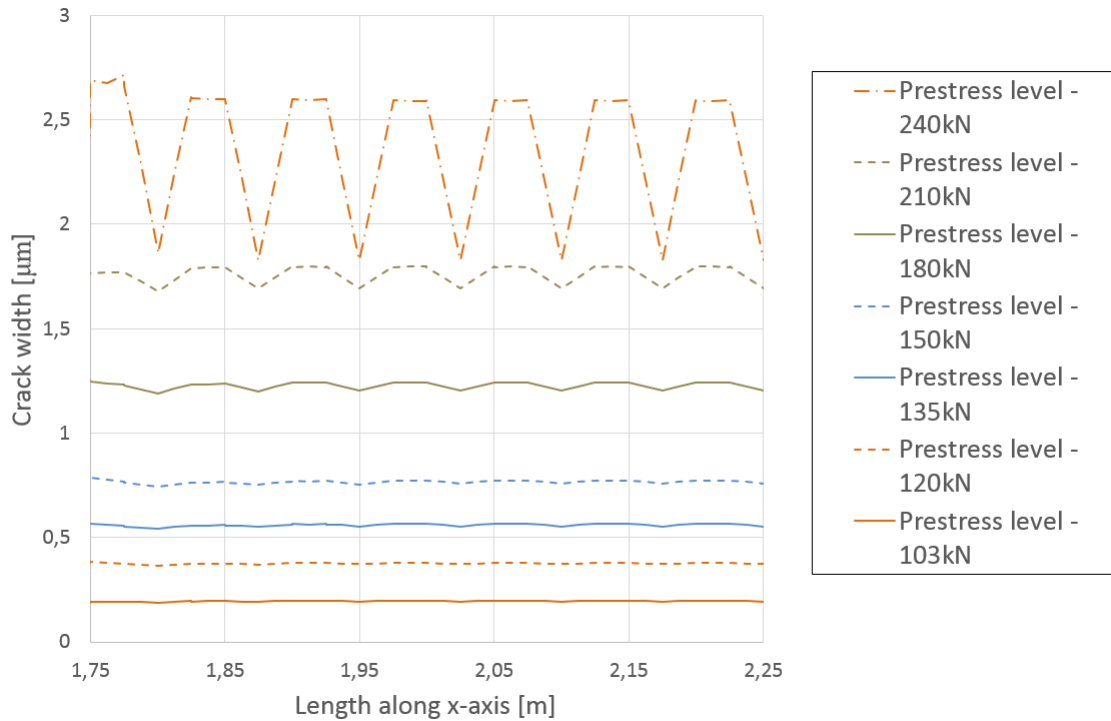


Figure 5.19: Crack growth on top side, after support

5.6 Ductility of the beam strengthened with prestressed CFRP laminate

Each beam was evaluated for their ductility in order to see the response when the prestressing level is increased. Ductility index is calculated accordingly to Fib Bulletin 14 (2001) and equations stated in section 2.3. All compressive depths are taken from the mid-span in the FE model.

The unstrengthened beam has symmetry in the reinforcement and will have a ductility index of $\xi = 0.435$, which is a reasonable ductility index at ultimate. The beam with passive CFRP laminate will have a ductility index below required index for ductility and therefore the best index. Ductility index is calculated at ultimate load for each simulation.

Table 5.7: Ductility index for different prestressing levels

Beam type	Compressive zone [mm]	Ductility index at ultimate ξ
Reference	100	0.435
Beam, Passive CFRP	88.5	0.385
Beam, prestress level 103 kN	102	0.443
Beam, prestress level 120 kN	105	0.456
Beam, prestress level 135 kN	108	0.469
Beam, prestress level 150 kN	110	0.478
Beam, prestress level 180 kN	115.75	0.5
Beam, prestress level 210 kN	117	0.508
Beam, prestress level 240 kN	125	0.543

Since only the beam with prestressing level 103 kN and prestressing levels below 103 kN will meet the requirement stated in Fib Bulletin 14 (2001), it is reasonable to believe that ductility index for some of the prestressing levels will be acceptable. This is because the compressive zone height is hard to distinguish from the FE model, due to irregularities in the compressive zone height over the cross section.

5.7 Strain in CFRP laminate

In figure 5.20, strain in the midpoint of the CFRP laminate and load is plotted to illustrate which strains where debonding and/or rupture of the CFRP might happen. As stated before, full-scale tests and laboratory tests showed that debonding took place at ~ 5 micro strains for the passive CFRP and rupture at ~ 10 micro strain for the prestressed CFRP. Theoretically, rupture should take place at 15 micro strain and lab tests showed 14 micro strain. Debonding is reasonable to believe happening between strains of 5-8 micro strains (SIA, 2004). The debonding zone, 5-8 micro strain, in figure 5.20 only applies for passive CFRP and rupture zone, ≥ 14 micro strain, for the prestressed CFRP. When the prestressing force is increased, the initial strain is increased simultaneously, which leads to higher utilization of the CFRP, higher cracking-, yielding- and ultimate load. This is captured by the FE model, but the concrete fails before the CFRP and therefore it will not reach theoretical rupture strain in the model.

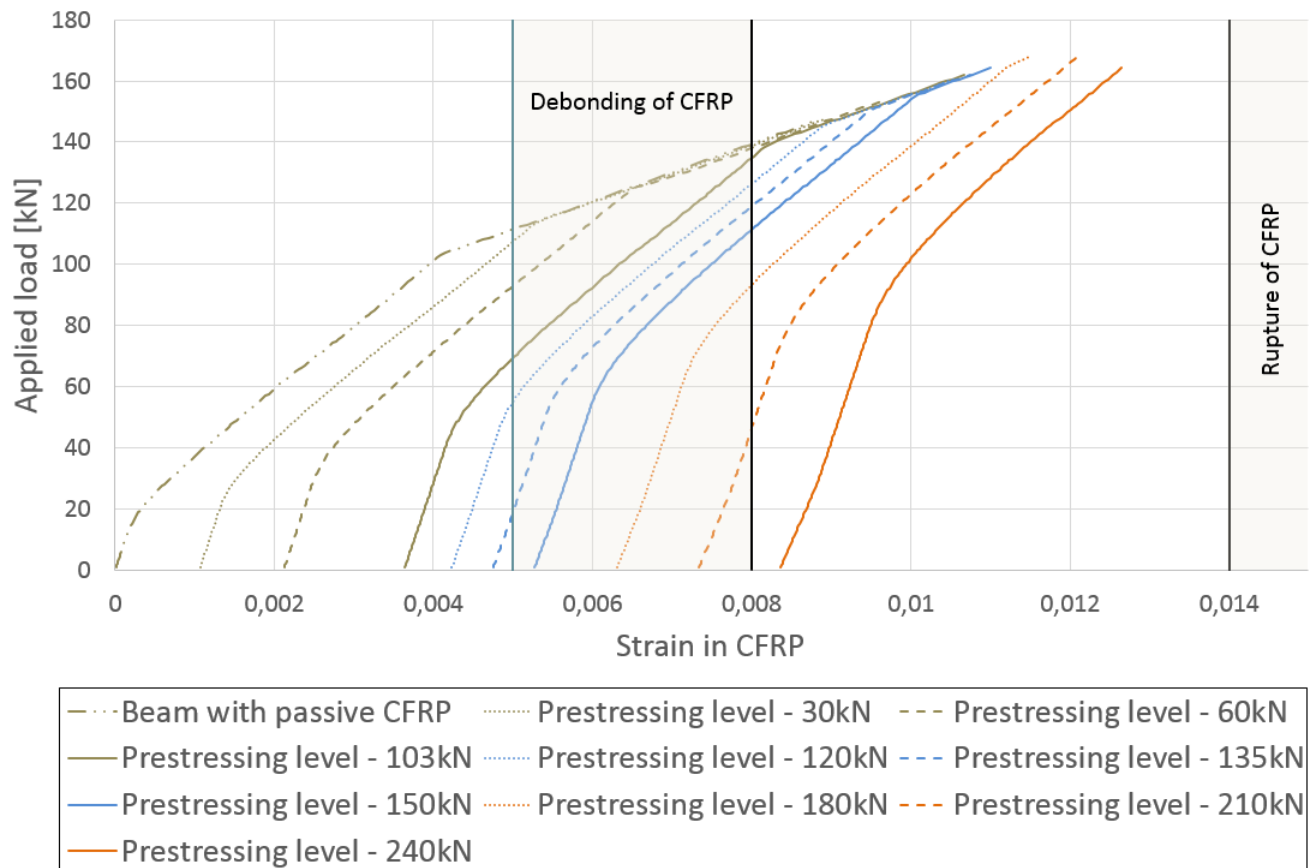


Figure 5.20: CFRP strain vs applied load

5.8 Optimization of prestressing force

To evaluate, according to the criteria stated in table 5.8, what prestressing level is optimal, all aspects have to be taken into account.

Table 5.8: Criteria for optimized prestressing force

- Yielding of reinforcement
- Rupture of CFRP
- Concrete crushing
- Ductility
- Crack widths

After FE simulations had been carried out, the first check to be done was to check if the reinforcement had started to yield. If the reinforcement had started to yield before concrete failure happened, the yielding capacity of the beam was determined. Next step was to check for possible failure modes. One failure mode was to check if the presumptions that the CFRP had reached strains above 14 micro strains, where the CFRP laminate should rupture. Meanwhile the concrete, in nearly all cases, suffered from a decreased load carrying capacity, due to lateral reduction/confinement as a consequence from top side cracking. It was assumed that all beams experienced concrete failure (local crushing and global crushing) when the FE simulation ended. This assumption was made due to the fact that that the FE model did not reach any other failure mode.

Since the FE simulations did not show strains above 14 micro strain in the CFRP laminate and due to the fact that none of the concrete beams had sustained any loading prior to strengthening with prestressed CFRP, the assumption was made that CFRP rupture was not able to happen. This because the concrete would fail before the maximum strain of 14 micro strain could be achieved in the CFRP laminate in the FE simulations. To reach appropriate CFRP strains, the CFRP had to be prestressed up to a level of 300 kN, which is equivalent to an initial CFRP strain of 11.6 micro strain. Since rupture was not attained the optimization scheme had to be updated and the optimization had to be checked for top side cracking and concrete crushing since this occurred before rupture. The risk of debonding is also a thing that needs to be taken into account when evaluating the prestressing force. The theory is stating that if the prestressing force is too low, e.g acting in a more passively way. The risk of debonding at CFRP strain less than 5 micro strains might be governing criteria. Due to the limitation of not incorporating the debonding failure in the FE model, this criterion will be illustrated as a lower strain limit of the CFRP. Since none of the FE models sustained strains as low as 5 micro strains, all FE models passed this criterion in the optimization of the prestressing force.

Table 5.9: Updated criteria for optimized prestressing force

- Yielding of reinforcement
- Rupture of CFRP
- Concrete crushing
- Ductility
- Cracks on top side of the beam
- Debonding risk of the CFRP laminate

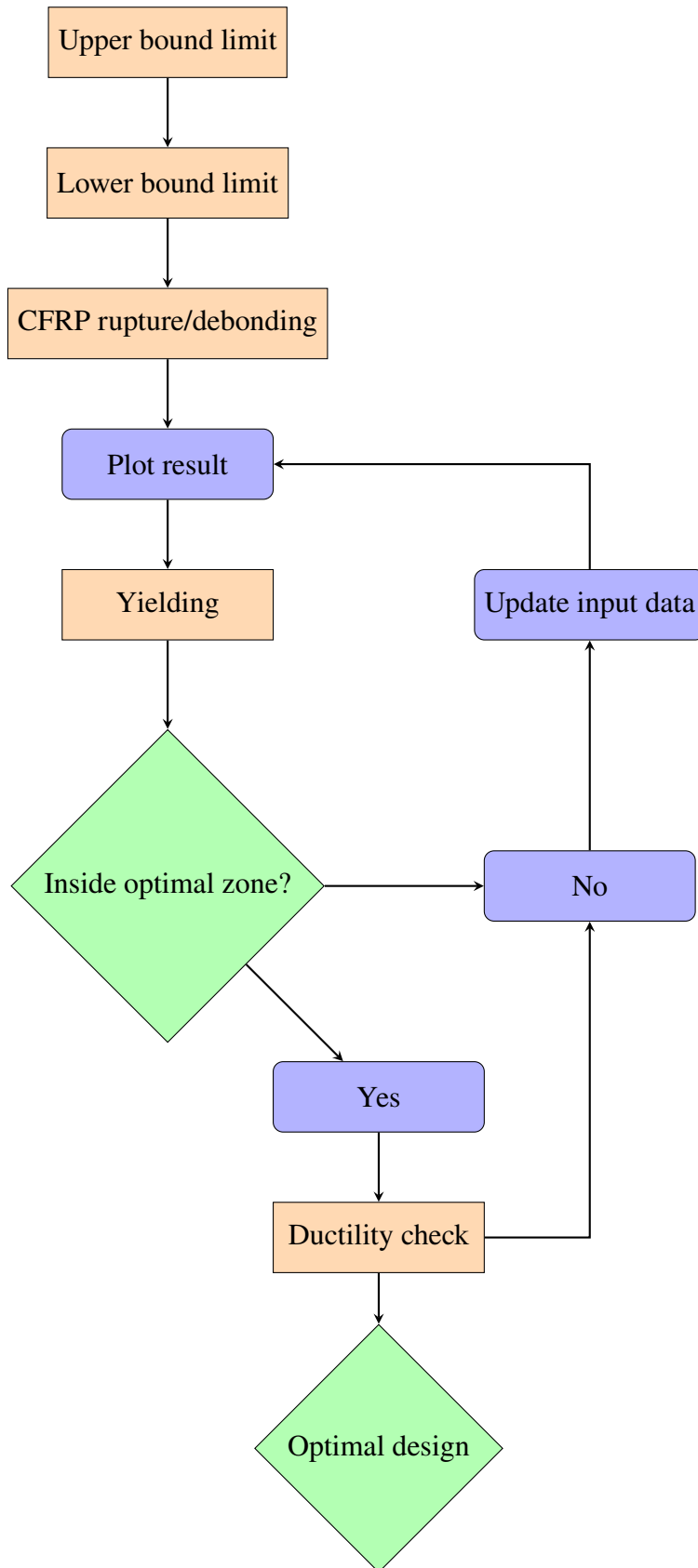
In figure 5.22 CFRP strain is plotted against concrete strain to visualize when concrete crushing is happening as well as the reduction of compressive strength of the concrete due to lateral confinement/reduction. In the red zone in figure 5.22, the reduction of compressive strength is visualized and this is happening due to increased strain at the top of the concrete, which can be seen as an increase of negative strain in figure 5.22. When the prestressing force in the CFRP laminate is increasing, the beam will be less ductile and fail earlier compared to when the prestressing force is not affecting the cracking on the top side of the beam in the prestressing phase.

Optimal prestressing force according to the new criteria would be when the concrete is not prematurely crushed and the cracking strain on the top side of the beam is below 0.00315 and sufficient ductility is achieved.

When evaluating the FE simulations, prestressing forces below 120 kN is showing the most promising results accordingly to the criteria. The ductility of this prestressing levels below 120 kN is ≤ 0.45 , which is the upper bound limit accordingly to Fib Bulletin 14 (2001). All prestressing forces below 120 kN will fulfill the ductility requirement, see figure 5.23. All simulations below 120 kN showed that the cracks on the top side were below 0.3 μm , which can be seen as a reasonable crack size that does not affect the lateral confinement/reduction in the FE model.

5.8.1 Work flow for optimizing prestressing force

- Before optimizing, find/choose appropriate input data for concrete, reinforcement, and CFRP and conduct FE-analysis.
- Step one is to evaluate appropriate upper bound limit for the concrete crushing strain from chosen concrete data.
- Step two is to evaluate appropriate lower bound limit for the concrete cracking strain on the top side of the beam.
- Step three is to find the rupture/debonding strain for the CFRP laminate.
- Step four is to plot the result from the FE-analysis
- Step five is to plot a line through all yielding points and check if enough yielding is achieved in the reinforcement.
- Find, with help of step one-five, the optimal zone for the prestressing force.
- If inside the optimal zone, check for ductility requirement.
- If not inside the optimal zone, update/change input data and FE-analysis. Go to step four.
- If ductility is fulfilled and within the optimal zone, desired prestressing force is achieved.



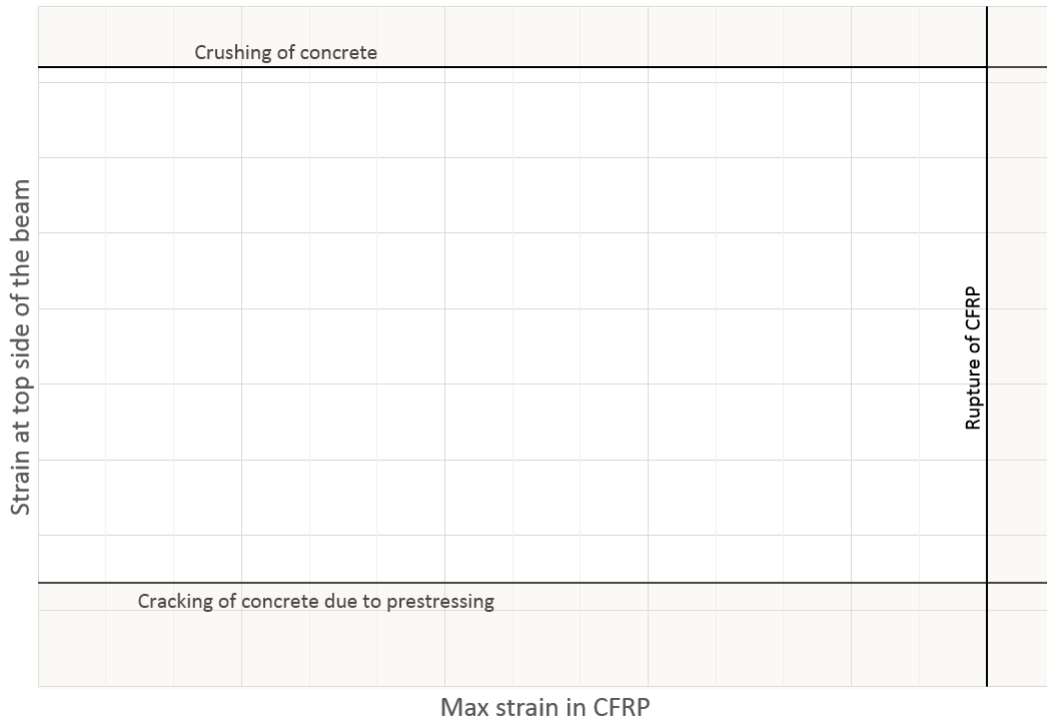


Figure 5.21: Optimization layout example

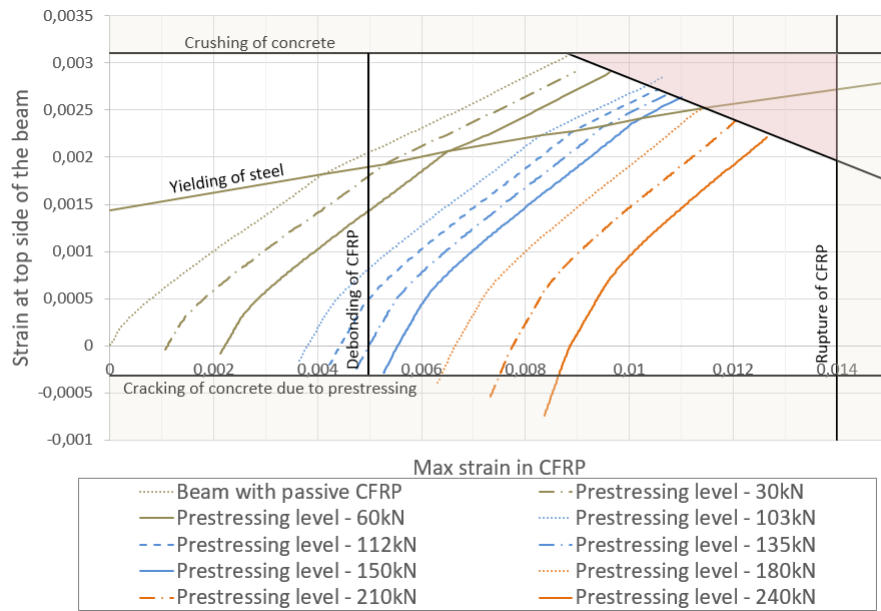


Figure 5.22: Optimization of FE beams

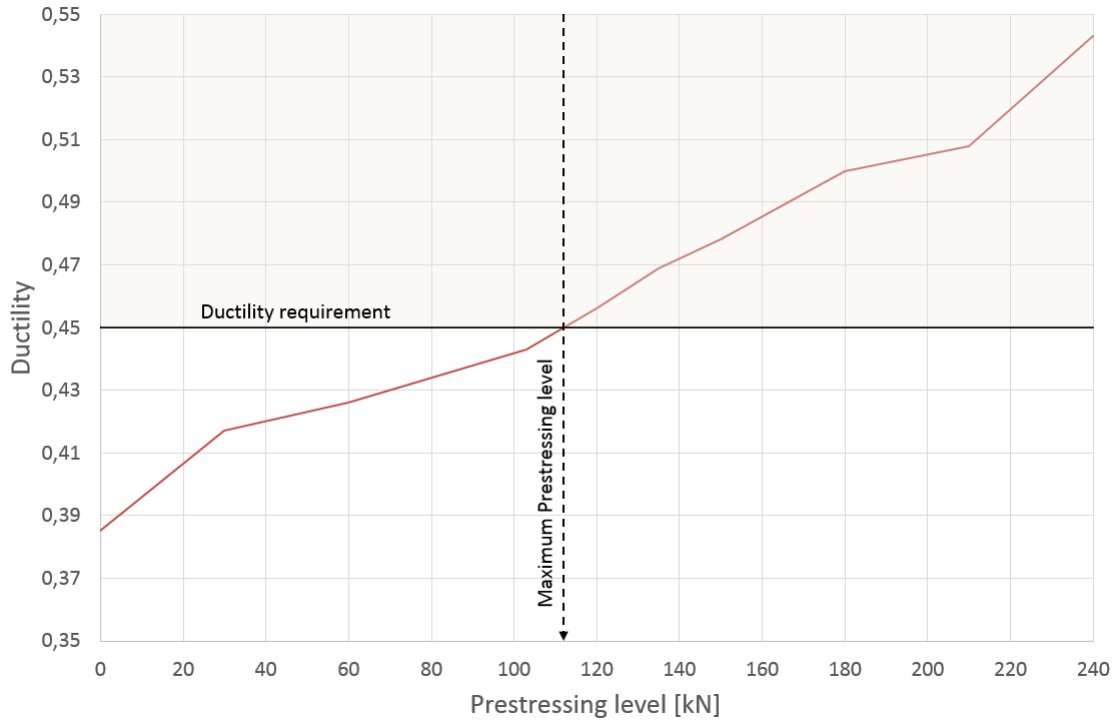


Figure 5.23: Ductility requirement accordingly to Fib Bulletin 14 (2001)

6 Discussion

All results obtained from the FE analysis are plausible and the trends are showing that the prestressing force can be increased with the result of decreased crack widths on the bottom side, an increase of cracking load, yield load and ultimate capacity. The major problem to not be able to verify the results of FE against the experimental tests completely is the modified E-modulus. Since the change of concrete E-modulus was done to match the full-scale tests it is reasonable to believe that the E-modulus used in the FE analysis is incorrect and in reality, it would be stiffer. With increased E-modulus the crack load, yield load, ultimate capacity would increase and crack widths would decrease as well. Since all beams sustained concrete crushing (local and global) and this is probably happening due to the low E-modulus of the concrete and it is reasonable to think that some of the prestressing levels would not have this failure mode.

Since none of the FE beams sustained any cracks or loading before strengthened with prestressed CFRP laminates, it was not possible to achieve rupture of the CFRP laminate before concrete failure. Fib Bulletin 14 (2001) is just treating strengthening of RC beams that have been sustained to loading and therefore probably cracking, which gives the concrete an initial strain. This will make it easier to reach theoretical rupture strain.

The only way of reaching rupture strain in the FE model is to increase the prestressing force of above 300 kN, which is not reasonable due to the ductility of the beam will decrease rapidly and the beam will sustain major top side cracking, which reduces the ultimate capacity of the beam significant. If the concrete E-modulus is increased to a value close to the reality, the FE model might be able to induce strains nearly rupture strain of the CFRP before concrete failure.

Another major issue that was found during the post processing of the results is the influence of the cracks on the top side. This phenomenon lowered the ultimate capacity of the beams significantly and to utilize the full potential of the CFRP, this needs to be dealt with.

The fact that the lab tests of the CFRP and the full-scale test showed that the CFRP can rupture earlier than the manufacturer states makes it hard to draw a line when the CFRP rupture in the FE model, which also makes this an uncertain factor. The explanation for this is that the CFRP laminate in the full-scale test had sustained stress concentrations from the GFRP plate during the prestressing phase.

The FE model could not capture the curing effect of the epoxy, which leads to prestressing and bonding of the prestressed CFRP in one step. This resulted in a stress concentration at the laminates end, resulting in a major crack which decreases the capacity of the FE model, but in reality should not be a problem.

6.1 Source of error

The comparison of the FE models with the experimental results shows similar behavior, both for the reference beam and CFRP beams with active and passive laminates. When modeling in FE programs such as DIANA some simplification has to be made in order for the model to run faster or due to insufficient data. Some simplifications that might be a source of error are:

- No bond slip is accounted for the reinforcement. The reinforcement is assumed to be perfectly embedded in the concrete.
- The surface interaction between the concrete, epoxy, CFRP laminate, supports and load prints are all assumed to be perfectly bonded and thus, slip cannot occur in between these materials.
- The FE model does not take into consideration initial cracking. The concrete beams used for the experimental tests were transported from an external manufacturer and subjected to stress during the transportation. This is most likely the reason to some initial cracking in the beams before the CFRP laminates were applied and before the actual testing of the beams. The initial cracking will result in lower cracking load in the test results.
- The fact that only one beam has been tested for each case might lead to unreliable results. To take in consideration some standard deviation and more than one beam for each case should be tested.

7 Conclusion

The aim of this master thesis is to analyze the structural behavior and crack widths of an EB prestressed CFRP reinforced RC beam and to be able to optimize the prestressing force so it is possible to improve the utilization rate of the CFRP.

- The results in this thesis show that the prestressing level can be increased to an equivalent prestressing force of 110-115 kN, which corresponds to a utilization to 27.90-29.17% of the CFRP ultimate capacity, with the in data used in the FE model.
- Ductility is an important factor and if this is the governing aspect in the design, ductility will decide how much prestressing force that can be applied.
- Crack widths will decrease with increasing prestressing force and smear out.
- To be able to utilize further, the cambering effect from the prestressing force need to be dealt with, reducing cracking on top side.
- For more verification, more full-scale tests need to be done, especially with beams that are not cracked in the beginning and additional FE analysis with appropriate in-data, e.g. from Eurocode or ACI.

8 Further studies

For further studies, the authors propose studies with GFRP externally bonded on the top side of the beam to investigate the cambering effect and crack reduction. Possible results from this could be that the crack width due to upwards bending from the prestressing can be lowered. This would save some capacity in the concrete and the reduction factor due to lateral cracking would be reduced.

To generate a more reliable FE model the authors propose that the experimental data is extracted from experiments, used with a reasonable standard deviation. For each case, there should be more than one experimental beam to be able to verify the experimental data with the results from FE models. The beams should also be constructed and tested in a reliable environment in order to ensure the quality of the material and experimental tests. Further in the FE model, incorporation of all types of CFRP debonding, to be able to capture all failure modes.

To be able to study the effects of externally bonding a prestressed CFRP laminate onto an already loaded concrete element, the authors suggest to continue with FE modeling and incorporate a loading phase prior to the strengthening. This might show that already existing cracks can be reduced and lost capacity of the element can be regained. The utilization of the CFRP laminate should be compared with a case where no prior loading has occurred.

The optimization scheme needs further verification and the authors propose that this is done with hand calculations and FE modeling with Eurocode values, to be able to distinguish the maximum upper bound and the maximum lower bound limit for the concrete. The strategy for the optimization has a lot of possibilities for refinement and incorporation of further limitations and demands.

References

- ACI, C. (1999). Building code requirements for structural concrete and commentary. *ACI 318-99*.
- DIANA FEA, D. (2015). Diana 10.0 user's manual.
- Dyresjö, P. & Eskilsson, M. (2016). An analytical approach for flexural strengthening of double-t slabs with prestressed cfrp laminates. Institutionen för bygg- och miljöteknik, Konstruktionsteknik, Chalmers tekniska högskola.
- Engström, B. (2014). *Restraint cracking of reinforced concrete structures*. Chalmers University of Technology.
- Engström, B., Al-Emrani, M., Johansson, M., & Johansson, P. (2013). *Bärande konstruktioner del 1*. Chalmers University of Technology.
- Fib Bulletin 14, I. F. f. S. C. (2001). *Externally bonded frp reinforcement for rc structures*.
- El-Hacha, R., Wight, R., & Green, M. (2001). Prestressed fibre-reinforced polymer laminates for strengthening structures. *Progress in Structural Engineering and Materials*, 3(2), 111–121. doi:10.1002/pse.76
- Haghani, R. & Al-Emrani, M. (2016). A New Method for Application of Pre-stressed FRP laminates for Strengthening of Concrete Structures. *IABSE Congress Stockholm*,
- Hong, S. & Park, S.-K. (2013). Effect of prestress levels on flexural and debonding behavior of reinforced concrete beams strengthened with prestressed carbon fiber reinforced polymer plates. *Journal of Composite Materials*, 47(17), 2097–2111. doi:10.1177/0021998312454318
- Kim, Y., Shi, C., & Green, M. (2008). Ductility and Cracking Behavior of Prestressed Concrete Beams Strengthened with Prestressed CFRP Sheets. *Journal of Composites for Construction*, 12(3), 274–283. doi:10.1061/(ASCE)1090-0268(2008)12:3(274)
- Lorenzis, L. D. & Teng, J. (2007). Near-surface mounted {frp} reinforcement: An emerging technique for strengthening structures. *Composites Part B: Engineering*, 38(2), 119–143. doi:http://dx.doi.org/10.1016/j.compositesb.2006.08.003
- Michels, J., Barros, J., Costa, I., Sena-Cruz, J., Czaderski, C., Giacomini, G., ... Zile, E. (2016). Prestressed FRP Systems. In C. Pellegrino & J. Sena-Cruz (Editors), *Design Procedures for the Use of Composites in Strengthening of Reinforced Concrete Structures* (19, Pages 263–301). RILEM State-of-the-Art Reports. DOI: 10.1007/978-94-017-7336-2_7. Springer Netherlands. Retrieved February 13, 2017, from http://link.springer.com/chapter/10.1007/978-94-017-7336-2_7
- Nordin, H. (2003). *Fibre Reinforced Polymers in Civil Engineering* (Doctoral dissertation, Luleå University of Technology).
- Nordin, H. (2005). Strengthening structures with externally prestressed tendons. 2005:06.
- Petre, D. & Zapalowicz, I. (2012). *Analysis of reinforced concrete slabs strengthened with textile reinforcement, non-linear finite element analysis* (Master's thesis).
- Rezazadeh, M., Barros, J. A., & Costa, I. G. (2014). Influence of prestress level on NSM CFRP laminates for the flexural strengthening of RC beams. Retrieved from https://www.researchgate.net/publication/263427704_Influence_of_prestress_level_on_NSM_CFRP_laminates_for_the_flexural_strengthening_of_RC_beams
- SIA, S. I. S. I.-u. A. (2004). Klebebewehrungen (externally bonded reinforcements).
- Täljsten, B., Blanksvärd, T., & Sas, G. (2016). *Kompositförstärkning av Betong* (Bulls Graphics AB). Svensk Byggtjänst.

- Täljsten, B., Carolin, A., & Nordin, H. (2003). Concrete structures strengthened with near surface mounted reinforcement of cfrp. *Advances in Structural Engineering*, 6(3), 201–213. doi:10.1260/136943303322419223. eprint: <http://dx.doi.org/10.1260/136943303322419223>
- Yang, J., Haghani, R., & Al-Emrani, M. (2017). Flexural strengthening of reinforced concrete beams using externally bonded frp laminates prestressed with a new method.
- Zoghi, M. (2013). *The International Handbook of FRP Composites in Civil Engineering*. DOI: 10.1201/b15806. CRC Press. Retrieved February 9, 2017, from <http://www.crcnetbase.com/doi/book/10.1201/b15806>

A Hand Calculations

Calculate the capacity of reference RC beam

Input data



Cross-section of the RC beam

$$h := 300\text{mm}$$

$$b := 200\text{mm}$$

$$a_b := 70\text{mm} \quad \text{distance between bottom reinforcement bar to concrete edge}$$

$$a_t := 70\text{mm} \quad \text{distance between top reinforcement bar to concrete edge}$$

Concrete properties C30/37 according to EC2

$$E_{cm} := 15\text{GPa}$$

$$f_{ck} := 30\text{MPa}$$

$$f_{cm} := 38\text{MPa}$$

$$f_{c,t,k5} := 2.0\text{MPa}$$

$$f_{c,t,m} := 2.03\text{MPa}$$

$$f_{c,t,k95} := 3.8\text{MPa}$$

$$\varepsilon_{cu} := 3.5 \cdot 10^{-3}$$

Steel rebar

$$A_{s,t} := 2\pi \cdot (8\text{mm})^2$$

$$A_{s,t} = 402.124 \cdot \text{mm}^2$$

$$A_{s,b} := 2\pi \cdot (8\text{mm})^2$$

$$A_{s,b} = 402.124 \cdot \text{mm}^2$$

$$E_s := 210\text{GPa}$$

confirm with lab test, 203 to 214 GPa

$$f_y := 460\text{MPa}$$

f.y.m=550-560 MPa in the lab test

$$\varepsilon_y := \frac{f_y}{E_s} = 2.19 \times 10^{-3}$$

CFRP laminate

$$t_f := 1.4\text{mm} \quad w_f := 80\text{mm}$$

$$A_f := t_f \cdot w_f = 112 \cdot \text{mm}^2$$

$$E_f := 210\text{GPa} \quad E.f = 230 \text{ GPa in lab test and 210 GPa from supplier}$$

$$\varepsilon_{\text{frp}} := 14 \cdot 10^{-3} \quad \text{14 to 15 millistrain according to lab test, I renamed the symbol from } \varepsilon.\text{frp} \text{ to } \varepsilon.f.u$$

$$\varepsilon_{f.u} := 14 \cdot 10^{-3}$$

$$f_{f.u} := 3.3\text{GPa} \quad \text{Ultimate strength } f.f.u = 3520 \text{ MPa in lab, 3300 MPa from supplier}$$

$$\text{Prestress level} \quad N_{\text{pre}} := 80\text{kN} \quad \text{the CFRP laminate was prestressed till 80 kN against the beam}$$

CFRP strain after relaxation according to the lab test

$$\varepsilon_{f.\text{ini}} := \frac{N_{\text{pre}}}{A_f \cdot E_f} = 3.401 \times 10^{-3} \quad \begin{array}{l} 3960 \text{ microstrain when prestress till 80 kN} \\ 3610 \text{ microstrain after 48 hr curing} \\ 3490 \text{ microstrain when 4 point bending start} \end{array}$$

$$\text{Excentricity} \quad e_f := \frac{h}{2} + \frac{t_f}{2} = 150.7 \cdot \text{mm} \quad \text{CFRP center to concrete beam center}$$



1. Calculate the cracking load ($E_s=210\text{GPa}$)



$$I_{\text{ref}} := \frac{1}{12} \cdot b \cdot h^3 + \frac{E_s}{E_{\text{cm}}} \cdot A_{s.t} \cdot \left(\frac{h}{2} - a_t\right)^2 + \frac{E_s}{E_{\text{cm}}} \cdot A_{s.b} \cdot \left(\frac{h}{2} - a_b\right)^2$$

$$I_1 := \frac{1}{12} \cdot b \cdot h^3 + \frac{E_s}{E_{\text{cm}}} \cdot A_{s.t} \cdot \left(\frac{h}{2} - a_t\right)^2 + \frac{E_s}{E_{\text{cm}}} \cdot A_{s.b} \cdot \left(\frac{h}{2} - a_b\right)^2 + \frac{E_f}{E_{\text{cm}}} \cdot A_f \cdot \left(\frac{h}{2} + \frac{t_f}{2}\right)^2$$

Neglect the effect of CFRP on changing the position of neutral axis

$$M_{\text{cr.mean.2}} := \frac{f_{c.t.m} \cdot I_{\text{ref}}}{h \cdot 0.5} = 7.065 \cdot \text{kN} \cdot \text{m}$$

$$M_{cr.mean.1} := \left(f_{c.t.m} + \frac{N_{pre}}{b \cdot h} \right) \cdot \frac{I_1}{h \cdot 0.5} = 12.504 \cdot kN \cdot m \quad \frac{N_{pre}}{b \cdot h} = 1.333 \cdot MPa$$

$$l_a := 1600mm - 60mm - 85mm = 1.455 \text{ m}$$



$$P_{cr.mean.ref} := \frac{M_{cr.mean.2}}{l_a} \cdot 2 = 9.712 \cdot kN$$

$$P_{cr.mean.passive} := \frac{M_{cr.mean.1}}{l_a} \cdot 2 = 17.188 \cdot kN$$

$$P_{cr.mean.prestressed} := \frac{M_{cr.mean.1} + N_{pre} \cdot e_f}{l_a} \cdot 2 = 33.76 \cdot kN$$



An alternative method to calculate the cracking load of beam with prestressed cfrp
Before loading the concrete beam was subjected to compression and bending due to prestressing

The strain of concrete on bottom edge before loading is

$$\epsilon_{c.b.1} := \frac{N_{pre}}{E_{cm} \cdot \left[b \cdot h + \left(\frac{E_s}{E_{cm}} - 1 \right) \cdot (A_{s.t} + A_{s.b}) \right]} + \frac{N_{pre} \cdot e_f}{E_{cm} \cdot I_{ref}} \cdot \frac{h}{2} = 3.066 \times 10^{-4} \quad \text{compression}$$

when the load increase from zero to cracking load $P_{cr.pre}$, the concrete at bottom edge started cracking.

$$\text{guess} \quad P := 50kN$$

$$\text{Given} \quad -\epsilon_{c.b.1} + \frac{0.5P \cdot l_a}{E_{cm} \cdot I_1} \cdot \frac{h}{2} = \frac{f_{c.t.m}}{E_{cm}}$$

$$P_{cr.pre} := \text{Find}(P)$$



$$P_{cr.pre} = 33.879 \cdot kN$$

2. Calculate the yielding load ($f_y=f.y.k=460MPa$, $E_s=210GPa$)

2.1 Yielding load of reference beam WITHOUT cfrp laminate



find the position of neutral axis (reference beam without CFRP)

Guess $x := 100\text{mm}$ Distance between NA and top edge of concrete beam

$$\text{Given } b \cdot x \cdot \frac{x}{2} + A_{s,t} \cdot \frac{E_s}{E_{cm}} (x - a_t) = A_{s,b} \cdot \frac{E_s}{E_{cm}} (h - x - a_b)$$

$$x_{c,k,ref} := \text{Find}(x)$$

$$x_{c,k,ref} = 85.331 \cdot \text{mm}$$

$$\text{When steel rebars in bottom side reach yielding strain } \epsilon_{y,ref} := \frac{f_y}{E_s} = 2.19 \times 10^{-3}$$

$$\text{Strain in rebar in top side } \epsilon_{s,t,ref} := \frac{\epsilon_{y,ref}}{h - x_{c,k,ref} - a_b} (x_{c,k,ref} - a_t) = 2.321 \times 10^{-4}$$

$$\text{Strain in concrete top edge } \epsilon_{c,ref} := \frac{\epsilon_{y,ref}}{h - x_{c,k,ref} - a_b} \cdot x_{c,k,ref} = 1.292 \times 10^{-3}$$

$$M_{y,k,ref} := \frac{E_{cm} \cdot \epsilon_{c,ref} \cdot x_{c,k,ref} \cdot b}{2} \left(h - a_b - \frac{x_{c,k,ref}}{3} \right) + E_s \cdot \epsilon_{s,t,ref} \cdot A_{s,t} (h - a_b - a_t)$$

$$M_{y,k,ref} = 36.469 \cdot \text{kN} \cdot \text{m}$$

As double check, choose neutral axis as rotation center:

$$M_{y,k,ref} := \frac{E_{cm} \cdot \epsilon_{c,ref} \cdot x_{c,k,ref} \cdot b}{2} \cdot \frac{2x_{c,k,ref}}{3} + E_s \cdot \epsilon_{s,t,ref} \cdot A_{s,t} (x_{c,k,ref} - a_t) \dots$$

$$+ f_y \cdot A_{s,b} (h - x_{c,k,ref} - a_b)$$

$$M_{y,k,ref} = 36.469 \cdot \text{kN} \cdot \text{m}$$

OK !



$$P_{y,k,ref} := \frac{M_{y,k,ref}}{l_a} \cdot 2 = 50.129 \cdot \text{kN}$$

2.2 Yielding load of beam with passive cfrp laminate



For cracked section find the position of neutral axis (consider the application of CFRP)

Use first moment of area method to find the neutral axis

Guess $\tilde{x} := 100\text{mm}$ distance between neutral axis and top edge of beam

$$\text{Given} \quad b \cdot x \cdot \frac{x}{2} + A_{s,t} \cdot \frac{E_s}{E_{cm}} (x - a_t) = A_{s,b} \cdot \frac{E_s}{E_{cm}} (h - x - a_b) + A_f \cdot \frac{E_f}{E_{cm}} \left(h - x + \frac{t_f}{2} \right)$$

$$x_{c,k} := \text{Find}(x)$$

$$x_{c,k} = 96.23 \cdot \text{mm}$$

When steel rebars in bottom side reach yielding strain $\epsilon_y = 2.19 \times 10^{-3}$

$$\text{Strain in rebar in top side} \quad \epsilon_{s,t} := \frac{\epsilon_y}{h - x_{c,k} - a_b} (x_{c,k} - a_t) = 4.295 \times 10^{-4}$$

$$\text{Strain in concrete top edge} \quad \epsilon_c := \frac{\epsilon_y}{h - x_{c,k} - a_b} \cdot x_{c,k} = 1.576 \times 10^{-3}$$

Strain of passive CFRP when the rebars in bottom side start yielding (Add)

$$\epsilon_{f,pss} := \frac{\epsilon_y}{h - x_{c,k} - a_b} \left(h - x_{c,k} + \frac{t_f}{2} \right) = 3.348 \times 10^{-3}$$

As double-check I choose the neutral axis position as rotation center

$$M_{y,k} := \frac{E_{cm} \cdot \epsilon_c \cdot x_{c,k} \cdot b}{2} \left(x_{c,k} - \frac{x_{c,k}}{3} \right) + E_s \cdot \epsilon_{s,t} \cdot A_{s,t} (x_{c,k} - a_t) \dots$$

$$+ f_y \cdot A_{s,b} (h - x_{c,k} - a_b) + E_f \cdot \epsilon_{f,pss} \cdot A_f \left(h - x_{c,k} + \frac{t_f}{2} \right)$$

$$M_{y,k} = 56.39 \cdot \text{kN} \cdot \text{m}$$

If use bending stiffness to calculate the M_y of passive cfrp beam

The moment inertial of cracked cross-section

$$x_{y,pss} := x_{c,k}$$

$$I_{y,pss} := \left[\frac{b \cdot x_{y,pss}^3}{12} + b \cdot x_{y,pss} \cdot \left(\frac{x_{y,pss}}{2} \right)^2 + \frac{E_s}{E_{cm}} \cdot A_{s,t} \cdot (x_{y,pss} - a_t)^2 \dots \dots \right. \\ \left. + \frac{E_s}{E_{cm}} \cdot A_{s,b} \cdot (h - x_{y,pss} - a_b)^2 \right. \\ \left. + \frac{E_f}{E_{cm}} \cdot A_f \cdot \left(h - x_{y,pss} + \frac{t_f}{2} \right)^2 \right]$$

$$M_{y,pss} := \frac{f_y}{h - x_{y,pss} - a_b} \cdot \frac{E_{cm} \cdot I_{y,pss}}{E_s} = 56.39 \cdot \text{kN} \cdot \text{m} \quad \text{It matches the result above}$$



$$P_{y,passive} := \frac{M_{y,pss}}{l_a} \cdot 2 = 77.512 \cdot \text{kN}$$

2.3 Yielding load of beam with prestressed cfrp laminate



when load is zero

Before loading, the concrete part was subjected to compression and bending due to prestressing force

The concrete strain in the top edge:

assume the cross-section is not cracked on top due to prestressing

$$\epsilon_{c,t,1} := \frac{-N_{pre}}{E_{cm} \cdot \left[b \cdot h + \left(\frac{E_s}{E_{cm}} - 1 \right) \cdot (A_{s,t} + A_{s,b}) \right]} + \frac{N_{pre} \cdot e_f}{E_{cm} \cdot I_{ref}} \cdot \frac{h}{2} = 1.552 \times 10^{-4} \quad \text{in tension}$$

$$\epsilon_{c,t,1} \cdot E_{cm} = 2.328 \cdot \text{MPa}$$

$$\frac{N_{pre}}{E_{cm} \cdot \left[b \cdot h + \left(\frac{E_s}{E_{cm}} - 1 \right) \cdot (A_{s,t} + A_{s,b}) \right]} = 7.57 \times 10^{-5} \quad \text{Neglect the crack effect}$$

$$\frac{N_{pre} \cdot e_f}{E_{cm} \cdot I_{ref}} \cdot \frac{h}{2} = 2.309 \times 10^{-4}$$

The steel bar in the top side:

$$\varepsilon_{s,t.1} := \frac{-N_{pre}}{E_{cm} \cdot \left[b \cdot h + \left(\frac{E_s}{E_{cm}} - 1 \right) \cdot (A_{s,t} + A_{s,b}) \right]} + \frac{N_{pre} \cdot e_f}{E_{cm} \cdot I_{ref}} \cdot \left(\frac{h}{2} - a_b \right) = 4.747 \times 10^{-5} \quad \text{Tension}$$

The steel bar in the bottom side:

$$\varepsilon_{s,b.1} := \frac{N_{pre}}{E_{cm} \cdot \left[b \cdot h + \left(\frac{E_s}{E_{cm}} - 1 \right) \cdot (A_{s,t} + A_{s,b}) \right]} + \frac{N_{pre} \cdot e_f}{E_{cm} \cdot I_{ref}} \cdot \left(\frac{h}{2} - a_b \right) = 1.989 \times 10^{-4} \quad \text{compression}$$

It is worthy to mention here that in the lab test the strain of rebar before loading was 2.8E-4

$$\frac{N_{pre} \cdot e_f}{E_{cm} \cdot I_{ref}} \cdot \left(\frac{h}{2} - a_b \right) = 1.232 \times 10^{-4}$$

The initial strain of CFRP laminate before loading

$$\varepsilon_{f,ini} = 3.401 \times 10^{-3} \quad \text{calculated from } N_{pre} \text{ theoretically}$$

$$\varepsilon_{f,1} := \varepsilon_{f,ini} = 3.401 \times 10^{-3} \quad \text{in tension}$$

load increase from 0 till cracking load P.cr

The neutral axis position is assumed in the center of concrete

$$x_{cr} := \frac{h}{2} = 150 \cdot \text{mm}$$

The corresponding secondary moment of inertia of the cross-section

$$I_{cr} := I_1 = 5.577 \times 10^8 \cdot \text{mm}^4 \quad \text{this is calculated before in section 1}$$

load increase from P.cr cracking load till yielding load P.y

Assume linear distribution of cross-sectional strain, and neglect the cracked concrete

the neutral axis position of cracked cross-section with passive CFRP was calculated in Section 2.2

$$x_{y.pss} = 96.23 \cdot \text{mm}$$

The neutral axis position of cracked beam with prestressed CFRP

$$x_{y.pre} := x_{y.pss} = 96.23 \cdot \text{mm}$$

Note: The following calculation using force equilibrium aims to validate the equation above

find the neutral axis position at yielding load

$$\text{Guess} \quad \underline{x} := 100 \text{mm}$$

$$\text{Given} \quad \frac{1}{2} \cdot b \cdot x \cdot E_{cm} \cdot \left(\epsilon_{c,t.1} + \frac{\epsilon_y + \epsilon_{s.b.1}}{h - x - a_b} \cdot x \right) \dots = A_{s,b} \cdot f_y \dots$$

$$+ A_{s,t} \cdot E_s \cdot \left[\epsilon_{s,t.1} + \frac{\epsilon_y + \epsilon_{s.b.1}}{h - x - a_b} \cdot (x - a_t) \right] + A_f \cdot E_f \cdot \left[\epsilon_{f.1} + \frac{\epsilon_y + \epsilon_{s.b.1}}{h - x - a_b} \cdot \left(h - x + \frac{t_f}{2} \right) \right]$$

$$x_{y.pre.valid} := \text{Find}(x)$$

$$x_{y.pre.valid} = 100.229 \cdot \text{mm} \quad \text{This approximate calculation matches with the result above}$$

The moment inertial of cracked cross-section

$$I_{y.pre} := \left[\frac{b \cdot x_{y.pre}^3}{12} + b \cdot x_{y.pre} \cdot \left(\frac{x_{y.pre}}{2} \right)^2 + \frac{E_s}{E_{cm}} \cdot A_{s,t} \cdot (x_{y.pre} - a_t)^2 \dots + \frac{E_f}{E_{cm}} \cdot A_f \cdot \left(h - x_{y.pre} + \frac{t_f}{2} \right)^2 \right]$$

$$+ \frac{E_s}{E_{cm}} \cdot A_{s,b} \cdot (h - x_{y.pre} - a_b)^2$$

Reaching yielding point P.y -- steel bars in the bottom side started yielding

The strain of rebar in the bottom side reached yielding strain

$$\epsilon_{s.b.2} := \epsilon_y = 2.19 \times 10^{-3}$$

Now make an equation in terms of the development of strain in rebars in bottom side

$$\text{Guess} \quad P_y := 80 \text{kN}$$

$$\text{Given} \quad -\epsilon_{s.b.1} + \frac{0.5P_{cr.pre} \cdot l_a}{E_{cm} \cdot I_{cr}} \cdot (h - x_{cr} - a_b) + \frac{0.5(P_y - P_{cr.pre}) \cdot l_a}{E_{cm} \cdot I_{y.pre}} \cdot (h - x_{y.pre} - a_b) = \epsilon_{s.b.2}$$

$$P_{y.pre} := \text{Find}(P_y)$$

$$P_{y.pre} = 110.086 \cdot \text{kN}$$

Check the strain values

Strain in concrete top edge at yielding load

$$\epsilon_{c,t.2} := \epsilon_{c,t.1} + \frac{0.5P_{cr.pre} \cdot I_a}{E_{cm} \cdot I_{cr}} \cdot x_{cr} + \frac{0.5(P_{y.pre} - P_{cr.pre}) \cdot I_a}{E_{cm} \cdot I_{y.pre}} \cdot x_{y.pre}$$

$$\epsilon_{c,t.2} = 2.146 \times 10^{-3} \quad \epsilon_{c,t.2} < \epsilon_{cu} = 1 \quad \text{OK}$$

Strain in CFRP laminate

$$\epsilon_{f,2} := \epsilon_{f,1} + \frac{0.5P_{cr.pre} \cdot I_a}{E_{cm} \cdot I_{cr}} \cdot (h - x_{cr}) + \frac{0.5(P_{y.pre} - P_{cr.pre}) \cdot I_a}{E_{cm} \cdot I_{y.pre}} \cdot (h - x_{y.pre})$$

$$\epsilon_{f,2} = 7.124 \times 10^{-3} \quad \epsilon_{f,u} = 0.014$$



$$P_{y.pre} = 110.086 \cdot \text{kN}$$

3. Calculate the ultimate load (f.y=f.y.k=460MPa, E.s=210GPa)

3.1 reference beam WITHOUT cfrp laminate



assume:

1. $\epsilon_c = \epsilon_{cu} = 3.5E-3$
2. steel started yielding before concrete crashing

$$\alpha := 0.810 \quad \beta := 0.416 \quad \epsilon_{cu} = 3.5 \times 10^{-3}$$

$$\text{Guess} \quad x_{aa} := 100 \text{ mm}$$

$$\text{Given} \quad A_s \cdot b \cdot f_y = \alpha \cdot f_{cm} \cdot b \cdot x + A_{s,t} \cdot E_s \cdot \frac{\epsilon_{cu}}{x} \cdot (x - a_t)$$

$$x_{u.ref} := \text{Find}(x)$$

$$x_{u.ref} = 49.683 \cdot \text{mm}$$

check the strain of rebar on bottom side

$$\epsilon_{s,b.3} := \frac{\epsilon_{cu}}{x_{u.ref}} \cdot (h - x_{u.ref} - a_b) = 0.013 \quad \epsilon_y = 2.19 \times 10^{-3} \quad \text{OK}$$

strain of rebar on top side

$$\epsilon_{s,t.3} := \frac{\epsilon_{cu}}{x_{u.ref}} \cdot (a_t - x_{u.ref}) = 1.431 \times 10^{-3} \quad \text{In tension}$$

Assumption is valid.

$$M_{u.ref} := \alpha \cdot f_{cm} \cdot b \cdot x_{u.ref} \cdot (x_{u.ref} - \beta \cdot x_{u.ref}) + A_{s,t} \cdot E_s \cdot \epsilon_{s,t.3} \cdot (a_t - x_{u.ref}) + A_{s,b} \cdot f_y \cdot (h - x_{u.ref} - a_b)$$

$$M_{u.ref} = 44.684 \cdot \text{kN} \cdot \text{m}$$



$$P_{u.ref} := \frac{M_{u.ref}}{l_a} \cdot 2 = 61.422 \cdot \text{kN}$$

3.2 beam with passive cfrp laminate

define the limitation of strain in CFRP when debonding happen

$$\epsilon_{f,deb} := 7 \cdot 10^{-3}$$

please change this value and make sure that this value matches with lab test or FE assumption

$$\epsilon_{f,deb} := 0.004968 \quad \text{Lab value}$$

$$\epsilon_{f,deb} := 0.00533 \quad \text{FE value}$$



assume:

1. failure of concrete crushing on top $\epsilon_c = \epsilon_{cu} = 3.5E-3$
2. steel started yielding before concrete crushing
3. debonding did not occur

$$\alpha := 0.810 \quad \beta := 0.416 \quad \epsilon_{cu} = 3.5 \times 10^{-3}$$

$$\text{Guess } x := 100 \text{ mm}$$

$$\text{Given } \alpha \cdot f_{cm} \cdot b \cdot x + A_{s,t} \cdot E_s \cdot \frac{\epsilon_{cu}}{x} \cdot (x - a_t) = A_{s,b} \cdot f_y + A_f \cdot E_f \cdot \frac{\epsilon_{cu}}{x} \left(h - x + \frac{t_f}{2} \right)$$

$$x_{u.pss} := \text{Find}(x)$$

$$x_{u.pss} = 71.667 \cdot \text{mm}$$

check the strain of rebar on bottom side

$$\epsilon_{s,b.2} := \frac{\epsilon_{cu}}{x_{u,pss}} \cdot (h - x_{u,pss} - a_b) = 7.733 \times 10^{-3} \quad \epsilon_y = 2.19 \times 10^{-3}$$

OK, assumption 2 valid

strain of rebar on top side

$$\epsilon_{s,t.2} := \frac{\epsilon_{cu}}{x_{u,pss}} \cdot (x_{u,pss} - a_t) = 8.14 \times 10^{-5} \quad \text{in compression}$$

strain of CFRP

$$\epsilon_{f,3} := \frac{\epsilon_{cu}}{x_{u,pss}} \cdot \left(h - x_{u,pss} + \frac{t_f}{2} \right) = 0.011 \quad \epsilon_{f,deb} = 5.33 \times 10^{-3}$$

$$\epsilon_{f,3} < \epsilon_{f,deb} = 0 \quad \text{Assumption 3 is not valid}$$

Second round to find the neutral axis

assume:

1. debonding failure $\epsilon_{f,3} = \epsilon_{f,deb}$
2. concrete on top have not reached crushing, $\epsilon_{c,t.3} < \epsilon_{cu}$
3. steel already started yielding

Guess $x_{n,n} := 100 \text{ mm}$

$$\text{Given} \quad b \cdot x \cdot E_{cm} \cdot \frac{\epsilon_{f,deb}}{h - x + \frac{t_f}{2}} \cdot x + A_{s,t} \cdot E_s \cdot \frac{\epsilon_{f,deb}}{h - x + \frac{t_f}{2}} \cdot (x - a_t) = A_{s,b} \cdot f_y + A_f \cdot E_f \cdot \epsilon_{f,deb}$$

$x_{u,pss} := \text{Find}(x)$

$$x_{u,pss} = 67.72 \cdot \text{mm}$$

Check the strains

Concrete strain on top edge

$$\epsilon_{c,t.3} := \frac{\epsilon_{f,deb}}{h - x_{u,pss} + \frac{t_f}{2}} \cdot x_{u,pss} = 1.549 \times 10^{-3}$$

$$\epsilon_{c,t.3} < \epsilon_{cu} = 1 \quad \text{OK, assumption 2 is valid}$$

steel rebar on top side

$$\varepsilon_{s.t.3} := \frac{\varepsilon_{f.deb}}{h - x_{u.pss} + \frac{t_f}{2}} \cdot (a_t - x_{u.pss}) = 5.217 \times 10^{-5} \quad \text{in tension}$$

$$\varepsilon_{s.t.3} < \varepsilon_y = 1 \quad \text{ok, not yielding}$$

$$M_{u.pss} := E_{cm} \cdot \varepsilon_{c.t.3} \cdot \frac{b \cdot x_{u.pss}}{2} \cdot \frac{2x_{u.pss}}{3} + E_s \cdot \varepsilon_{s.t.3} \cdot A_{s.t} \cdot (a_t - x_{u.pss}) \dots$$

$$+ f_y \cdot A_{s.b} \cdot (h - x_{u.pss} - a_b) + E_f \cdot \varepsilon_{f.deb} \cdot A_f \cdot \left(h - x_{u.pss} + \frac{t_f}{2} \right)$$

$$M_{u.pss} = 66.34 \cdot \text{kN} \cdot \text{m}$$



$$P_{u.pss} := \frac{M_{u.pss}}{l_a} \cdot 2 = 91.189 \cdot \text{kN}$$

3.3 Beam with prestressed CFRP laminate

Define the limitation of strain at CFRP fracture

$$\varepsilon_{f.fra} := \varepsilon_{f.u} = 0.014 \quad \text{Theoretical strain}$$

$$\varepsilon_{f.fra} := 0.01129 \quad \text{Real rupture strain from FE}$$



assume:

1. failure mode is CFRP fracture $\varepsilon_{f.fra} = \varepsilon_{f.u} = 14$ millistrain

2. Concrete on top have not reach crushing $\epsilon_{c.t.3} < \epsilon_{cu}$
3. Steel bars in bottom side yielded

find the neutral axis position at failure load

Guess $x := 100\text{mm}$

Given
$$\frac{1}{2} \cdot b \cdot x \cdot E_{cm} \cdot \left(\epsilon_{c.t.1} + \frac{\epsilon_{f.fra} - \epsilon_{f.1}}{h - x + \frac{t_f}{2}} \cdot x \right) \dots = A_{s.b} \cdot f_y + A_f \cdot E_f \cdot \epsilon_{f.fra}$$

$$+ A_{s.t} \cdot E_s \cdot \left[\epsilon_{s.t.1} + \frac{\epsilon_{f.fra} - \epsilon_{f.1}}{h - x + \frac{t_f}{2}} \cdot (x - a_t) \right]$$

$x_{u.pre} := \text{Find}(x)$

$x_{u.pre} = 83.904 \cdot \text{mm}$

Check the strains

Concrete strain on top edge

$\epsilon_{c.t.2} := \epsilon_{c.t.1} + \frac{\epsilon_{f.fra} - \epsilon_{f.1}}{h - x + \frac{t_f}{2}} \cdot x_{u.pre} = 3.453 \times 10^{-3}$ almost reaching 3.5 millistrain

$\epsilon_{c.t.3} < \epsilon_{cu} = 1$ OK, assumption 2 is valid

steel rebar on top side

$\epsilon_{s.t.2} := \epsilon_{s.t.1} + \frac{\epsilon_{f.fra} - \epsilon_{f.1}}{h - x_{u.pre} + \frac{t_f}{2}} \cdot (a_t - x_{u.pre}) = -4.585 \times 10^{-4}$ in tension

$\epsilon_{s.t.3} < \epsilon_y = 1$ ok, not yielding

Steel rebar on bottom side strain is larger than ϵ_y

$$M_{u,\text{pre}} := E_{\text{cm}} \cdot \varepsilon_{\text{c.t.3}} \cdot \frac{b \cdot x_{u,\text{pre}}}{2} \cdot \frac{2x_{u,\text{pre}}}{3} + E_{\text{s}} \cdot \varepsilon_{\text{s.t.3}} \cdot A_{\text{s.t}} \cdot (a_{\text{t}} - x_{u,\text{pre}}) \dots$$

$$+ f_{\text{y}} \cdot A_{\text{s.b}} \cdot (h - x_{u,\text{pre}} - a_{\text{b}}) + E_{\text{f}} \cdot \varepsilon_{\text{f.fra}} \cdot A_{\text{f}} \cdot \left(h - x_{u,\text{pre}} + \frac{t_{\text{f}}}{2} \right)$$

$$M_{u,\text{pre}} = 109.441 \cdot \text{kN} \cdot \text{m}$$



$$P_{u,\text{pre}} := \left(\frac{M_{u,\text{pre}}}{l_{\text{a}}} \right) \cdot 2 = 150.434 \cdot \text{kN}$$

B CFRP Manufacture

Tekniskt faktablad

StoFRP Plate

Kolfiberlaminat för förstärkning av betong- och stålkonstruktioner



Karakteristik

Användning	<ul style="list-style-type: none"> ytmonterat förstärkningssystem för ökad bärförmåga hos befintliga betongkonstruktioner som kolfiberlaminat
-------------------	---

Egenskaper	<ul style="list-style-type: none"> olika möjligheter beträffande E-modul och area
-------------------	--

Teknisk data

StoFRP Plate S 50 C	Fibertyp	höghållfast kolfiber
StoFRP Plate S 80 C	Fiberorientering	0° (alla bärande fibrer i laminatets längdriktning)
StoFRP Plate S 100 C	Tvärsnittsareor	1,4 x 50 = 70 mm ²
StoFRP Plate S 120 C		1,4 x 80 = 112 mm ²
StoFRP Plate S 150 C		1,4 x 100 = 140 mm ²
kolfiberlaminat		1,4 x 120 = 168 mm ²
peel-ply på två sidor		1,4 x 150 = 210 mm ² andra tvärsnitt kan tas fram på begäran
	Draghållfasthet (min)	2800 MPa
	Draghållfasthet (medel)	3100 MPa
	Elasticitetsmodul (min)	163 GPa
	Elasticitetsmodul (medel)	170 GPa
	Brottöjning, f	ca 16‰
	Längder på laminat	upp till 100 m
	Lagringstid	obegränsad
	Förpackning	i rullar eller lådor, beroende på laminatlängd
StoFRP Plate IM 60 C	Fibertyp	högmodul kolfiber
StoFRP Plate IM 80 C	Fiberorientering	0° (alla bärande fibrer i laminatets längdriktning)
StoFRP Plate IM 100 C	Tvärsnittsareor	1,4 x 60 = 84 mm ²
kolfiberlaminat		1,4 x 80 = 112 mm ²
peel-ply på två sidor		1,4 x 100 = 140 mm ²
	Draghållfasthet (min)	2900 MPa
	Draghållfasthet (medel)	3300 MPa
	Elasticitetsmodul (min)	200 GPa
	Elasticitetsmodul (medel)	210 GPa
	Brottöjning, f	ca 14‰
	Längder på laminat	upp till 100 m
	Lagringstid	obegränsad
	Förpackning	i rullar eller lådor, beroende på laminatlängd
StoPox SK 41, epoxilim	Fakta	ett lösningsmedels- och nonylfenolfritt tixotrop epoxilim, speciellt framtaget för förstärkning av konstruktioner med StoFRP Plate E eller IM.
	Blandningsförhållande	bas : hårdare 100 : 25 viktdelar
	Densitet +20° C	1800 kg/m ³

Tekniskt faktablad

StoFRP Plate

Viskositet	tixotrop
Potlife 100 g, +20° C	30 min
Skjuvhållfasthet	≥12 MPa
Elasticitetsmodul	≥ 2 GPa
Åtgång	0,063 kg/m x laminatets bredd (cm)

Appliceringsanvisning

Tillkapning kolfiber	Kolfiberlaminaten kapas lättast med en rondell. Linda det område som ska kapas med t.ex. maskeringstejp. Slipa lätt området som har kapats för att avlägsna kolfiberflisor.
Behandling av limytor	Kolfiberlaminatet kommer levererade med en s.k. "peel-ply", vilken avlägsnas innan limning. Rengör ytan alldeles innan limning med acetone. Laminaten skall handhas med varsamhet, smuts, fett eller dylikt får ej finnas på ytan vid limning. Lämpligen används rena plasthandskar. Betongytan sandblästras eller slipas så att slamskiktet avlägsnas och ballasten friläggs. Betongytan skall vara fri från partiklar av damm, olja eller andra föroreningar. Dammsugning eller tryckluft för rengöring skall användas.
Klimat	Temperaturen på betongytan ska vara minst 10°C samt minst 3°C över rådande dagpunkt. Vid limning ska den relativa fuktigheten i luften understiga 80%. Dessa förhållanden måste vara uppfyllda under limmets hela uthärdningsförlopp.
Blandning av primer	För blandning kan användas omrörare alt. elektrisk bormaskin. Blanda därefter StoPox 452 EP enligt anvisning: Blanda noggrant med långsamgående visp (max 300 varv/min.), tills en homogen massa uppstår. Det är viktigt att även röra om vid sidorna och i botten, så att härdaren blir jämnt fördelad. Blandningstid minst 3 minuter. Arbeta inte ur leveransbehållaren! Håll över materialet i en ren behållare efter blandningen och rör om ordentligt. Temperaturen på de enskilda komponenterna måste vid blandningen uppgå till minst +15 C.
Påföring av primer	Se till att betongytan är rengjord enligt ovan. En fördel med StoPox 452 EP är att den är diffusionsöppen. Primern appliceras med pensel eller roller.
Blandning av lim	För blandning kan användas omrörare alt. elektrisk bormaskin. Blanda därefter StoPox SK 41 enligt anvisning: Rör om komponent A, och tillsätt därefter hela komponent B. Blanda noggrant med långsamgående visp (max 300 varv/min.), tills en homogen massa uppstår. Det är viktigt att även röra om vid sidorna och i botten, så att härdaren blir jämnt fördelad. Blandningstid minst 3 minuter. Arbeta inte ur leveransbehållaren! Håll över materialet i en ren behållare efter blandningen och rör om ordentligt. Temperaturen på de enskilda komponenterna måste vid blandningen uppgå till minst +15 C.
Montering av laminat	Innan laminatet monteras ska lim påföras, normalt påförs lim såväl på betong som på laminat. För att underlätta påföringen av lim på laminat finns en speciell limpåförare, StoDivers Applikator, som passar till samtliga laminat. En limtjocklek motsvarande 1-2 mm är lämpligt. Följande appliceringsgång kan följas: 1. Applicera lim på den behandlade och rengjorda betongytan 2. Applicera lim på rengjort kolfiberlaminat 3. Montera laminatet 4. Applicera tryck med gummiroller 5. Skrapa bort överskottslim
Att tänka på	Viktigt att tänka på är: - att aktsamhet vid hantering av epoxiprodukter vidtas - att föreskriven skyddsutrustning används

Tekniskt faktablad

StoFRP Plate

	<ul style="list-style-type: none"> - att kanterna på laminaten kan bli vassa vid kapning - att flera lager av laminat inte bör appliceras ovanpå varandra - att skyddsplasten på laminatets utsida kan avlägsnas så att eventuella fläckar av epoxi försvinner
Rengöring	Efter användning, rengör genast alla verktyg med aceton där inte annat anges.
Litteratur	<p>Hassanzadeh M., 2000, "Beständighet hos kompositmaterial för infrastrukturkonstruktioner", Uppdragsrapport nr. U00.07, Lunds Tekniska Högskola, Avdeln för Byggnadsmaterial, p 22, 2000.</p> <p>Täljsten B., 1994, "Plate Bonding, Strengthening of Existing Concrete Structures with Epoxy Bonded Plates of Steel or Fibre Reinforced Plastics", Doctoral Thesis 1994:152D, ISSN 0348-8373, Luleå University of Technology, p 308, 1994.</p> <p>Täljsten B., 1998, "Strengthening of Building Structures with FRP-Fabrics", IABSE Colloquium, Berlin 1998, "Saving Buildings in Central and Eastern Europe", ISBN 3-85748-094-8, and CD-publication.</p> <p>Täljsten B., 2001, "Full Scale Tests on Concrete Structures Strengthened with Plate Bonding in Sweden", Conf. Proceedings: Concrete Under Severe Conditions – Environment and Loading, University of British Columbia, Vancouver June 18-20, 2001, Edt. Banthia N., Sakai K. and Gjörv O.E., ISBN 0-88865-782-X, pp 2132 – 2142.</p> <p>Täljsten, B., 2002, "FRP Strengthening of Existing Concrete Structures, Design Guidelines", ISBN:91-89580-03-6, Division of Structural Engineering, Luleå University of Technology, p 228, 2002.</p>
Övrigt	
Säkerhet	<p>Säkerhetsdatablad finns på www.sto.se</p> <p>Observera informationen angående hantering av produkten, lagring och avfallshantering.</p>
Särskilda upplysningar	
	<p>Information och uppgifter i detta tekniska faktablad är avsett för normal applicering respektive produktens lämplighet för detta och är baserad på vår nuvarande kunskap och erfarenhet. Det befriar dock inte användaren från det egna ansvaret att undersöka ändamål och lämplighet.</p> <p>Användning som inte entydigt omnämns i detta tekniska faktablad får endast utföras efter samråd med Sto Scandinavia AB. Utan godkännande sker detta på användarens eget ansvar. Detta gäller framför allt för kombinationer med andra produkter.</p> <p>Genom utgivningen av ett nytt tekniskt faktablad upphör alla tidigare versioner att gälla. Den senaste utgåvan finns tillgänglig på www.sto.se</p>

Sto Scandinavia AB
 Box 1041
 581 10 Linköping
 Telefon 020-37 71 00
 Telefax 013-37 71 37
 kundkontakt@stoeu.com
www.sto.se

C Reinforcement lab test

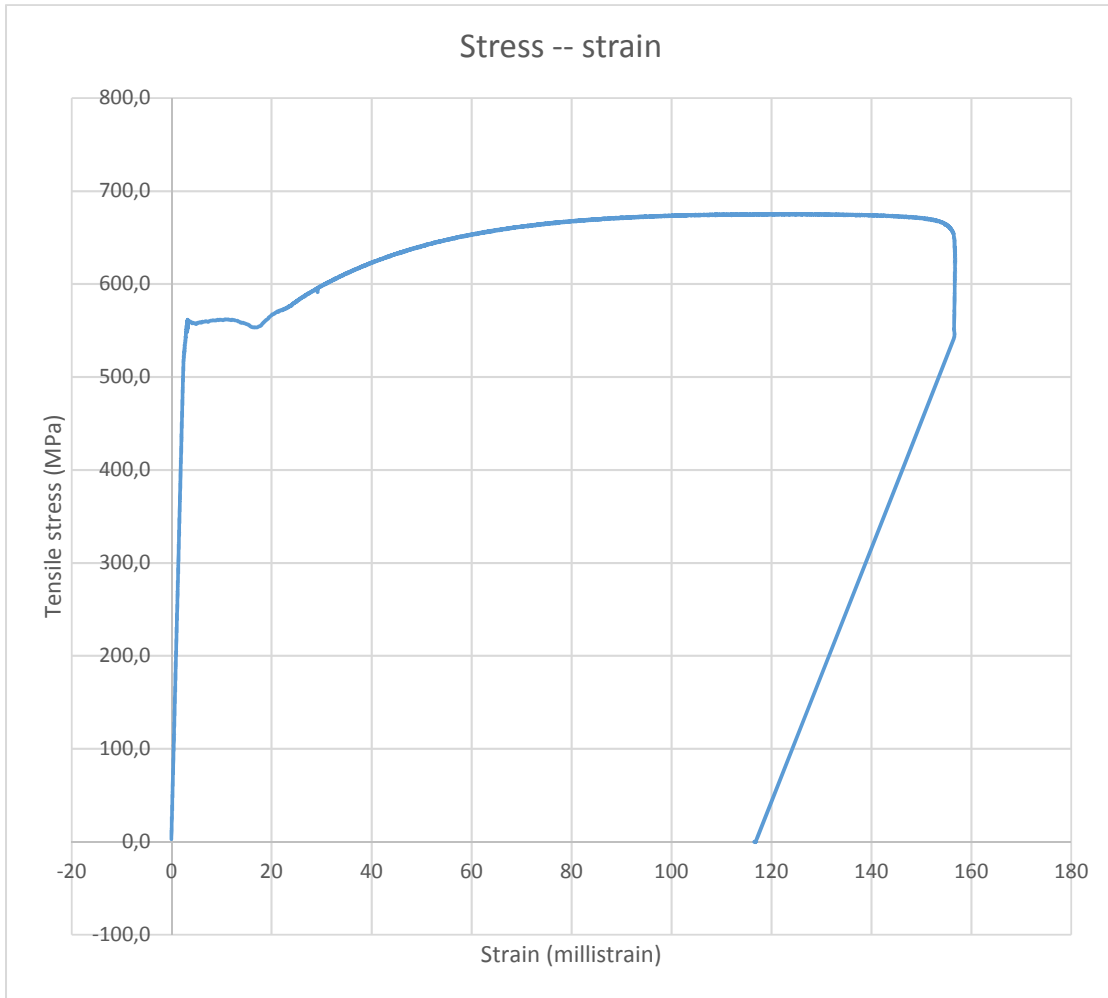
Reinforcement lab test

bar1 (first loaded in compression unintended)			
Diameter	15,3 mm		
Area	184 mm ²		
Clamping l_c	248 mm		
Ext-mtr	50 mm		
f.u	680 MPa		
stress 1.0	-210,9	-1,0	$\epsilon=1,0$ millistrain
stress 2.0	-413,534	-2,0	$\epsilon=2,0$ millistrain
E.s in comp	203,8 GPa		
f.y	550 MPa		
$\epsilon.y$	2,698433 millistrain	theoretically	

bar2			
Diameter	15,3 mm		
Area	184 mm ²		
Clamping l_c	248 mm		
Ext-mtr	50 mm		
f.u	676 MPa		
stress 1.0	228,9	1,0	$\epsilon=1,0$ millistrain
stress 2.0	442,2	2,0	$\epsilon=2,0$ millistrain
E.s	214,8 GPa		
f.y	560 MPa		
$\epsilon.y$	2,607128 millistrain	theoretically	

Note:

It is suggested to use the properties of Bar 2 as input data in FEM Tension hardening after yielding, check sheet ' B2'



D Concrete lab test

Concrete cylinders under compressive test

ID	Diameter	Height	days	Compressive strength 180 (MPa)	Variation	H/D	H/D factor	Age factor [ref 3]	Size effect--alt 1. / Calibrated strength		Size effect--alt 2. [ref 2]	
									$f_{c,m}(150 \text{ cylinder, } 28 \text{ days, } H/D=2.0)$	$f_{c,m}(150 \text{ cube, } 28 \text{ days, } H/D=2.0)$	$f_{c,m}(150 \text{ cylinder, } 28 \text{ days, } H/D=2.0)$	$f_{c,m}(150 \text{ cube, } 28 \text{ days, } H/D=2.0)$
Specimen 1	45	90	90	53,6	-11%	2	1,000	0,86	1,06	48,83	1,079	49,69
Specimen 2	45	95	95	59,5	-2%	2,111	1,008	0,86	1,06	54,63	1,077	55,49
Specimen 3	45	96	96	62,7	4%	2,133	1,009	0,86	1,06	57,66	1,076	58,51
Specimen 4	45	109	109	61,7	2%	2,422	1,028	0,86	1,06	57,78	1,076	58,65
Specimen 5	45	111	111	65,1	8%	2,467	1,031	0,86	1,06	61,14	1,075	62,01
avg (1-5)				60,52						56,0		56,9

ref 1 R. Pudinotti 2013, based on ACI 214.4R & BS1881
 ref 2 F. Indelicato (1997), Estimate of concrete cube strength by means of different diameter cores: A statistical approach
 ref 3 EC 2, section 3.1.2

f _{ck} (MPa)	Strength classes for concrete C30/37												Analytical relation / Explanation		
	12	16	20	25	30	35	40	45	50	55	60	70		80	90
f _{ck,0.05} (MPa)	15	20	25	30	37	45	50	55	60	67	75	85	95	105	f _{ck} = f_{ck} + 8 (MPa)}
f _{ck,0.05} (MPa)	20	24	28	33	38	43	48	53	58	63	68	78	88	98	f _{ck} = f_{ck} + 8 (MPa)}
f _{ck,0.05} (MPa)	1,6	1,9	2,2	2,6	2,9	3,2	3,5	3,8	4,1	4,2	4,4	4,6	4,8	5,0	f _{ck} = 0,30 \cdot f_{ck}^{0,23} \cdot C^{0,50} \cdot 10^{0,10} + f_{ck}^{0,70} \cdot C^{0,50} \cdot 10^{0,10}}
f _{ck,0.05} (MPa)	1,1	1,3	1,5	1,8	2,0	2,2	2,5	2,7	2,9	3,0	3,1	3,2	3,4	3,5	f _{ck} = 0,7 \cdot f_{ck}}
f _{ck,0.05} (MPa)	2,0	2,5	2,9	3,3	3,8	4,2	4,6	4,9	5,3	5,5	5,7	6,0	6,3	6,6	f _{ck} = 1,3 \cdot f_{ck}}
E _{cm} (GPa)	27	29	30	31	33	34	35	36	37	38	39	41	42	44	E _{cm} = 220 \cdot (f_{ck} + 10)^{0,23}}
ε _{ck} (‰)	1,8	1,9	2,0	2,1	2,2	2,25	2,3	2,4	2,45	2,5	2,6	2,7	2,8	2,8	see Figure 3.2
ε _{ck} (‰)															ε _{ck} (‰) = 0,17 \cdot f_{ck}^{0,23}}
ε _{ck} (‰)															see Figure 3.2
ε _{ck} (‰)															ε _{ck} (‰) = 2,0 \cdot 10^{-5} \cdot (f_{ck} + 10)^{0,23}}
ε _{ck} (‰)															see Figure 3.3
ε _{ck} (‰)															ε _{ck} (‰) = 2,0 \cdot 10^{-5} \cdot (f_{ck} + 10)^{0,23}}
n															see Figure 3.3
ε _{ck} (‰)															ε _{ck} (‰) = 2,0 \cdot 10^{-5} \cdot (f_{ck} + 10)^{0,23}}
ε _{ck} (‰)															see Figure 3.4
ε _{ck} (‰)															ε _{ck} (‰) = 1,75 + 0,55 \cdot (f_{ck} + 50) / 100}

Table 3.1 Strength and deformation characteristics for concrete

EN 1992-1-1:2004 (E)

Concrete class evaluation
 C30/37 informed by supplier
 C45/55 size effect from ACI 214.4R-03
 C35/45 Size effect from F. Indelicato 1997

E CFRP lab test

CFRP_1	25 mm
Width	1,4 mm
Thickness	35 mm ²
Area	120,2 kN
Max. Force	15,73 millistrain
Max. strain	29,7 0,004
Force 04	94,3 0,012
Force 12	230,6 GPa
E.cfrp	3434 MPa
f _u	

CFRP_2	25 mm
Width	1,4 mm
Thickness	35 mm ²
Area	126,3 kN
Max. Force	14,4 millistrain
Max. strain	30,6 0,004
Force 04	103,2 0,012
Force 12	259,1 GPa
E.cfrp	3608 MPa
f _u	

CFRP_3	25 mm
Width	1,4 mm
Thickness	35 mm ²
Area	120,2 kN
Max. Force	10,559 millistrain
Max. strain	40,8 0,004
Force 04	96,9 0,008
Force 08	400,5 GPa
E.cfrp	3434 MPa
f _u	

CFRP_4	25 mm
Width	1,4 mm
Thickness	35 mm ²
Area	126,1 kN
Max. Force	10,559 millistrain
Max. strain	91,65524 0,005
Force 05	117,6097 0,006
Force 06	741,6 GPa
E.cfrp	3603 MPa
f _u	

	f _u	E.cfrp	
CFRP_1	3434	230,6	
CFRP_2	3608	259,1	overestimated due to unreliable values of strain gauges
CFRP_3	3434	400,5	overestimated due to unreliable values of strain gauges
CFRP_4	3603	741,6	overestimated due to unreliable values of strain gauges
Avg	3520	230	
from suppl	3300	210,0	

According to technical data sheet, f_u=3300MPa, elastic modulus 210 Gpa, ultimate strain 14 millistrain

